The role of the histone variant macroH2A1 in muscle physiology and pathophysiology

Melanija Posavec

TESI DOCTORAL UPF / 2014

Thesis Director:
Marcus Buschbeck, PhD
Chromatin Metabolism and Cell Fate Group
Institute of Predictive and Personalized Medicine of Cancer

TABLE OF CONTENTS

DISCUSSION

MacroH2A1.1 is the least investigated and least understood histone variant. It always provoked lot of discussion as it was found to bind NAD+-derived metabolites *in vitro*. Having observed dominant expression of macroH2A1.1, a structural component of chromatin, in highly metabolic skeletal muscle tissue, we hypothesised that macroH2A1.1 could allow chromatin to respond to local metabolic environment changes via its metabolite binding-pocket. Here we discuss our data on macroH2A1 splicing during myogenic differentiation, the role of macroH2A1.1 and its metabolite-binding capacity in myoblast fusion and myotube maturation. We further put our finding that macroH2A1.1 regulates myoblasts' metabolic properties and muscle fiber type profile in mice into the context of previous knowledge and discuss its possible relevance for the whole body health state. As further detailed below, we believe that our results encourage the idea that macroH2A1.1 could be one of the long sought mechanisms allowing chromatin to adapt to its metabolic environment ultimately defining an adapted cellular phenotype.

MacroH2A1 splicing switch accompanies physiological myogenic differentiation and results in dominant macroH2A1.1 expression in mature myotubes and muscles

MacroH2A1 splicing switch where macroH2A1.2 gets completely exchanged with time during differentiation for the metabolite-binding macroH2A1.1 characterizes physiological myogenic differentiation process (Fig. 43**.)**. The fact that macroH2A1.1 correlates with terminally differentiated cells supports the finding that macroH2A1.1 conversely correlates with cell proliferation as reported for cancer cell lines (Novikov et al., 2011). Also the fact that terminally differentiated skeletal muscles contain only post-mitotical nuclei and express only macroH2A1.1 establishes macroH2A1.1 as a part of cell cycle exit signature. Also looking at macroH2A1.1 protein levels in healthy and aRMS cells - cancer cells of myogenic origin - macroH2A1.1 shows clearly higher expression in healthy than in aRMS cells. Interestingly, the aRMS cell lines Rh30 and Rh4 showed impaired or delayed macroH2A1 splicing switch. Moreover, Rh30 cells known to be more metastatic, contain more *macroH2A1.2* than Rh4 cells and actually never completely downregulate *macroH2A1.2* upon differentiation, providing another piece of evidence that macroH2A1.2 might act pro-cancerous as previously suggested by others (Dardenne et al., 2012; Sporn et al., 2009) or at least favour proliferation as reported by Novikov *et al.* (Novikov et al., 2011). However, we cannot state this with certainty for myoblasts as we have not assessed proliferation. Nevertheless, the "overly" expressed *macroH2A1.2* upon differentiation in the presented model of Rh30 metastatic aRMS resembles other studies on metastatic cancer models (Dardenne et al., 2012; Sporn et al., 2009). Rh30 lack

macroH2A2 which might be a coincidence as many cell types do not express macroH2A2, but is interesting to point out as macroH2A2 was shown to be a tumour-suppressor (Kapoor et al., 2010). This leaves the possibility that in the case of Rh30 cells, lack of macroH2A2 and incomplete macroH2A1 switch contribute to metastatic properties of these cells. During mouse myoblast differentiation, both total *macroH2A1* and *macroH2A2* levels decreased slightly until the end of differentiation. In the case of macroH2A1, this reduction is a consequence of the drastic drop of *macroH2A1.2*. Even though the functional significance of the total macroH2A pool decrease upon differentiation remains poorly demonstrated, one argument could be that terminally differentiated nuclei just do not need to sustain similar high amounts as proliferating cells. This might be due to the fact that they do not need to extensively reorganize their genome as most of it was already silenced (probably through many other mechanisms of epigenetic regulations) and therefore need less macroH2A which could otherwise render their genes inactive, but responsive to defined signal induction (Buschbeck et al., 2009; Gamble et al., 2010; Ouararhni et al., 2006). In contrast to mouse myoblast, our results on human primary myoblasts showed that the total *macroH2A1* transcript pool remained constant during differentiation and also *macroH2A2* mRNA levels did not drop. Whether the macroH2A mRNA levels correspond to protein levels still remains to be investigated. Additional distinction between mouse and human cells was observed when ratio of macroH2A1 isoforms was analyzed in proliferation. While mouse proliferating myoblasts contain 3-4-times more mRNA of *macroH2A1.2* than *macroH2A1.1*, in human cells the levels of *macroH2A1.2* are only approximately 1.5-fold higher than *macroH2A1.1.* Whether this reflects distinct epigenetic set-ups in these two species or whether it implies any metabolic differences, so far we can only speculate, as protein levels have not been compared between mouse and human cells and no functional studies have been performed.

How exactly the splicing switch of macroH2A1 is regulated is not fully understood, but we have been able to add the splicing factor RBFox2 to the list of regulators of *macroH2A1.1* levels. We also showed that macroH2A1.2 is positively regulated in myoblasts by Ddx5 and Ddx17 splicing factors, just as previously reported in a breast cancer model (Dardenne et al., 2012).

How the genome localization of the two splicing isoforms is organized and reorganized during differentiation is not fully understood. Nevertheless, our ChIP-seq analyses provided first data on macroH2A1.2 and macroH2A1.1 genome-wide distribution in proliferating and differentiated C2C12 myoblasts, contributing in that way to the understanding of epigenetic landscape remodelling upon myogenic differentiation (Asp et al., 2011; Vethantham et al., 2012) We suggest that the two macroH2A1 isoforms during differentiation exchange at their genomic loci of enrichment, as no drastic differences were seen when the genome distribution

was analysed. What might change extensively upon isoforms switch on the chromatin is the local macroH2A1.1- or macroH2A1.2-associated environment. Distinct factors might associate specifically with each isoform and modulate chromatin structure and gene expression in differentiation-dependent manner. Specific macroH2A1.2 and macroH2A1.1 effects on gene behaviour in myoblasts and myotubes nuclei still need to be further investigated just as our ChIP-seq data need to be crossed with other existing ChIP-seq profiles in order to better understand the contribution of macroH2A1 in the context of chromatin to myogenic differentiation.

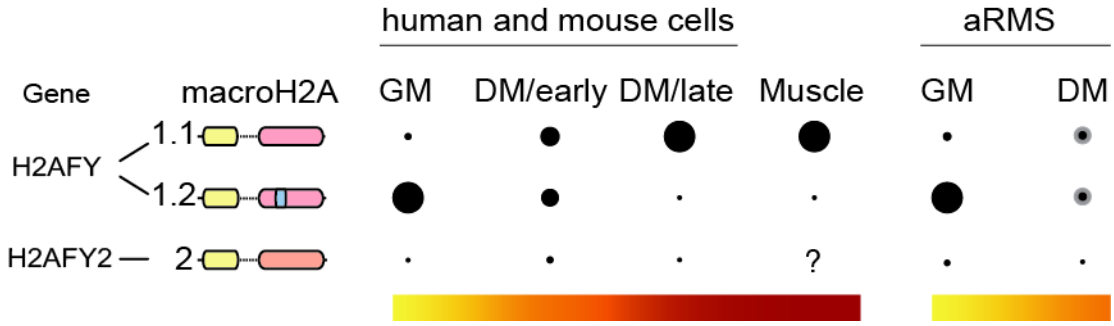

Figure 43. MacroH2As in myogenic differentiation. The size of the bubble represents the expression. Questionmark means not assessed. In the case of aRMS cell lines, the grey dots represent Rh30 cell line behaviour, while the black dots represent both Rh30 and Rh4 cell line.

MacroH2A1/MacroH2A1.1-deficieny destabilizes the myogenic differentiation gene program

MacroH2A1 KO mice were found to have no overt developmental phenotypes (Changolkar et al., 2007), but rather metabolic defects as for example a 50% incidence of spontaneous liver steatosis in females (Boulard et al., 2010). That these mice would develop without any bigger developmental defect was not expected and how this happens is not completely clear. From analysis of macroH2A in cancer, stem cells and somatic reprogramming, we can conclude that a major function of these histone variants is to maintain the differentiated state stable. Hence, it will be interesting to test how mice develop in stressed conditions. In adult mice, we could show by cardiotoxin-induced muscle regeneration that macroH2A1 KO mice, even though they can regenerate their muscles, suffer from failing to form full-sized fibers. This late fusion defect was confirmed also when primary macroH2A1 KO myoblasts were differentiated in culture. Primary KO myotubes contained lower number of myonuclei per myotube and had smaller diameters. Smaller myotube diameter can be attributed to lower fusion rate, but also decreased protein synthesis as myotubes grow both by myonuclei accretion and protein synthesis (Sandri, 2008).

Also C2C12 myoblasts showed impaired fusion when macroH2A1.1 was depleted. Several dozen reports on macroH2A since its discovery indeed support the statement that macroH2A is necessary for proper differentiation and development. In contrary, macroH2A1.2-depleted myoblasts form very nice and mature myotubes. Apparently myoblasts and myotubes represent different cell types that have different epigenetic requirements. Possibly in the cell types where both isoforms are present their relative ratio defines the degree of differentiation and proliferative drive (Dardenne et al., 2012; Novikov et al., 2011). Cells of early developmental stage as human and mouse ES cells, induced pluripotent stem (iPS) cells, and zebrafish embryos exhibited impaired differentiation when any of the macroH2A proteins was removed (Barrero et al., 2013b; Buschbeck et al., 2009; Creppe et al., 2012; Pasque et al., 2012). Importantly, in these models macroH2A1.1 levels were almost undetectable and macroH2A1.2 and macroH2A2, the only macroH2A proteins present, were responsible for the described pro-differentiation functions. Therefore, the timing of the appearance or increment of the different macroH2A1 isoforms expression probably adjusts the isoforms function as pro-differentiation factors, as studies done so far imply that models of adult cells depend on macroH2A1 isoforms ratio but early developmental stages cells do not, exemplified by the fact that macroH2A is virtually absent in the zygote (Nashun et al., 2010). Finally, all this does not explain nor support the fact that macroH2A1 KO mice demonstrate normal development. One of the explanations is that in mouse utero development is more robust and less sensitive to environmental fluctuations that could impact on macroH2A1-containing chromatin. Another possibility is that macroH2A1 KO mice were not extensively enough studied to identify more subtle developmental phenotypes. As further detailed below, we could indeed identify alterations when performing a more profound characterization of muscle tissues. Another explanation is that diminishing two isoforms of opposite functions might balance the KO phenotype. It is also possible that mice, as mammals tend to have more complex epigenetic mechanisms with many layers of gene regulation, can buffer to a certain degree the loss of one epigenetic mechanism. This would be consistent with a previous studies done in Zebrafish where upon deletion of macroH2A2 as the only developmentally expressed macroH2A protein, the animals though they exhibited multiple developmental defects, contained all organs (Buschbeck et al., 2009). Taken together that macroH2A-deficient zebrafish develop complete with all its organs and that mice have only very subtle phenotypes affirm that macroH2A histone variants are epigenetic modulators and not master regulators. Or in other words said, macroH2A histone variants seem not to be crucial for cell fate decision-making, but rather the proper execution of a specific differentiation/developmental gene expression profile.

Knock-down of macroH2A1.1 in differentiating myoblasts led to the deregulation of around 800 genes. That this was not a mere consequence of delay in differentiation but a real deregulation was shown by the direction of the deregulation of the genes upon macroH2A1.1 knock-down. Genes were shown to be upregulated or downregulated upon differentiation, but after the knock-down exhibited really diverse regulation. This goes in line with previously reported macroH2A-deficiency effects where improper differentiation of mouse ES cells, human iPS cells or teratomas was observed upon macroH2A1-depletion (Barrero et al., 2013b; Creppe et al., 2012). In total, macroH2A proteins are accepted as stabilizers of more differentiated states due to all the pro-differentiation evidence collected but also because of reprogramming facilitation upon macroH2A removal (Barrero et al., 2013a; Pasque et al., 2011; Pasque et al., 2012). We did not observe reduced proliferation capacity in primary KO cells nor in mice during muscle regeneration (as the KO mice muscles did not appear smaller), as opposed to other studies where removal of specific macroH2A induced proliferation capacity changes. MacroH2A1.2-deficiency would imply decreased proliferative capacity if relying on previous studies on macroH2A1.2 in cancer (Dardenne et al., 2012; Novikov et al., 2011; Sporn et al., 2009), or increased proliferation as observed in human primary keratinocytes or melanoma cells (Creppe et al., 2012; Kapoor et al., 2010), but none of this was observed. As the total H2AFY gene KO eliminates both macroH2A1.2 and macroH2A1.1, the KO cells could have been relying on other compensatory mechanisms to stabilize their cell fates during development or as already mentioned, the simultaneous loss of two isoforms with opposing functions might balance the phenotype. It is conceivable that lack of macroH2A1.1 could act in favour of proliferation and would therefore counterbalance the depletion of macroH2A1.2.

We have observed no defect in the commitment of primary KO cells to differentiation, which is comparable to studies on ES cells where induction of differentiation genes was detected upon differentiation in macroH2A1-deficient cells, but it was less efficient as compared to control cells (Barrero et al., 2013b; Creppe et al., 2012). When macroH2A1.1-depleted C2C12 cells were differentiated, they all committed as witnessed by various differentiation markers tested, but showed obvious fusion defects as a late differentiation phenotype. This is another piece of evidence that macroH2A1/macroH2A1.1 contribute to the execution of an adequate gene expression program possibly by stabilizing the underlying chromatin structure but that its absence does not abrogate cell fate transitions *per se*. Nevertheless, it could represent a risk factor for altered chromatin function as genome-wide studies showed that in muscle main osteogenic and adipogenic factors bear active chromatin marks like H3K4me2/3 (Asp et al., 2011). Large-scale gene expression analysis of macroH2A1.1-depleted C2C12 myotubes demonstrated that many genes involved in adhesion, cell motility and extracellular structures are

affected. Since these processes are crucial for fusion, we argue that the genes regulated by macroH2A1.1 and detected in our large-scale expression analysis could be responsible for the observed fusion defect. Other previously reported such as *Il4*, *Tmem8c*, *Cdh15* (M-cad) and *Nfatc2* (Simionescu and Pavlath, 2011) were not affected. Notably, macroH2A1.1 does not act just specifically on myoblast/myotube related genes, but as a matter of fact on genes involved in proper functions of different cell types. Additionally, macroH2A1.1 and macroH2A1.2 drive expression of *Tmem171* and *Cdhr1* genes in contrary directions. The control of genes involved in cell motility, adhesion and extracellular matrix regulated by the two macroH2A1 isoforms in an opposing manner might be even more important in the context of cancer and metastasis and could provide another explanation for the differential functions attributed to both isoforms in cancer.

MacroH2A1 isoforms exhibit specific regulation on muscle mass homeostasis genes

The other aspect that appears different in myoblasts and myotubes is the metabolic environment and their intrinsic preference for metabolic pathways. Intriguingly, macroH2A1.2 can be found in highly proliferative cells such as pluripotent cells or cancer cells that rely on aerobic glycolysis (Creppe et al., 2012; Dardenne et al., 2012; Novikov et al., 2011; Sporn and Jung, 2012), but also in proliferating myoblasts; as opposed to macroH2A1.1 found in more differentiated or terminally differentiated cells and myotubes. Muscle mass control and the metabolic properties of the muscle are intimately related (Sandri, 2008; Sandri et al., 2006; Schiaffino and Reggiani, 2011). We have defined a set of muscle mass and metabolism homeostasis-related genes to be affected by macroH2A1.1 knock-down. These include the *Mstn* gene, that encodes the myokine myostatin and whose upregulation could even be seen in proliferating myoblasts, and also the genes *Fst*, *Igf-1*, *Igf-2*, *Pdgfr, Slc2a4* and *Fstl1*. Increased myostatin levels have been reported to reduce muscle mass albeit to different extents (Durieux et al., 2007; McFarlane et al., 2006; Reisz-Porszasz et al., 2003; Zimmers et al., 2002). MacroH2A1.1-depleted cells exhibit increased *Mstn* expression and a mild reduction of *Fst*, which encodes follistatin, the inhibitor of myostatin. Whether the phenotype could partly be explained by the follistatin – myostatin axis, which participates in both fusion and hypertrophy, would need to be addressed. Also, we have not explored the expression of activin receptors nor their activation upon myostatin binding in macroH2A1.1 knock-down cells. Therefore at this point it is hard to argue that *Mstn* expression changes are the main or major cause of the observed phenotype. Moreover, both *Igf-1* and *Igf-2* are deregulated in the absence of macroH2A1.1 but in opposite directions. Igf-1 and Igf-2 positively control muscle mass but by

acting on distinct processes. While Igf-1 acts on protein synthesis and myonuclei number, Igf-2 seems to promote differentiation of primary myoblasts (reviewed in Philippou et al., 2007). Whether the deregulation of Igf expression seen in our studies makes sense in the light of the phenotype observed remains to be further investigated: cells commit well to myogenic differentiation which might be due to *Igf-2* increase but fail to form bigger and more mature myotubes, maybe as a consequence of *Igf-1* reduction. Igf-1 can inhibit atrogenes expression (Sacheck et al., 2004), but we could not detect any change in the expression of the two atrogens encoded by the *Trim63* and *Fbxo32* genes. While addition of Igf-1 downregulates *Trim63* and *Fbxo32* mRNA synthesis, the downregulation of Igf-1 might have no evident effect. Still, our current dataset does not provide enough evidence to give support neither to the Igf-1 and Igf-2 axis in control of macroH2A1.1-deficient myotubes fusion and size. Nevertheless, one could argue that all the deregulated genes involved in muscle mass homeostasis contribute synergistically to the phenotype of macroH2A1.1-depleted cells.

Some of these genes involved in muscle mass were likewise detected deregulated upon macroH2A1.2 depletion, such as *Fst* and *Igf-2*. Interestingly, in macroH2A1.2 knock-down cells *Fst* was upregulated, which could have provoked decreased myostatin action in those myotubes. Whether the Mstn signalling was really diminished in these cells, we cannot assert as myostatin – activin receptors signalling pathway activation remains to be tested. Yet, more explanation of increased myotubes size could be explained by the upregulation of *Myh4* fiber type gene coding for hypertrophy-submissive fibers (Schiaffino and Reggiani, 2011), and upregulation of some fusion factors tested – *Tmem8c*, *Nfatc2*, *Cdh15*. In total, genes deregulation pointed toward possibility of myotube increment, which could explain the observed tendency of macroH2A1.2-deficient myoblasts to form larger myotubes. *Tmem171* and *Cdhr1*, as already mentioned, are both downregulated upon macroH2A1.1 knock-down but upregulated upon macroH2A1.2 knock-down. These data point out that genes regulated equally or similarly by both macroH2A1 isoforms might depend just on the macro domain generally, no matter if it can or does bind metabolites or not. Conversely, other genes, such as *Tmem171*, *Cdhr1*, *Igf*, *Fst* and *Mstn* evidently depend on different macro domains and one could argue that they depend on macroH2A1.1, especially those related to metabolic functions of muscle. Still, in our rescue experiments in C2C12 cells we could observe equally successful rescue using wild type or G224E mutant, which resembles macroH2A1.2 in the sense that it cannot bind metabolites of macroH2A1.1. Though at first sight the rescue experiments argue against uniqueness of metabolite-binding macroH2A1.1 isoform function, the real question that has never been addressed is whether the metabolites were really bound or present in those conditions. In order to ensure metabolite accessibility, one could modulate NAD+ levels through nutrients

availability/starvation to activate sirtuins (Canto et al., 2009) and change therefore ADPr and *O*AADPr concentrations. If in this experimental set-up any change between the wild type and mutant macroH2A1.1 would be observed, this would give first strong support to the physiological role of macroH2A1.1 metabolite binding pocket.

Interestingly, *Mstn* was the only upregulated gene (by macroH2A1.1 knock-down) that was robustly rescued by the introduction of rescue transgenes. Although our gene expression analysis showed that macroH2A1.1 represses half of the genes, while the other half gets induced by macroH2A1.1 removal, the upregulation was greater than the downregulation of the genes. And though we cannot assure which of the targets are directly influenced by macroH2A1.1 and which not, we do propose that macroH2A1.1 removal acts bi-modally: removal of macroH2A1.1 alters chromatin structure locally and globally altering therefore genes expression. Possibly the right localization of macroH2A1.1 in the chromatin upon the rescue requires more time and energy and is not that easily established. Also, as macroH2A was shown to present just one layer of repressiveness (Nesterova et al., 2002), removing it might induce more broad chromatin alterations that are harder or impossible to erase. This might happen for pure steric reasons. The genes that are controlled by macroH2A1.1 incorporation in the chromatin might exhibit this "hard-to-rescue" pattern. On the contrary, gene expression changes early after re-introduction of macroH2A1.1 in the nucleus might reflect incorporation-dependent regulation via local metabolite-binding of macroH2A1.1. This implies that rather the macro domain and not the histone fold are involved in the regulation. For this recue experiments using transgenes separating macro domain and histone fold would provide further insight. The way we conduct experiments, enough time is most likely provided for gene expression changes to occur as a consequence of chromatin rearrangement as we let cells to be rescued during 3-4 days. Nevertheless, why we could detect very few upregulated genes rescued requires further analysis.

Inhibition of myostatin has proven to immensely boost muscle mass increase in many animal models and even in humans (Schuelke et al., 2004). We did not observe substantial changes of myotubes size when macroH2A1.1 was overexpressed, but this might be because the *Mstn* downregulation was not strong enough or simply because it is harder to observe these changes in a time-limited cell culture setting. Also, another function described for myostatin is regulating insulin signalling in mice liver (Hittel et al., 2010). The possibility that macroH2A1 and myostatin form a pathway that is conserved in different insulin-responsive tissues is intriguing and seeks for more research.

Metabolite-binding macroH2A1.1-dependent functions revealed in myotubes using the binding pocket mutant G224E

When primary KO myoblasts were rescued with transgenes encoding either wild-type macroH2A1.1 or the G224E point mutant unable to bind metabolites in vitro, a difference could be observed between the two conditions. MacroH2A1.1-rescued myotubes looked well formed and mature and only very few cells could be detected on the plate that did not fuse. Control infected KO myoblasts exhibited a fusion defect where only nascent but no mature myotubes myotubes could be detected. This indicates that indeed macroH2A1.1 is necessary for completion of proper myogenic differentiation. G224E mutant-rescued myotubes looked differently than the control or the macroH2A1.1-rescued cells. Though there were mature myotubes detected, not all cells successfully fused and grew as the wild type macroH2A1.1-rescued myotubes. This observation provides first evidence that the metabolite binding-capacity of macroH2A1.1 contributes to the formation of proper myotubes. How metabolite-binding could exert such an influence on fusion, it is not clear.

It remains a big speculation whether metabolite binding pocket can sense the metabolic environment and can directly make the cells respond adequately to nutrients available and metabolic needs. At the present it is further poor speculation that such a function could enable full development of myotubes.

The increase in macroH2A1.1 upregulation and the even more pronounced reduction in macroH2A1.2 expression become evident in myogenic differentiation right after the serum withdrawal and can be understood as a response to the consequential change in metabolism. That changes of metabolism occur with changes in cell fate is widely accepted. For example the Warburg effect is characteristic of cancer and pluripotent cells (Vander Heiden et al., 2009) and the redox state was shown to influence myoblasts differentiation (Fulco et al., 2003). In favour of the metabolic distinction of proliferating myoblasts and differentiated myotubes goes also our LC/MS-MS profile of relevant metabolites. ADPr, which macroH2A1.1 can bind, heavily drops with differentiation. As ADPr is rapidly formed from sirtuin side-product OAADPr, our data supports the previous that sirtuin expression and activity decrease with differentiation (Fulco et al., 2003). The same authors also showed that if sirtuins are downregulated when myoblasts were simulataneously starved, fusion of the myoblasts improved (Fulco et al., 2008). This would imply that the best fusion would be observed when least ADPr is present, which in turn would limit the fraction of macroH2A1.1 macro domain that could be bound to ADPr. However, our preliminary observation in rescue experiments with the G224E mutant in primary KO myoblasts suggest at least a partial involvement. New tools and additional experiments will be needed to sort out the molecular details.

MacroH2A1.1 regulates fiber type genes and metabolic characteristics of C2C12 cells

MacroH2A1.1 is most dominantly expressed in fully formed myotubes and muscles. One of the initial observations in the knock-down and rescue experiments performed in C2C12 cells was that levels of macroH2A1.1 correlated with a change in medium color indicative of extracellular acidification. To better understand this metabolic alteration became the focus of our interest. We investigated in details how macroH2A1.1-depleted cells react on glucose addition after a period of starvation. By measuring the acidification rate, we uncovered reduced glycolytic flexibility in macroH2A1.1-depleted cells. After a period of starvation, cells will try to utilize glucose with a maximal rate to compensate quickly for the possible NAD+/NADH ratio changes and the drop in ATP levels. In the knock-down cells this does not happen suggesting that macroH2A1.1 will enable the cells to maximally use glycolysis as energy replenishing path. Interestingly, in our analysis of substrate utilization preferences of macroH2A1.1-depleted cells we observed that these cells preferentially use glucose as energy source. Though at first sight contradictory, it makes sense. If the cells are inefficient in production of energy and balancing the redox state through glycolysis, they might actually try to increase the glucose transport into the cells as a feed-back mechanisms to compensate for the inefficient glycolysis. And truly, in our gene expression analysis we find the *Slc2a4* gene encoding the Glut4 transporter of the glucose 1,6-fold upregulated in the macroH2A1.1 knock-down cells. Indeed, Glut4 mRNA has been shown to be upregulated in muscles of fasted animals (Canto et al., 2010). We could find more simple carbohydrates to be preferentially used by macroH2A1.1-depleted cells, as for example mannose and maltose. Maltose is a disaccharide composed of two units of glucose and is has been suggested that it provokes a similar metabolic effect as glucose (Young and Weser, 1971), but at the same time provides twice as much energy when metabolized. Pazienza *et al.* report that liver cancer cells augment insulin-dependent glucose uptake after macroH2A1.1 overexpression, but not after macroH2A1.2 overexpression (Pazienza et al., 2014). MacroH2A1.1-overexpressing liver cells could favour glucose conversion into glycogen which is an accepted mechanism to keep glucose stores for other tissues (Zhang et al., 2014), while switching to other sources like fatty acids for energy production. Pazienza and colleagues suggest that macroH2A1.1-overexpressing cells act protective by modulating their metabolism (Pazienza et al., 2014). The issue in the paper by Pazienza *et al.* arrises because HepG2 macroH2A1.2-overexpressing cells show comparable glycogen synthesis to macroH2A1.1-overexpressing cells, even though macroH2A1.2-overexpressing cells did not show increased glucose uptake. Interestingly, in the Hepa1-6 cell line tested, the authors show upregulation of genes involved in glucose utilization upon macroH2A1.2 overexpression and downregulation in

the case of macroH2A1.1 overexpression (Pazienza et al., 2014). These discrepancies could have occurred as cell line-specific events.

Next to *Slc2a4*/Glut4, we found also other relevant genes – *Pparγ* (1,32-fold), *Fabp3* (approximately 3-fold), *Pdk4* (1,2-fold as measured by qRT-PCR) – to be upregulated by macroH2A1.1 knock-down. All these genes were positively regulated upon macroH2A1.2 overexpression and addition of exogenous fatty acids (FAs) as reported by Pazienza *et al*. While Fabp3 should facilitate transport of fatty acids to mitochondria for their oxidation, Pdk4 should save the pyruvate from getting converted to acetyl-CoA in periods of energy stress. Substrate switching from glucose to fatty acids is normal after fed-to-fasted transition and is normally found in muscle when energy-deprived, as for example after prolonged exercise (Zhang et al., 2014). The reverse switch is also a physiological event after feeding when insulin stimulates muscle to dispose majority of glucose (Kelley and Mandarino, 2000). Nonetheless, in obese and type 2 diabetes (T2D) patients this fails to happen and moreover, Kim *et al.* have shown that prolonged infusion of fat in rats can lead to acute insulin resistance (Kim et al., 2006b). CD36, a fatty acid transporter with a main role in muscle, activates fatty acid flux during starvation, which correlates with decreased insulin concentrations and AKT signalling, leading to enhanced fatty acid utilization (Nahle et al., 2008). Interestingly, the independent analysis by two labs of livers from macroH2A1 KO mice showed upregulated *CD36* levels (Boulard et al., 2010; Changolkar et al., 2007). Furthermore, we found genes encoding components of the AKT signalling pathway to be downregulated in macroH2A1.1-deprived C2C12 cells. Altogether, we can argue that macroH2A1.1-depleted cells seem to feel energy-deprived due to limited glucose availability, as a consequence of impaired glycolytic flexibility. This fake "starvation situation" they then try to compensate by upregulating the genes involved in fatty acids utilization. The fact that we observed glucose and other carbohydrates to be preferentially utilized by macroH2A1.1 knock-down cells can be a misleading piece of data as we just tested simple sugars, amino acids and di-peptides.

We also provide evidence that the maximal respiratory capacity of the knock-down cells is compromised in the knock-down cells. Our experiments showed that macroH2A1.1-depleted committed myoblasts show declined maximal respiratory capacity when mitochondria were uncoupled using FCCP. Nonetheless, basal respiration levels were essentially equal pointing out that if the cells experience no energy stress demands, they will do fine. But if any energy stress is induced, the macroH2A1.1 knock-down cells will perform worse. Seeing the compromised mitochondrial respiratory capacity and also increased *Fabp3* levels, we decided to check how the knock-down cells oxidize fatty acids. FAs feed into the TCA cycle when oxidized, which can be monitored through oxygen consumption. Upon starvation free FAs get mobilized from

triglycerides (Dole, 1956; Fredrickson and Gordon, 1958; Gordon and Cherkes, 1956) and uncouple mitochondria of the starved cells causing increase in oxygen consumption not due to FA oxidation (Divakaruni and Brand, 2011). If the cells are starved, but exogenous FAs are added, the exogenous FAs will preferentially be metabolized over endogenous free FAs. Our experiment consisted of starving the macroH2A1.1-depleted cells in order to prime them for FA oxidation. Our data confirmed previously seen compromised mitochondrial respiratory capacity. Oxidation of both endogenous or egoxenous FAs was reduced in macroH2A1.1-depleted cells. Even though the knock-down cells, just as the control cell, rely on exogenous FAs if energy stressed, they show lower rates of oxygen consumption. *Fabp3* was our top upregulated target, but fatty acids mobilization is a separate process from oxidation by the mitochondria. Carnitine palmitoyltransferase I (Cpt1b isoform in the muscle) initiates the priming of exogenous FAs for oxidation. We observed almost neglectable increase of *Cpt1b* expression upon macroH2A1.1 knock-down (though the correct way would be to check the Cpt1b behaviour upon the exogenous FAs addition), while Pazienza *et al.* observed increased *CPT2* and decreased *CPT1a* levels upon exogenous FA administration in macroH2A1.2-overexpressing cells. When we checked oxygen consumption due to uncoupling by free FAs, we could again observe a decrease. The knock-down cells in all conditions (plus or minus exogenous FAs, plus and minus Cpt1 inhibitor etoxomir) exhibited diminished ATP production, which is consistent with our starvation hypothesis.

Can fiber type shift in macroH2A1 KO muscles be a cause of systemic metabolic defects?

Analyzing our large-scale gene expression array, we found fiber type genes to be deregulated. *Myh7*, *Myh7b*, *Myh2*, *Myh1*, *Myh4* and *Myh8* were all differentially expressed upon the macroH2A1.1 knock-down. We found this extremely important considering that *myosin heavy chain* genes encode key structural proteins of fiber types that define the function of muscles (Schiaffino and Reggiani, 2011), but also define muscle fiber metabolism which can profoundly impact other tissues and whole body health through glucose tolerance and insulin sensitivity (Daugaard et al., 2000; Henriksen et al., 1990; Lillioja et al., 1987; Song et al., 1999). We found that the fiber types genes downregulated were those of the extremes: coding for the most oxidative and the most glycolytic fiber type; *Myh7*, *Myh7b*, and *Myh4*. Conversely, *Myh2* and *Myh1* genes were upregulated. These genes code for fast fiber types, IIa and IIx, that exhibit higher oxidative potential than type IIb fibers but lower than type I fibers (Schiaffino, 2010). Importantly, our analysis on metabolic properties of macroH2A1.1-depleted cells correlates

with these expression data as indeed these cells suffer from decreased glycolytic flexibility and impaired mitochondrial respiration capacity.

The type I fibers play important role in insulin resistance and the onset of T2D (DeFronzo and Tripathy, 2009), in addition to regulating fat accumulation and mobilization. Type IIb fibers are great glucose consumers and are prone to undergo hypertrophy or atrophy, depending on nutrient availability, hormonal control and physical activity. In order to test whether we observe only a fiber type encoding genes switch in culture or whether this alterations could be linked to metabolic changes in adult mice, we analyzed muscle tissue composition of macroH2A1 KO mice. MacroH2A1 KO mice so far have been shown to exhibit mild metabolic defects such as liver steatosis in females (Boulard et al., 2010) and worsen glucose clearance in male macroH2A1 KO mice (Changolkar et al., 2007), but in both macroH2A1 KO models the metabolic phenotypes have been correlated with deregulated genes implicated in lipid metabolism in the liver, such as already mentioned *CD36*, *Lpl* and *Serpina7*. In one case the steatosis was correlated with *Serpina7* upregulation and its effect on increased lipid metabolism, while in the other increased *Lpl* and *CD36* liver levels were claimed to be responsible for only scarce worsening of glucose clearance in male macroH2A1 KO mice. Although both studies provide correlations, a possible insight into regulation mechanism has been proposed just by Boulard *et al.* since they show that macroH2A1 was enriched on the *Serpina7* promoter specifically in females. In the case of *Serpina7*, it is possible that the gene expression alteration observed arises as a consequence of macroH2A1 removal and consequential alterations in chromatin structure. Yet, for other genes it is not clear whether they might be deregulated as a consequence of rebutting the possible energy stress. It is widely accepted that muscle is responsible for majority of glucose cleared under insulin control (Schiaffino and Reggiani, 2011) and improper muscle functions have been implicated in many pathological states such as T2D and obesity. Neither of the studies commented anything on the muscles in the macroH2A1 KO mice. We describe for the first time a metabolic change in muscles of macroH2A1 KO mice. We investigated several muscles and could show that the fiber type profile in soleus and tibialis muscles is altered in macroH2A1 KO mice. Importantly, we did not observe unidirectional change of the fiber profile. We observed that in the fast muscle tibialis the glycolytic fibers change towards the oxidative and slower fiber type. In soleus the most oxidative fiber type I changes into less oxidative and faster fibers IIa. This is important as type I fibers are more active in glucose disposal, burn more energy daily and can utilize fat as fuel source after prolonged period of starvation (Schiaffino and Reggiani, 2011). Type I fibers positively correlate with insulin sensitivity and glucose tolerance (Daugaard et al., 2000; Henriksen et al., 1990; Lillioja et al., 1987; Song et al., 1999). Whether these muscle alterations

can explain the metabolic phenotype of macroH2A1 KO mice needs more proof. A comprehensive study like metabolic profiling using metabolic cages could provide further insight into metabolic alterations in the macroH2A1 KO mice. The KO mice could also be fed high fat diet (HFD). We anticipate that they might exhibit insulin sensitivity changes. As already in not-challenged conditions 50% of the macroH2A1 KO female mice suffer from liver steatosis, one can hypothesise that the ectopic fat accumulation could get more extreme upon HFD. It is interesting that in one macroH2A1 KO mice study male mice, shown to have more type II fibers (Welle et al., 2008), exhibit slight glucose disposal issue, while females, who should be better in utilizing fat by muscles, exhibit liver steatosis in the second study. Additionally, exercise experiments could give evidence on whether these mice, due to fiber type profile changes, exhibit altered physical competence and whether they also suffer from impaired ATP production, like the very pronounced phenotype of compromised ATP production in C2C12 cells depleted of macroH2A1.1.

This analysis of the fiber profiles indeed goes in line with our initial finding on macroH2A1.1 depletion-induced fiber type genes changes. We can affirm that the specific fibers do not just change their oxidative and glycolytic properties but that indeed the fiber type profile changes since we could show the differences in the KO muscles using specific fiber type antibodies. In summary, what the macroH2A1 KO mice have are mediocre muscles: less oxidative or not as glycolytic as they should be. Additionally, the importance of myostatin in insulin resistance and T2D was also recognized (Hittel et al., 2010; Palsgaard et al., 2009). Whether there could be any correlation between the metabolic defects of macroH2A1 KO and possible plasma or muscle myostatin levels, is not clear.

And while for humans fiber type I is extremely important, one should take care when applying the same logics to mice. Mice have very few muscles with type I fibers, but have many with type IIb and type IIX. Therefore the changes we see in soleus could represent minority of the metabolic changes induced as opposed to the loss of type IIb fibers, which could have a more profound impact on the metabolism of these mice. We could not corroborate type IIx alterations in the KO muscles as we did not test specific antibody against it. Nevertheless, we could observe type IIa fibers improper increased occurrence in both soleus and tibialis. We also did not test the regenerated muscles fiber type profile but it would be interesting to see whether it gets even more impaired or the muscles manage to maintain at least approximately normal fiber type distribution.

Finally, we propose that macroH2A1.1 fine-tunes myoblasts/myotubes/muscles properties by priming them for the right metabolic responsiveness (Fig. 44).

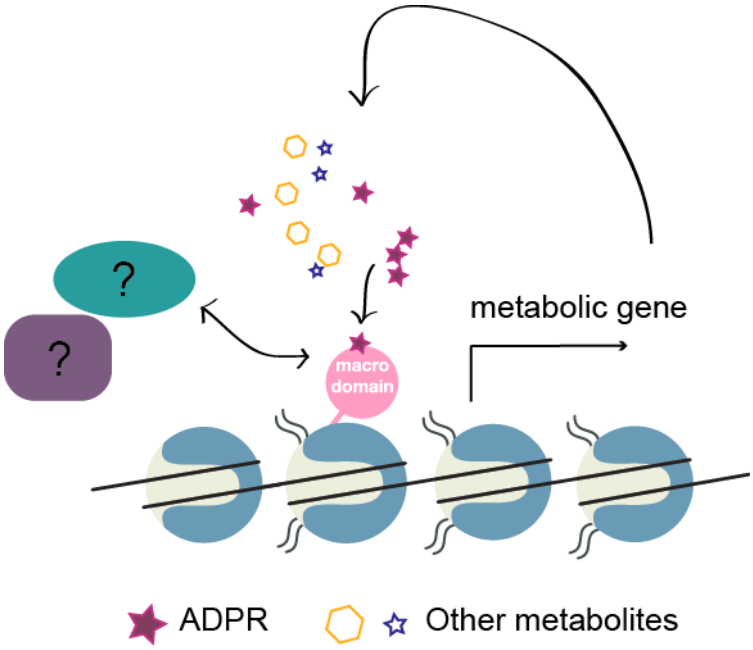

Figure 44. Hypothetical working model for metabolite-sensing macroH2A1.1 function in determining metabolic profile of a cell. MacroH2A1.1, upon incorporation into chromatin could bind to locally available ADPr or *O*AADPr. Through this binding macroH2A1.1 could sense the local environment and adequately regulate metabolic gene expression and define the metabolic profile of the cell. Other players possibly assisting in this metabolite sensing-dependent regulation of gene expression are still unknown.

FUTURE DIRECTIONS

While we have gained important new insight in macroH2A function in particular in the context of muscle, our results have allowed us to define new questions and hypotheses. Here I would like to suggest possible future directions that could be taken to further advance this exciting project.

1. To profound our knowledge on macroH2A1 KO phenotype using physiology methods such as use calorimetry to study whole metabolism. To challenge mice with different diets sich as high fat diet and to observe macroH2A1-dependent changes in fat metabolism such as ectopic fat accumulation. To use starvation and re-feeding protocols and acute exercise to study how KO mice can deal with energy stressed situations
2. In culture perform additional rescue studies comparing wild-type and pocket mutant transgenes in the context of changing metabolite concentrations to further clarify the contribution of the macroH2A1.1 binding pocket
3. Perform rescue experiment using macro1.1 domain stand alone transgene to see whether macroH2A1.1 depletion-induced changes depend on locus-specific chromatin incorporation and direct gene regulation or as a consequence of global nuclear metabolite binding
4. Perform rescue studies using macroH2A1.2 to determine whether macroH2A1.2 behaves like a loss-of-function of macroH2A1.1 in terms of metabolite-binding.
5. Determine whether altering the expression of macroH2A1 isoforms in aRMS cell lines improves their limited capacity to exit cell cycle and to differentiate. Whether macroH2A1 could serve in gene therapy of rhabdomyosarcoma, is still far fetched, but worth trying as rhabdomyosarcoma tend to be very devastating tumours with the worst outcome for the young patients.
6. To test bioenergetical potential of macroH2A1.2-deficient cells. We would argue that these cells would not exhibit the same metabolic defects, as macroH2A1.2 does not bind NAD+-derived metabolites. If macroH2A1.2 binds something else and some other relevant metabolites, remains a mystery, just as for macroH2A2.

SUMMARY OF RESULTS

In our study we aimed to elucidate the physiological function of metabolite-binding macroH2A1.1, an isoform of the histone variant macroH2A1 generated by alternative splicing. After identifying skeletal muscle as the tissue expressing highest levels of the isoform, we have focused our studies on myogenic differentiation and muscle-related functions. By analysing mouse and human myoblasts-derived immortal cell lines as well as primary muscle precursor cells and tissues from macroH2A1-deficient mice, we came to the following conclusions:

1. MacroH2A1 isoforms switch during myogenic differentiation. The non-metabolite binding isoform macroH2A1.2 is predominantly expressed in proliferating myoblasts and the metabolite-binding macroH2A1.1 in myotubes.
2. This physiological process is impaired in soft tissue cancer cells of myoblast origin.
3. During late differentiation macroH2A1.1 is required for proper fusion and myotube maturation. This process is only partially dependent on the integrity of the metabolite-binding pocket.
4. *In vivo* this is reflected by a reduced regeneration capacity in macroH2A1-deficient mice.
5. MacroH2A1.1 and macroH2A1.2 diverge in gene regulation. In myotubes macroH2A1.1 is required for proper activation of genes involved in adhesion, motility and Akt signalling, while macroH2A1.2 represses genes promoting fusion.
6. A subset of genes is shared by both macroH2A1 isoforms and includes muscle growth-related genes.
7. Loss of macroH2A1.1 alters the bioenergetic and metabolic properties of committed myoblasts.
8. Loss of macroH2A1.1 alters the relative expression of myosin heavy chain encoding genes that in muscle are markers of fiber types with different metabolic capacities. This change correlates with a change in the fiber type composition of muscles in macroH2A1-deficient mice.
9. MacroH2A1 KO mice show obvious fiber type profile shift, which might explain their metabolic phenotype.

ABBREVIATIONS

5mC = 5-methylcytosine
Acadm = medium chain acyl-CoA dehydrogenase, mitochondrial
Acetyl-CoA = acetyl Coenzyme A
AceCS2 = acetyl-CoA synthase 2
ActRIIB = activin receptor IIB
ADP = adenine diphosphate
ADPr = ADP-ribose
AMP = adenine monophosphate
AMPK = AMP-activated protein kinase
APLF = Aprataxin-PNK-like factor
AR = androgen receptor
aRMS = alveolar rhabdomyosarcoma
Ash2L = Set1/Ash2 methyl transferase
ATP = adenine triphosphate
Atp9a = probable phospholipid-transporting ATPase IIA
BDNF = bran derived neurotrophic factors
cADP = cyclic ADP
CELF1 = CUG triplet repeat binding protein 1
CD36 =fatty acid translocase
Cdh15 = cadherin 15
Cdhr1 = cadherin related family member 1
CDK8 = cyclin-dependent kinase 8
ChIP = chromatin immunoprecipitation
ChIP-seq = ChIP coupled to parallel massive sequencing
c-MET = hepatocyte growth factor receptor
CoxVb = cytochrome c oxidase subunit Vb
Cpt1a, b = carnitine palmitoyltransferase 1a,b
Cpt2 = carnitine palmitoyltransferase 2
CSA = cross-sectional area
Cycs = cytochrome c, somatic
Days P.I. = days post-injury
Ddx5/17 = dead box protein 5/17
DM = differentiation medium
DM1 = myotonic dystrophy 1
DNMT1 = DNA methyl transferase 1
DNMT3a = DNA methyl transferase 3a
DNMT3b = DNA methyl transferase 3b
ECAR = extracellular acidification rate
eMHC = embryonic myosin heavy chain
ES cells = embryonic stem cells
Esrra = estrogen-related receptor α
ETC = electron transport chain
Eto = Etomoxir, Cpt1 inhibitor
Ezh2 = enhancer of zeste homolog 2
FAs = fatty acids
Fabp3 = fatty acid-binding protein 3
FAD = flavin adenine dinucleotide
Fbxo32 = f-box only protein 32
FFA = free fatty acids
FGFR4 = fibroblast growth factor receptor 4
FOXO1/3 = forkhead box protein O1/3
Fst = follistatin
Fstl1 = follistatin-like 1

GC = gastrocnemius
Glut4 = glucose transporter type 4
GM = growth medium
GO = Gene Ontology
GOA = GO Annotation
GST = glycolytic stress test
GST = Glutathione S-transferase
GTPbp4 = nucleolar GTP-binding protein 1
HAT = histone acetyltransferase
HDAC = histone deacetylase
HFD = histone fold domain
HKMT = histone lysine methyltransferases
HKDM = histone lysine demethylase
hn-RNP-L = heterogenous nuclear ribonucleoprotein L
IDH1 = isocitrate dehydrogenase 1
IDH2 = isocitrate dehydrogenase 2
IGF-1 = insulin-like growth factor 1
IGF-2 = insulin-like growth factor 2
Il-4 = interleukin-4
Il-6 = interleukin-6
Il-7 = interleukin-7
iPS cells = induced pluripotent stem cells
Itga11 = integrin α11
JMJ = Jumonji domain
KAT = histone acetyl transferase
KO = knock-out
LC-MS/MS = liquid chromatography coupled to tandem mass spectrometry
LDH = lactate dehydrogenase
Lpl = lipoprotein lipase
LSD1 = lysine-specific demethylase 1
LSD2 = = lysine-specific demethylase 2
mADPRRyl / PARyl = mono(ADPr) or PARylated protein
MBNL1 = muscleblind-like splicing regulator 1
MBNL2 = muscleblind-like splicing regulator 2
MEF2 = myocyte enhancer factor-2
mH2A = macroH2A
MHC = myosin heavy chain
MRF4 = muscle-specific regulatory factor 4
Mstn = myostatin
MST = mitochondrial stress test
MT = myotubes
mTOR = mammalian target of rapamycin
Myf5 = myogenic factor 5
Myf 6 = myogenic factor 6
Myh = myosin heavy chain gene
MYOD/MYOD1 = myoblast determination protein (1)
Myog = myogenin
NA = nicotinic acid
NAD+ = Nicotinamide adenine dinucleotide
NADH = Nicotinamide adenine dinucleotide, reduced
NADP+ = Nicotinamide adenine dinucleotide phosphate
NADPH = Nicotinamide adenine dinucleotide phosphate, reduced
NAM = nicotinamide

NAMN = nicotinic acid mononucleotide
NAMPT = NAM phosphoribosyltransferase
NFATc2 = nuclear factor of activated T-cells, cytoplasmic 2
NMN = nicotinamide mononucleotide
NMNAT = NMN adenyltransferase
NR = NAM riboside
*O*AADPr = *O*-acetyl-ADPr
OCR = oxygen consumption rate
O-GlcNac = β–N-acetylglucosamine
P38 MAPK = p38 mitogen-activated protein kinase
PAR = poly-ADPr
PARG = poly(ADP)-ribose glycohydrolase
PARP1 = poly(ADPr)-ribose polymerase 1
PARP2 = poly(ADPr)-ribose polymerase 2
PAX3 = paired box protein Pax3
PAX7 = paired box protein Pax7
PDE = phosphodiesterase
Pdgfb = platelet-derived growth factor subunit β
Pdgfr = platelet-derived growth factor receptor β
Pdk4 = pyruvate dehydrogenase kinase, isoenzyme 4
PGC1α = peroxisome proliferator-activator receptor γ co-activator 1α
PI3K/AKT = phosphatidylinositol-4,5-biphosphate 3-kinase/Protein kinase B
PKM2 = pyruvate kinase M2
PRC1 = Polycomb Repressive Complex 1
PRC2 = Polycomb Repressive Complex 2
PRMT = protein arginine N-methyltransferase
PTB = polypyrimidine tract-binding protein 1
PTM = posttranslational modification
Q = quadriceps
Qki = protein quaking
qRT-PCR = quantitative PCR after reverse transcription
RbFox1= RNA binding protein fox-1 homolog 1
RbFox2 = RNA binding protein fox-1 homolog 2
RC = respiratory chain
RFLP = restriction fragment length polymorphism
RMS = rhabdomysoarcoma
ROS = reactive oxygen species
SAH = *S*-adenosylhomcysteine
SAM = *S*-adenosylmethionine
SC = satellite ells
SDH = succinate dehydrogenase
Serpina7 = serpin peptidase inhibitor, clade A (alpha-1 antiproteinase, antitrypsin), member 7
SIRT1 = sirtuin 1
Slc2a4 = solute carrier family 2, facilitated glucose transporter member 4
Sucnr1 = succinate receptor 1
Tbg = thyroid hormone-binding protein
TGFβ = transforming growth factor β
Thrsp = thyroid hormone responsive SPOT14 homolog gene
Tmem8c = protein Tmem8c (myomaker)
Trp = tryptophan
Trx = trithorax protein
TES = transcription end site

TSS = transcription start site
UDP-GlcNac = uridine diphosphate-GlcNac
T, TA = tibialis anterior
T2D = type 2 diabetes
TCA cycle = tricarboxylic acid cycle
TDCS = two distinct columns strategy
Tdh = threonine dehydrogenase
TET = ten-eleven translocation protein
Tmem171 = transmembrane protein 171
Trim63 = E3 ubiquitin-protein ligase Trim63
Vegfa = vascular endothelial growth factor A

MATERIAL AND METHODS

Mice and MacroH2A1 KO generation

As mice colony was maintained in Lyon, France, all the experiments on mice were approved by CREA Rhone-Alpes (France) committee. Mice were housed in cages standardly with littermates of the same sex. A 12 hours light-dark cycle was maintained and the animals were fed standard rodent chow diet (SAFE #A04-10 and SAFE #A03-10 for breeders; Perotech Sciences Inc., Toronto, ON, Canada).

To generate macroH2A1 knock-out (KO) mouse, exon 2 of the *H2afy* gene was replaced with the neomycin resistance cassette by homologous recombination in the E14.1 ES cells originated from 129/Ola strain. After the homologous recombinants were confirmed, two distinct ES clones baring one mutated allele were injected into the C57Bl/6 blastocyst and later transferred into pseudopregnant females. Of them, one clone resulted in having high-level chimeras and transmitting the mutation to further generations after crosses into C57Bl/6 strain (Boulard et al., 2010).

Cardiotoxin-induced muscle regeneration in vivo

Approximately 2 months old WT and macroH2A1 KO littermates, both females and males, were operated in order to inject cardiotoxin (Latoxan) into the muscles quadriceps, gastrocnemius and tibialis anterior of both hindlimbs. In details, mice were sedated with intraperitoneal injection of ketamine (50 mg/kg) and medetomidine (1 mg/kg) (both products provided by the PRBB Animal Facility, Barcelona). After they fell asleep, their legs were shawed, disinfected with Betadine (MEDA Pharma), a minimal cut on the skin was made and 50 µl of cardiotoxin of concentration 10^{-5} M (0,08 mg/kg) were injected per muscle per leg. 2-3 stitches were made at the place of the cut and mice were woken up by injection of Atipamezol (2 mg/kg, provided by the PRBB Animal Facility, Barcelona) intraperitonealy. During the whole procedure the animals were placed on an electrical blanket to keep their body temperature constant.

Cell culture and isolation of primary myoblasts

C2C12 mybolasts were obtained from Monica Suelves. The cells were grown in DMEM (Gibco) containing 20% FBS (Invitrogen) and 1% Penicillin-Streptomycin (Gibco) (GM, growth medium). Primary myoblasts were maintained in Ham's F10 (Gibco) medium complemented with 20% FBS (Invitrogen), 10 ng/ml of bFGF (Invitrogen), 0,1% Fungizone (Invitrogen), Penicillin-Streptomycin. For primary myoblasts maintenance, cell culture plates were coated with Rat tail collagen I (BD Biosciences) for 2h at 37ºC and afterwards washed

twice with PBS. For differentiation, cell culture plates were Matrigel treated (BD Biosciences) for 1h at 37ºC and washed with Ham's F10 medium. Differentiation medium (DM) for all cell cultures was DMEM supplemented with 2% Horse serum (Gibco) and Penicillin-Streptomycin. To induce differentiation, cells were washed once with PBS and DM was added. When time-course experiments were performed, fresh DM was added every 2 days. GP2 cells used for retroviral production were grown in DMEM containing 10% FBS and Penicillin-Streptomycin.

To isolate primary myoblasts, legs from WT and macroH2A1 KO mice were processed. All steps were performed at room temperature, except for the Pronase incubation (see below). All muscles from all limbs of a mouse were taken and fat and connective tissue were cleaned off. The muscles were cut in very small pieces and incubated with 1% Pronase (Calbiochem) and 25 mM Hepes of pH 7 for 1h at 37ºC in a water bath while shaking. After the incubation Pronase was removed by pelleting the digested muscle pieces and resuspending them in the medium containing serum. Digested muscle pieces were additionally disrupted by passing them through pipette and finally filtered through Steriflip Vacuum-driven filters (Milipore). The filtrate was spinned for 10' at 1400g and in the meantime Percoll (GE Healthcare), that has been put to shaking previously, gradient was prepared as followed: in a 15 ml falcon 1,5 ml of 60% Percoll was overlayed slowly and carefully with 11,5 ml of 20% Percoll. Correctly prepared gradient enables to visualise the border between the two different Percoll concentrations. Filtered and spinned cells were resuspended in fresh medium containing Penicillin-Streptomycin and without FBS. The resuspended cells were loaded onto the Percoll gradient and everything was spinned at 2000 x g for 25' without break. After centrifugation, a specific cloud of cells visible at the border of the two Percoll concentrations containing isolated primary myoblasts was collected and put in a separate 50 ml tube. PBS was filled in to wash off the Percoll by centrifugation at 900 x g for 15 min. Supernatant was removed, cells were resuspended in fresh growth medium and counted. Primary myoblasts are recognizable for their very round morphology and brightness. Cells were seeded onto corresponding collagen-coated plates and passaged as needed.

Table 3. Percoll Solutions Preparations

Percoll Concentration	Percoll Solution	PBS 10X	90% Percoll Solution	DMEM+P/S	Ham's F10+P/S
90%	9 ml	1 ml			
60%			3.3 ml	1.7 ml	
20%			6.6 ml		23.4 ml

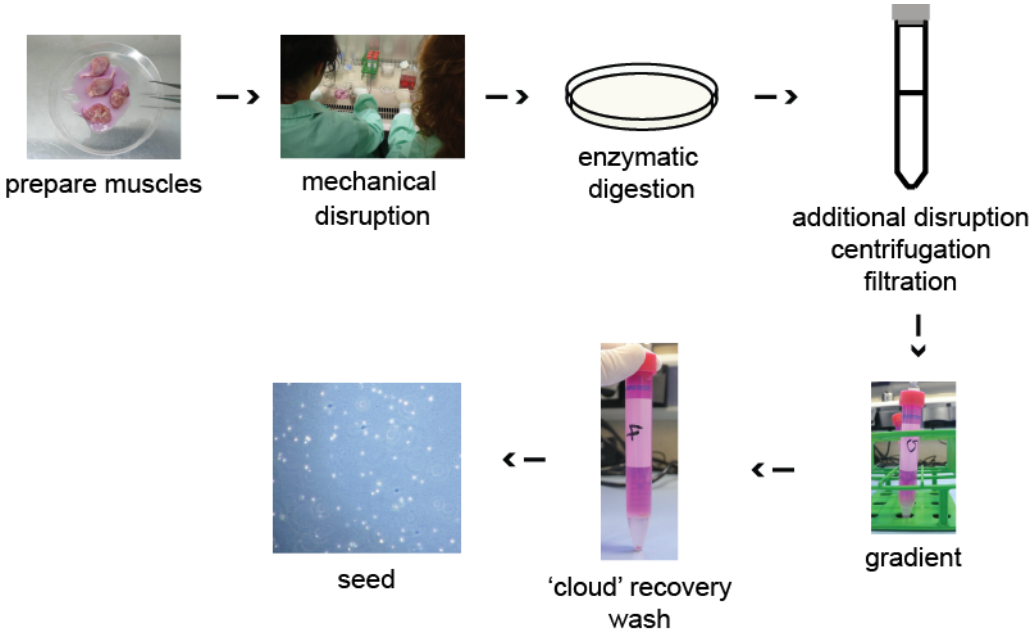

Figure 45. Schematic explanation of mouse primary myoblasts isolation.

Human primary myoblasts were kindly provided by Monica Suelves. Two primary cell lines, 13A and E3 were maintained in growth medium: DMEM (Biowhittaker), containing 10% FBS (Hyclone), 15 ng/ml of bFGF (Invitrogen), 10 ng/ml EGF and 1% insulin 1 mg/ml (Sigma-Aldrich) were added. Cells were grown on 0,1% gelatin (Sigma-Aldrich) coated plates. To wash the cells prior trypsinization, Hank's Balanced Salt Solution (HBSS, Gibco) was used. In order to differentiate the cells, they were seeded at high confluency and the medium was changes for DM (2% HS) containing 1% insulin 1 mg/ml (Sigma-Aldrich) the day after.

Alveolar rhabdomyosarcoma cell lines Rh30 and Rh4were kindly provided by Oscar Martinez Tirado, and were cultured at lower confluence in DMEM and RMPI (Gibco) medium supplemented with 10% FBS. For differentiation, the same DM as for mouse myoblasts was used.

Mouse embryonic stem (ES) cells were maintained in minimal medium supplemented with 10% of FBS (Hyclone), Penicillin-Streptomycin., 1% non-essential amino acids, 1% sodium pyruvate, 1% glutamax (all Gibco) and 0,2% β-mercaptoethanol, and grown on 0,1% gelatin coated plates. Leukemia inhibitory factor was produced in house from a plasmid and used a concetration of 1000u/ml to keep the cells self-renewing.

Antibody-containing hibridoma supernatant production

Both MF20 and F1.652 hibridoma cells were obtained from Pura Muñoz-Canoves, originally coming from Developmental Studies Hybridoma Bank.

MF20, anti-sarcomeric myosin heavy chain antibody production

Growth medium of MF20 hibridoma cells contained DMEM, 15% FBS, 1% Penicillin-Streptomycin and 1% of Hypoxantine (Sigma-Aldrich) and 1% of Thymidine (Sigma-Aldrich). Cells were grown in 20 ml containing suspension of growth medium in T-75 flasks, at the density of 0,2 – 1 X 10^6, until enough cells were produced. To induce antibody production, medium containing 2% FBS was used. Supernatant was collected 7-10 days after induction by spinning the medium and filtering it through 0.45 mm filters (Milipore). After testing it in WB and IHC or IF, the antibody-containing supernatant was aliquoted and stored at -80ºC.

F1652, anti-embryonic myosin heavy chain antibody production

F1.652 hibridoma cells were grown in DMEM supplemented with 10% FBS, 1% Penicillin-Streptomycin, 1% non-essential aminoacids (Gibco), L-glutamine (Gibco) and sodium-pyruvate (Gibco), in suspension in T-75 flasks. When enough cells were produced, they were seeded at the density of 0.8 – 1 X 10^6 and 2%FBS-containing medium was added to induce antibody production. After 7-10 days, the medium was centrifuged and filtered and the supernatant was tested by WB and IHC. Aliquots were stored at -80ºC.

Anti-macroH2A1 antibody purification

Bacterial culture was grown with 0,4 mM IPTG over night at 18 ºC in order to induce protein expression. The next day the bacteria were pelleted, lysed with lysis/wash buffer and lysozyme (Sigma-Aldrich), incubated on ice and additionally sonicated. After sonication, 1% of Triton X-100 was added and the lysate was incubated 20' on ice. The GST-protein-containing lysate was mixed with 500 μl of GSH-beads (Glutathione reduced beads, Amersham), previously blocked with 1% BSA (Bovine serum albumin, Sigma-Aldrich), for 2 h at 4 ºC on a rotating wheel. Beads were then poured into a 2 ml column (Thermoscientific) and lysate was passed 3 times in order to bind and retain GST-protein. Afterwards, the column was extensively washed (with 100 volumes) with the lysis/wash buffer containing 1% Triton X-100 and then with lysis/wash buffer alone. Once this was done, the cross-linking of the GSH-beads and GST-protein was perfomed. The GSH-beads bound to GST-protein first were taken out of the column, washed twice with 200 mM tri-ethanolamine pH 8,2, and then the cross-linking was performed during 30' using 20 mM di-methyl-pimelimidate (DMP, Sigma-Aldrich) in 200 mM tri-ethanolamine (Sigma-Aldrich). Afterwards, the fraction of not cross-linked GST-potein was removed using 15 mM reduced GSH (Sigma-Aldrich). Serum originating from the rabbit immunized with GST-macro1.2 fusion protein was centrifuged to remove debris, 0,05% Triton X-100 was added and incubated with the beads 2 h in a tube on a rotating wheel and afterwards the serum was

passed 3 additional time through the column to capture antibody on the the cross-linked GST-protein on the beads. For column washing, TBST (10 mM Tris, 135 mM NaCl, 0,05% Triton X-100) was used. In order to elute the bound antibody, 0,1 M glycine pH 2,5 was used. The antibody was collected into tubes containing 100 µl of 1 M Tris pH 8. Anti-GST antibody was purified out of the serum using GST-column. Five consecutive purifications were done using a pump each time to ensure more capture by constant serum flow through the column. We then proceeded to anti-macroH2A1.2 antibody purification. Importantly, this antibody recognizes both macroH2A1.1 and macroH2A1.2 proteins, as they differ in only 30 amino acids and the antibody was raised against the entire macro domain (more than 200 amino acids long). We performed 4 consecutive purifications using GST-macro1.2-column and also assured over-night flow through the column. The antibody was dyalyzed t PBS containing 20% glycerol (w/v, Sigma-Aldrich).

Table 4. Buffers used for anti-macroH2A1 antibody purification

Buffer	Composition
Lysis/wash	50 mM Tris-HCl pH 8 10 mM EDTA 150 mM NaCl 1 mM Leupeptine 1 mM PMSF
TBS	10 mM Tris pH 7,5 135 mM NaCl
TBST	TBS 0,05% Triton X-100

Plasmid constructs

Flag-tagged mouse macroH2A1.1 was cloned from C2C12 cells cDNA using specific oligos. The sequence of the cloned Flag-macroH2A1.1 was verified using pCMV specific oligos and the construct was cloned into pBabe puro backbone. The sequence was again verified using pBabe specific oligos. The G224E pocket-binding mutant was cloned by Stratagene site-directed mutagenesis starting from pCMV or pBabe Flag-macroH2A1.1.

Flag-tagged human macroH2A1.2 was cloned previously as described in (Buschbeck et al., 2009).

Transfection and retroviral infection

8 million of GP2 cells were seeded 4h prior to transfection in a P10 plate in 8ml of complete growth medium. When attached, the cells were transfected with 8 μg of desired retroviral construct and 3.6 μg packaging plasmid using the calcium-phosphate precipitation technique. Briefly, the plasmid DNA was mixed with 125 mM $CaCl_2$ and 1X HBS (2X HBS: 272 mM NaCl, 2,8 mM Na_2HPO_4, 55 mM HEPES; pH 7) in a total volume of 800 μl and when the whitish precipitates formed, the mixture was put onto the cells. Transfection efficiency was controlled checking the green signal of GFP-containing retroviral construct. This construct had no puromycin resistance gene so it also served as a selection control. If the GFP signal was present in more than 40-50% of the cells the day after transfection, 6ml of fresh medium was put on cells and they were left 48 h to produce viral particles.

For retroviral infection of myoblasts, C2C12 myoblasts were seeded the day prior to infection onto 6-well plates at the density of 10000 cells per well. 2 wells of a 6-well plate were infected with the viral supernatant coming from a single P10 plate mixed with ¼ of fresh medium and 8 μg/ml polybrene (Sigma-Aldrich).

Primary myoblasts were seeded 24-48 h prior to infection onto collagen-coated plates (10000 cells/well of a 6-well plate) or matrigel-treated plates (40000 cells/ well of a 6-well plate). The day of the infection, viral supernatant was filtered (0.45 mm, Milipore) and mixed with fresh medium as for C2C12 cells with the exception that polybrene was used at the concentration of 6μg/ml and that bFGF was adjusted to the total amount of virus-containing medium. C2C12 cells were centrifuged with added viral medium for 50' at 1000 x g and 32ºC. Primary myoblasts were centrifuged 45' at 800 x g and 32ºC. After centrifugation, plates were incubated 1,5h more in the incubator. After that, viral medium was replaced by fresh complete growth medium. As the infection efficiency was high (as followed by high GFP signal – usually 70% and more morning after infection), puromycin selection was always skipped for primary myoblasts. Infected primary myoblasts were either seeded for proliferation tests or differentiated directly on matrigel - treated plates adding DM when 70% confluency was achieved.

Retroviral infections of mouse ES cells to induce the knock-down of macroH2A1 were perfomed essentially as infections of myoblasts, with slight differences, as described earlier (Creppe et al., 2012). Cells were selected using 2mg/ml puromycin.

siRNA transfections

siRNAs used were described in Dardenne *et al.* (Dardenne et al., 2012) and ordered from Invitrogen. After verifying the knock-down effect and testing concentrations of siRNA to be used, 10 nM of siRNA was chosen as the concentration of siRNA that knockes down

satisfactorily and has no toxic effect on the cells. C2C12 myoblasts were counted and 25000 cells were seeded onto 6-well plates in 2ml of growth medium without antibiotics the day prior to siRNA transfection. For a well of 6-well plate, 500µl of OptiMEM (Gibco) was mixed with 0,5 µl of 50 µM siRNA. Lipofectamine RNAiMAX Transfection Reagent (Invitrogen) was added. After 20' of siRNA-Lipofectamine RNAiMAX mixture incubation the cells were transfected. The transfection mix was left on the cells for 24 h when GM was replaced for DM (not containing antibiotics) together with new siRNA transfection mix in order to ensure the knock-down effect during the whole course of myoblast differentiation. Fresh DM was added again with siRNA transfection mix every 2 days.

RNA isolation from cells and muscles and cDNA synthesis

Total RNA from cells was isolated using Invitrogen PureLink^{TM} RNA kit for RNA isolation. In brief, cells, just collected and washed well with PBS or previously collected and stored as pellets at -80ºC, were resuspended in 300 or 600 µl Lysis buffer containing 1% b-mercaptoethanol and passed through a sterile syringe 10 times. Equal volume of 70% ethanol was added and the mixture was vortexed thoroughly. The solution was loaded onto the column provided in the kit and RNA was bound onto the column by centrifugation at 12000 x g for 30'' at room temperature. The RNA was sequentially washed with Wash buffer I and twice with Wash buffer II containing ethanol, provided as well in the kit. Last spin was performed in order to remove the ethanol possibly left on the column. Elution was done using RNase-free water supplied in the kit. Elution volume was determined as a function of initial cell number used for RNA extraction.

For extracting RNA from muscles, mortar in liquid nitrogen and pestle were used in order to pulverize the muscle. From there, small part was separated for total DNA extraction, while the rest of the sample was used to extract RNA using the kit mirVana miRNA Isolation kit (Invitrogen), as it includes a Phenol/Chlorophorm extraction step that ensures a better conservation of RNA and break down of cell components. To extract RNA from primary myoblasts and primary myotubes PureLink RNA Mini kit was used, as it has smaller columns more adequate for low cell number samples. DNase-treatment (Invitrogen) of the samples was performed on the column after the first Wash I buffer wash. As recommended by the manufacturer, DNase mix was prepared using 10 µl of DNase, 8 µl of 10X Reaction buffer and 62 µl DEPC-treated water. 80 µl of DNase mix were left on the column for 10' and later on additional Wash I buffer wash was performed. The protocol was continued as above described.

Concentration and quality of extracted RNA was checked on Nanodrop (Thermoscientific).

Usually, 1 µg of RNA was used for cDNA synthesis using the First strand cDNA synthesis kit (Fermentas), according to the manufacturer's instructions. Shortly, 1 µg of RNA was mixed with 1 µg of oligo(dT) and nuclease-free water until the volume of 11 µl. This was incubated 5' at 65 ºC in the thermocycler. 4 µl of 15X Reaction buffer, 1 µl of RiboLock RNase Inhibitor, 2 µl of dNTP mix and 2 µl of M-MMLV Reverse Transcriptase were added to the RNA-oligo(dT) mix and the entire mixture was incubated 1h additionally at 37 ºC followed by a termination heating at 72 ºC for 5'.

Transcriptomics Analysis

C2C12 myoblasts were seeded and transfected with macroH2A1.1 siRNA as described above. Cells were collected at day 4 of the differentiation, washed well with 1X PBS and stored as pellets at -80ºC. Experiment was repeated for more than 6 times. Once all the pellets were collected, RNA was extracted at once and aliquots of RNA were made. A small aliquot was used to transcribe the RNA into cDNA using the oligo(dT) (as above described) and the knock-down of macroH2A1.1 was tested in all biological replicates. 4 experiments with most successful macroH2A1.1 knock-down were selected, RNA was quantified and quality was checked performing Eukaryote Total RNA Nano assay by our Genomics facility (run by Lauro Sumoy, IMPPC). RNA was amplified and loaded onto the microarray slide Agilent SurePrint G3 Mouse GE 8x60K Microarray. Bioinformatical analysis was performed by Roberto Malinverni from the Marcus Buschbeck laboratory.

Data analysis and statistics

Bioinformatical analysis was mostly performed by Roberto Malinverni from the Buschbeck laboratory. To detect the genes differentially expressed LIMMA was used (Smyth, 2004). The differentially expressed genes were selected with a cut-off of a q-value of 0,05 calculated after false discovery rate (FDR) correction. The Gene Ontology analysis was performed using R. package "ChIPpeakAnno" (Zhu et al., 2010), using p-value of 0,01 like maximally significant, and 30 like minGOterm (minimum count in a genome for a GO term to be included). A Boferroni multiple hypothesis testing adjustment was finally applied to adjust the enrichment result. REVIGO online software was used to summarize gene ontologies after initial Gene Ontology analysis (Supek et al., 2011).

The reads obtained by ChIP-Seq for macroH2A1 and Input samples were cleaned based on the quality and trimmed using Sickle (Joshi, 2011) and Cutadap (Martin, 2011), and aligned with the mouse genome (NCBIM37/mm9) using Bowtie (Langmead et al., 2009) version 0.12.7.

Two mismatches were allowed for the alignment within the seed and only reads mapping to a single position in the genome were used. To detect genomic regions enriched for multiple overlapping (broad peaks) SICER software version 1.4.1 was used (Zang et al., 2009). For macroH2A1 peaks calling a p-value cut-off of 1 x 10-5 and a FDR of 5% were used, while parameters of window and step were set on 1000 and 3000, respectively, as described in the paper. Genes were considered target genes if a peak was found in the gene body or on the 5' at distance of 3kb to TSS, or at 3' at a distance fo 3kb to TES. The annotation of the peaks was performed using ChIPpeakAnno package (Zhu et al., 2010). The enriched profile around gene body was calculated using ngsplot version 2.0 (Shen et al., 2014).

Data were represented as mean ± standard deviation. Student t-test or Wilcoxon test (as indicated) were used to calculate statistical significance.

Semi-quantitative Reverse Transcriptase Polymerase Chain Reaction analysis (qRT-PCR)

cDNA was used directly or diluted up to 10 times in order to perform the semi-quantitative RT-PCR analysis. A mix containing 5 µl SybrGreen (Roche), 0,5 µl of forward and 0,5 µl of reverse oligo (stock at 10 µM) and 2 µl of Milli Q water was mixed with 2 µl of cDNA in a well of 96-well plate. Each sample was analyzed in duplicate. Milli Q water was used as the negative control. Single product amplification was controlled doing the standard curve. Relative expression was represented as concentration ratio of the gene of interest and average of 2 housekeeping genes. When analysing *macroH2A1.1* and *macroH2A1.2* relative expression, the samples were normalized also by a reference sample containing equimolar ratios of amplicons of *macroH2A1.1* and *macroH2A1.2*. Oligo amplification efficiency and amplicon length were taken into account when preparing the reference sample. In that way we could observe the direct ratio of both splicing isoforms in a specific sample and on the same scale. The same was done for *macroH2A1* and *macroH2A2* relative expression.

Oligos for qRT-PCR were designed in order to span different exons so that by controlling the size of the amplicon genomic DNA contaminations can be avoided. Previously published oligos by us or other labs are also listed and the original publication is pointed out. All oligos were ordered desiccated and resuspended for the stock to be at final concentration of 100 µM. For qRT-PCR analysis, oligo stocks were at 10 µM and the final concentration in the SybrGreen mix was 0,5 µM. All oligos were checked for single product amplification and efficiency doing the standard curve and running the product on 1% agarose gel.

Table 5. qRT-PCR reaction conditions.

Reaction	Temperature/ºC	Duration	Cycles
Preincubation	95	8’	1
Amplification	95	10’’	45
	60	20’’	
	72	15’’	
Melting curve	95	15’’	1
	65	1’	
	96	endless	
Cooling	40	30’’	1

Restriction Fragment Length Polymorphism (RFLP)

Restriction Fragment Length Polymorphism was used in order to qualitatively assess the amount of macroH2A1 isoforms in different samples used. Essentially, cDNA obtained from RNA was used directly to perform the PCR reaction using oligos specifically annealing on exon 5 and exon 8 of the *macroH2A1* gene.

Table 6. RFLP Reaction mix.

Reagent	Final quantity or concentration/reaction
cDNA	25 ng
Oligo F 10 µM (exon 5)	0,1 µM
Oligo R 10 µM (exon 8)	0,1 µM
dNTPs (25 mM each)	250 mM
Reaction buffer 10X with 25 mM Mg^{2+}	1X
HotMaster *Taq* DNA Polymerase 5PRIME (5 units/µl)	1,25 U

Once the PCR reaction was done, 20µl of the product was taken and digested with 1 µl of HpaII (MspI, ThermoScientific) restriction enzyme in 1X Tango buffer (Fermentas) for 2 h at 37ºC. The digested product was run on 2% agarose gel (agarose, Condalab, dissolved in 1X TE) for 55’ at the speed of 90V.

Table 7. PCR reaction conditions.

Reaction	Temperature/ºC	Duration	Cycles
Initial Melting	94	2’	1
Melting	94	20’’	35
Oligo Annealing	60	10’’	
Amplification	65	20’’	
Termination	65	5’	1
Hold	16	endless	1

Proliferation assay

Primary myoblasts coming from WT and macroH2A1 KO mouse and from rescue experiments were assayed for proliferation. 10000 cells per plate were seeded onto 6-well plates previously coated with collagen in GM and left to grow for 72h. Fresh GM was added every 2 days. Cells were counted at 24, 48 and 72 h with Scepter (Milipore) cell counter and the results are represented as growth curves. 2 pairs of WT-KO female and 2 pairs of male primary myoblasts were tested in 2 independent experiments for each WT-KO pair.

Immunohistochemistry and Fusion assays

100000 and 40000 cells of primary myoblast cultures were seeded either on Matrigel-coated 6-well or 12-well plates, respectively, in GM that was replaced for DM the next day. Cells were monitored, fixed in 3,7% formaldehyde (FA) (Sigma-Aldrich) at the point of terminal differentiation or as stated elsewhere, washed well with 1XPBS and stained immediately or stored at 4ºC in 1X PBS containing 0,05% sodium-azide (Sigma-Aldrich). After fixation and washing, cells were permeabilized with 0,3% Triton X-100-containing PBS for 15’ at RT and blocked with 100% FBS during 30’ at RT. Afterwards the cells were stained with eMHC antibody (F1.652 neat hybridoma supernatant produced as stated above) and subsequently washed in 0,2% Tween-containing PBS and stained with anti-mouse secondary antibody coupled to Horse Radish Peroxidase (HRP) diluted in Tween-containing PBS diluted (DakoCytomation). Diaminobenzidine substrate (DAB, Sigma-Aldrich) was dissolved in PBS and 30% H_2O_2 (Sigma-Aldrich) was added. The substrate mix was then added onto cells and staining reaction was stopped after few minutes with distilled water. Photos of the cells were taken with the Leica DMI6000B microscope (Leica) and differentiation and fusion index were assessed. Differentiation index was represented as the ratio of nuclei in eMHC-positive cells and total nuclei analysed. Fusion was checked and fusion index was determined for each

experiment. In order to obtain the average number of nuclei per myotube, myonuclei were counted in all myotubes. Approximately the same number of nuclei was counted in conditions that were compared. Relative maximal diameter was measured using ImageJ program and defining the maximal diameter as the widest part of the myotubes, measuring it perpendicularly to the myotube axis.

C2C12 cells, seeded on 6-well plates at density of 150000 cells per well, were fixed at different time points with 3,7% FA and afterwards washed well with 1X PBS. Staining was performed as with primary myoblasts.

The details on antibodies and concentrations used are listed in the **table X**.

Table 8. List and composition of solutions used for Immunohistochemistry.

Buffer	Composition
Permeabilization buffer	0,3% Triton X-100 in 1X PBS
IHC Wash buffer	0,2% Tween (Sigma-Aldrich) in 1X PBS
DAB substrate buffer	0,67 mg/ml DAB 0,024% H_2O_2

Muscle histology, histochemistry and immunohistochemistry

Histology

Muscles of WT and macroH2A1 KO mouse were collected at different time points, immediately after the animals were sacrificed, snap-frozen in liquid nitrogen and stored at -80ºC until use. For Haematoxylin and Eosin (H&E) staining, transversal sections of muscles 10 μM thick were prepared and stained to assess the general histology of the muscles during cardiotoxin-induced muscle regeneration. Hematoxylin stain Gill's 2 (Sigma-Aldrich) was used as manufacturer advised. The 0,1% Eosin Y Phloxine B (Sigma-Aldrich) solution was used. The muscle sections were stained 1' in hematoxylin and then washed extensively with tap water until the water was clear. Then, eosin staining of 5' was performed and afterwards the sections were rinsed in 75% ethanol and twice in absolute ethanol. Finally, muscle sections were dehydrated passing twice through absolute ethanol and cleared in xylene twice. Finally, the sections were mounted.

Table 9. List and composition of solutions necessary for H&Estaining.

Buffer	Composition
Hematoxylin stain Gill's 2	**purchased**
0,1% Eosin Y Phloxine B	purchased; in acidified ethanol

Histochemistry

For histochemical stainings muscles were cut and the staining were performed immediately, without freezing the sections.

Succinate dehydrogenase (SDH) staining was performed on freshly cut snap-frozen muscles samples. Essentially, muscle cuts of 10μM of both WT and macroH2A1 KO mouse were put on the same glass slide to avoid staining difference between slides. The cuts were incubated in Incubation solution of pH 7.2-7.6 containing Nitroblue tetrazolium (Sigma-Aldrich) for 1h in a dark wet chamber at 37ºC. After the incubation, cuts were washed quickly 4 times in distilled water and afterwards passed through acetone of different concentrations (30%, 60%, 30%, 30'' each). 4 quick washed with distilled water were done again and afterwards the cuts were dehydrated and mounted. Samples were analysed on Leica DMI6000B microscope and Leica M80 lupa (Leica).

Table 10. List and composition of solutions necessary for SDH staining.

Buffer	Composition
0,2 M phosphate buffer pH 7,4	0,2 M KH_2PO_4 0,2 M Na_2HPO4
0,2 M succinic acid	Succinic acid, anhydrous crystalline disodium salt
0,2% Nitroblue tetrazolium (Nitro-BT)	Nitroblue tetrazolium 98%
Incubation solution	50 mM succinic acid 50 mM phosphate buffer 0,1% Nitro-BT

Immunohistochemistry

Immunostainings using monoclonal antibodies against type I (A4840), type IIa (A474) and type IIb (BF-F3) fibers were performed on muscle sections in controlled conditions using Ventana UltraView Universal DAB machine, property of the Hospital Universitari Germans Trijas i Pujol (Can Ruti, Badalona), with the help of the technician Maria Angela Fernandez. Prior to the staing procedure in the Ventana machine, muscle sections were fixed in cold 100% acetone at RT for 10'. After the staining the samples were dehydrated in ethanol as stated above and mounted. The details on antibodies and concentrations used are listed in the Table 14.

Protein Analysis

C2C12 cells were collected and washed well with 1XPBS. They were either processed directly or the cell pellets were stored at -80ºC until use. Cell pellets were lysed in 100µl WB lysis buffer containing 0,5% SDS and additionally sonicated (Diagenode). After the lysis protein concentration was determined using BCA Protein Assay Kit (ThermoScientific) and reading the absorbance at the spectrophotometer SPECTRAmax 340PC (BioNova). Equal quantities of samples were loaded onto polyacrilamide gels. Samples were run for necessary time in the polyacrilamide gels and then transferred to nitrocellulose membrane (Whatman, GE Healthcare) at 220 mA during a minimum of 1 h. Once the transfer was over, the membranes were blocked using 5% non-fat milk (Nestle) in TBST during minimum of 15 min. Membranes were incubated with primary antibody over night and day after, after extensive TBST washing, the membrane was incubated in appropriate secondary-HRP conjugated antibody (DakoCytomation) for 1h at RT while shaking. After this incubation, membranes were again well washed in TBST and ThermoScientific chemiluminescent reagent mix in 1:1 ratio was used to incubate the membrane for 1 minute. Incubated but dried membrane was overlayed with the photohgraphic film (GE Healthcare). The film was usually exposed for a time interval of few seconds to few minutes. Long exposures of the films were almost always avoided. After exposure the film was developed with the FujiFilm FPM-100A developer.

Table 11. List and composition of solutions used for Protein Analysis.

Buffer	Composition	Working concentration
WB Resolving buffer 4X pH 8,8	1,5 M Tris 0,4% SDS,	1X
WB Stacking buffer 4X pH 6,8	500 mM Tris 0,4% SDS,	1X
WB Running buffer 10X	250 mM Tris 2 M Glycine 10 g/l SDS	1X
WB Transfer buffer 10X	250 mM Tris 1,92 M Glycine	1X
TBST wash buffer 10x	140 mM NaCl 250 mM Tris 27 mM KCl	1X
Blocking 5% milk in TBST	5% Non-fat (Nestle) milk dissolved in 1X TBST	
WB Total lysis buffer	ChIP Elution buffer (see **table X**) diluted 1:1 in water	
Laemmli buffer 5X	250 mM Tris HCl pH 6,8 50% Glycerol 10% SDS	1,25-2X

	14,3 M b-mercaptoethanol 0,05% Blue Bromphenol	
10% NaN3	10% sodium-azide	0,05%
Ponceau	0,5% Ponceau S dissolved in 1% acetic acid	reusable

Table 12. Gel concentrations and compositions used for WB Resolving gels.

Resolving gels	8%	10%	12%	14%
Acrylamide 30% (BioRad)	2,6 ml	3,3 ml	3,89 ml	4,6 ml
WB Resolving buffer 4X pH 8,8	2,5 ml	2,5 ml	2,5 ml	2,5 ml
H20	5,2 ml	4,5 ml	3,91 ml	3,2 ml
APS 10% (Sigma-Aldrich)	80 µl	80 µl	80 µl	80 µl
TEMED (Amresco)	8 µl	8 µl	8 µl	8 µl

Table 13. Gel concentrations and compositions used for WB Stacking gel.

Stacking gel	4%
Acrylamide 30% (BioRad)	0,5 ml
WB Stacking buffer 4X pH 6,8	360 µl
H20	2,1 ml
APS 10%	30 µl
TEMED (Amresco)	3 µl

Table 14. List of antibodies and concentrations used.

Antibody	Supplier	Working concentration
macroH2A1	Homemade	1:1000
macroH2A1.1	Provided by Andreas Ladurner Laboratory, Homemade	1:1000
macroH2A1.2	Provided by Andreas Ladurner Laboratory, Homemade	1:500
macroH2A2	Homemade	1:1000
eMHC (F1.652)	Provided by Pura Muñoz-Canoves	Supernatant directly
Sarcomeric MHC (MF20)	Provided by Pura Muñoz-Canoves	Supernatant directly
MyoD	Santa Cruz	1:1000
Myogenin (F5D)	Santa Cruz	Supernatant directly
H3	Abcam	1:5000
Secondary anti-mouse-HRP conjugated antibody	DakoCytomation	1:3500

Secondary anti-rabbit-HRP conjugated antibody	DakoCytomation	1:3500
A4840 (fibers type I)	Provided by Pura Muñoz-Canoves	1:100
A474 (fibers type IIa)	Provided by Pura Muñoz-Canoves	1:100
BFF3 (fiber type IIb)	Provided by Pura Muñoz-Canoves	1:100

Chromatin Immunoprecipitation (ChIP) and ChIP-Sequencing

Chromatin Immunoprecipitation was performed on proliferating C2C12 myoblasts and terminally differentiated myotubes (day 4 after changing to DM) in cultures. To use only fully differentiated and fused myotubes, 4 days after switching the fully confluent C2C12 myoblasts to DM, the cells were washed of with PBS and 4ml of 1X Trypsin (Gibco) was used to separate the fully differentiated and fused myotubes from non-fused cells. Trypsinisation was done extremely fast (less than 20 sec) in order to avoid myotube damaging and enriched myotubes were collected in excess of FBS-containing medium in order to inactivate trypsin. Enriched myotubes were then fixed with 1% FA in suspension during 10' at RT on a rotating wheel. The time of fixation was controlled and the reaction was quenched with 0,125 M glycine during 5' also rotating on RT. After quenching, the myotubes were well washed with 1X PBS and stored at -80ºC. Proliferating C2C12 myoblasts were fixed in plates shaking with 1% FA during 10' at RT. The reaction was quenched as for enriched myotubes and the cells were extensively washed and stored as fixed pellets. Special High-clarity Polypropylene Conical blue tip 15ml falcons (BD Falcon) were used to store pellets as the sonicator tips (Diagenode) fit well on those tubes. To proceed with the chromatin immunoprecipitation, pellets were thawed on ice and extraction of nucleis was initiated by resuspending softly (without vortexing and strong pipetting up and down) the cells in Lysis buffer I containing PMSF and Leupeptin (both purchased from Sigma-Aldrich) (see table 15. further down) and left 10' on ice. Lysed cells were spinned at 5000 x g for 5' at 4ºC. Supernatant was discarded and nuclei were resuspended in Lysis buffer II containing PMSF and Leupeptin. After 10' incubation on ice, nuclei were completely disrupted by sonicating the samples 10' using Bioruptor sonicator (Diagenode). After sonication the samples were briefly centrifuged to remove debris. A small volume was taken out to check the size of the sheared chromatin: the aliquot was mixed with Lysis buffer 2, IP dilution buffer, Proteinase K (Sigma-Aldrich), $CaCl_2$ and NaCl and shaken over night at 65ºC. The next day Phenol/Chlorophorm (Sigma-Aldrich) extraction of DNA was performed: 1 volume of Phenol/Chlorophorm mix was added to the aliquot mix, vortexed thoroughly, spinned 5' at 5000

rpm and afterwards the upper phase containing DNA was recovered and the DNA was precipitated adding 3 volumes of absolute ethanol and 0,1 volume of 3 M sodium acetate. After 20' of incubation at -20ºC, the samples were spinned, washed with 70% ethanol, dried and resuspended in 75 µl of water. Concentration was determined and 2 µg of sample was run on the 1% agarose gel to check the size of the sheared chromatin. 35 µg of sheared chromatin were used for each IP reaction and diluted with 9 volumes of IP dilution buffer. All samples were incubated with antibodies in the same volume, as Lysis buffer II was used to adjust the volumes. Samples were precleared with 20 µl of pre-blocked (in 1% BSA for 30' rotating at 4ºC) slurry Ab binding beads (Diagenode, not blocked with any DNA) for 2h at 4ºC rotating. From precleared lysates input sample was taken (10% of the total volume) which was stored until later at 4ºC and to the rest of the lysate 3-5 µg of specific antibody were added. To pull down the chromatin fraction enriched for specific antibody, samples were rotated for 2h or over night (o/n) at 4ºC. The following day the capture with beads was performed by rotating during 2h at 4ºC using the same beads. Beads were spun down and washed twice with each of these buffers in this order: Mixed Micelle wash buffer, LiCl/Detergent wash buffer, Buffer 500. First wash was quick and the second was up to 5' rotating on a wheel at RT. Finally a quick wash with TE buffer was performed. Enriched chromatin was eluted with elution buffer and additional vortexing. After two elutions, reverse cross-linking was performed using NaCl at a final concentration of 200 mM and shaking the samples o/n at 65ºC. The next day the samples were digested with Proteinase K in a solution of EDTA and Tris pH 6,5 for 3h at 45ºC. To the digested samples 1 volume of phenol/chlorophorm was added and the upper phase was recovered, which was mixed with another volume of Chlorophorm (Sigma-Aldrich). Again the aqueous upper phase was recovered and the enriched DNA was precipitated including glycogen, 3 volumes of absolute ethanol and 0,1 volume of 3 M sodium acetate. After -20ºC incubation, DNA was pelleted, washed with 70% ethanol and dried. The DNA was finally resuspended in 50 µl of water. The precipitated DNA was analyzed by qRT-PCR using input diluted 1/50 to normalize directly loaded IP samples.

For Chip-sequencing, DNA was enriched by ChIP and quantified using Qubit™ dsDNA HS Assay (Invitrogen). 20 ng of enriched DNA was used for library generation and direct massive parallel sequencing on Illumina Genome Analyzer at the EMBL facility, Heidelberg.

Table 15. List and composition of solutions necessary for ChIP.

Buffer	Composition
FA solution	11% FA in 1X PBS
1,25 M Glycine	dissolved in 1X PBS
Lysis buffer I	5 mM PIPES pH 8

	85 mM KCl 0,5% NP-40 1 mM PMSF 50 µg/ml leupeptin
Lysis buffer II	1% SDS 10 mM EDTA pH8 50 mM TRIS pH 8.0 1 mM PMSF 50 µg/ml leupeptin
IP dilution buffer	1% TRITON X-100 150 mM NaCl 2 mM EDTA pH8 20 mM TRIS pH 8.0 1 mM PMSF 50 µg/ml leupeptin
Mixed Micelle Wash buffer	150mM Final 20 mM Tris-HCl pH 8.1 5 mM EDTA pH 8.0 5% sucrose (w/v) 0,02% NaN_3 1% Triton X-100 0,2% SDS
LiCl/detergent wash	0,5% deoxycholic acid (w/v) 1 mM EDTA 250 mM LiCl 0,5% NP-40 (v/v) 10 mM Tris-HCl pH 8.0 0.2% NaN_3
Buffer 500	0.1% deoxycholic acid (w/v) 1 mM EDTA 50 mM HEPES, pH 7.5 500 mM NaCl 1% Triton X-100 (v/v) 0,2% NaN_3
Elution buffer	1% SDS 100 mM $NaHCO_3$
0,5 M EDTA pH 8	
1 M Tris pH 8	
10% BSA (BioRad)	BSA dissolved in 1X PBS
1X PBS pH 7,4	136 mM NaCl 2,7 mM KCl

Phenotype Microarrays

Phenotype microarray experiments were performed following protocols provided by Biolog Inc. Essentially, C2C12 myoblasts were seeded as for transcriptomics anaylsis with the exception that 48h after the first siRNA transfection, cells were trypsinized, counted and resuspended in Biolog MC-0 medium (IF-M1 medium 50 ml, Pen/Strep 1,1 ml, 80 µl l-Glutamine, 2,65 ml

FBS) and seeded at density 10000 cells per 50 µl per well onto Biolog Phenotype MicroArrays™ plates PM-M1 and PM-M2 (Biolog Inc) that were calibrated at RT over night, both conditions in duplicate. Cells were incubated in a normal cell culture incubator. Part of the cells was stored to check the efficiency of the knock-down. The next day 10 µl of Redox Dye Mix (Biolog Inc) was added very quickly to each well and the plate was put in the plate reader. Two absorbencies were read – 590 nm and 750 nm. First reading was performed immediately after Redox Dye Mix adding and the next read were performed at 4h post-adding the Redox Dye Mix. After 4h in the wells containing positive control (a-*D*-glucose) the reaction was saturated as the colour was intense dark purple. The calculations were done as following: the second absorbance was used as the background and was subtracted from the values of A590. All values were normalized for (divided by) the average of the positive control, D-glucose, of the control cells. To represent the differences, values obtained from the control cells were deducted from the macroH2A1.1 knock-down values.

Oxygen Consumption and Extracellular Acidification Rate Measurements and FAO Assay

Analysis of oxygen consumption (OCR) and extracellular acidification (ECAR) rates was performed using a Seahorse XF96 Flux Analyzer (Seahorse Bioscience). In details, C2C12 myoblasts were treated as for Phenotype MicroArrays. 24h post-siRNA transfection cells were seeded into 2 XF 96-well cell culture microplates and incubated over night in a normal CO_2 containing incubator. On the next day, two different tests were performed: Mitochondrial Stress Test (MST) and Glycolytic Stress Test (GST). For MST, the normal medium of the cells was replaced with 90 µl of minimal medium containing 0,2% FBS, 25 mM glucose, 1 mM Hepes, Penicillin/Streptomycin, L-Glutamine (it is important not to add any buffering agent so the pH can change according to the possible metabolic changes of the cells). The plate was incubated for 2h at 37ºC in a $C0_2$ free incubator before starting the experiment. In the meantime different compounds were loaded onto the sensor cartridge: at the position A oligomycin, position B FCCP, position C Rotenone/Antimycin A mix, position D normal minimal medium; 30 µl in the drug injection port of each well. Following instrument and cartridge calibration, the XF microplate together with the sensor cartridge was loaded into the XF Analyzer to record oxygen consumption as well as extracellular acidification rates. The measurement protocol consisted of 5 loops of 4 min mixture and 5 min OCR/ECAR measurement times for each of the component added to the microchamber. At the end of the assay, 20 µl of Proteinase K (10 mg/ml) was added to the media and left over night. The following day 180 µl of GelDye mix (Biotrium, 3 µl of GelDye per 100 ml of PBS) was added to the digested microplate content, the whole solution

was mixed and 50µl of it was transferred to a transparent black walls 96-well plate and absorbance was read (533 nm excitation, 590 nm emission) to quantify the DNA and adjust for potential differences in cell densities. To perform the GST, a minimal medium was prepared as for MST but containing no glucose. Cells were incubated with this minimal medium (in starvation conditions) for 2h. In the meantime the sensor cartridge was prepared loading two compounds - glucose and 2-deoxy-glucose – and afterwards calibrated. To record the OCR and ECAR, total measurement protocol was following: 5 loops of 4 min mixture and 5 min measurement for each component added. To quantify the DNA, the same procedure as for MST was employed.

Fatty acid oxidation assay (FAO) was performed also as indicated in the technical leaflet. 24 –h post-siRNA transfection the C2C12 cells were seeded onto XF 96-well plate. 24 h prior the assaying, the medium of the cells was replaced for substrate-limited medium (DMEM containing 0,5 mM glucose, 1 mM glutamax, 0,5 mM carnitine and 1% FBS). 45' prior the assay, the cells were washed twice with the FAO medium (111 mM NaCl, 4,7 mM KCl, 1,25 mM $CaCl_2$, 2 mM $MgSO_4$, 1,2 mM NaH_2PO_4 supplemented with 2,5 mM glucose, 0,5 mM carnitine and 5 mM HEPES at pH 7,4).FAO assay medium was added to the cells (135 µl) and incubated in CO_2-free incubator for 45'. In the meantime assay cartridge was loaded with the same compounds as for the MST. Shortly prior the assay (15'), 15 µl of 400 µM Etomoxir (Eto) or vehicle were added to corresponding wells, to allow Eto uptake and binding to Cpt1. Just prior to starting the assay, XF Palmitate-BSA FAO Substrate or just BSA was added to the appropriate wells (30 µl/well). To record the OCR and ECAR, total measurement protocol was following: 5 loops of 4 min mixture and 5 min measurement for each component added. To quantify the DNA, the same procedure as for MST was employed.

Targeted metabolomics

For mass spectrometry analysis of the metabolites composition in proliferating myoblasts and differentiated myotubes, the samples were normalized by the nuclei number. Of the original sample sent to mass spectrometry, 10% was taken out. To count the nuclei in each sample, Hoechst 33342 staining was performed. From stock solution of 10 mg/ml (Molecular Probes, Invitrogen, provided by IGTP Flow Cytometry Facility) using 1X PBS, a solution of 5 µg/ml concentration was prepared and kept in dark. When needed, the 5 µg/ml solution was further diluted with PBS to obtain 1 µg/ml working solution. A triplicate of proliferating myoblasts pellets and a triplicate of differentiated myotubes was resuspended in Lysis buffer I (see Table 15.), using additionally syringe to break down well the myotubes. After spinning, the isolated nuclei were resuspended in 1 µg/ml Hoechst 33342 working solution and a 37ºC incubation

followed for 20'. The samples were protected from light all the time. Incubated samples were mixed with 100 µl of Perfect-Count Microspheres (provided by IGTP Flow Cytometry Facility) and passed through the flow cytometer. The number of nuclei per volume in each sample was calculated by the formula:

$$\text{Absolute count (cells/µl)} = \frac{\text{Number of cells of the target subpopulation counted}}{\text{Total number of microspheres counted}} \times \text{Num of Perfect-Count/µl (specified by manufacturer)}$$

The rest of the sample was processed to perform Liquid chromatography-MS/MS analysis. The metabolites of interest included metabolites of NAD+ metabolism: ADP-ribose, nicotinamide, nicotinamide mononucleotide, AMP, NAD+ and NADH. For the quantification of the 6 metabolites of interest, first the desired metabolites standards were analysed to enable selection of the right reaction to monitor. Later, the biological samples were processed using liquid chromatography coupled to a triple quadrupole mass spectrometer (QqQ) (Agilent 6490 with iFunnel technology and Agilent 7000, respectively) in multiple reaction monitoring (MRM) mode was performed. For each condition we tested three different biological replicates and each biological replicate was run twice (as analytical duplicate). Finally, the data was analysed and quantification was done, finally representing the data as relative area normalized for the cell number.

Primers

siRNAs targeting splicing factors in mouse cells were kindly provided by dr. Didier Auboeuf (Centre Léon Bérard, Lyon).
All other oligos were purchased from Invitrogen.

Table 16. List of siRNAs.

siRNA Name	Sequence
si Control	cguacgcggaauacuucgatt
si macroH2A1.1#1	cgacaaacacugacuucuatt
si macroH2A1.1#2	ccgacaaacacugacuucutt
si macroH2A1.2 #1	gcuuugagguggaggccau
si macroH2A1.2 #2	ugacauugaccuuaaagau

Table 17. List of PCR, RFLP and qRT-PCR primers.

Method	Oligo Name	Sequence
q RT-PCR	myogenin_mm_qRTPCR_212_fwd	ggtgtgtaagaggaagtctgtg
q RT-PCR	myogenin_mm_qRTPCR_375_rev	taggcgctcaatgtactggat
q RT-PCR	Mouse mH2A1_qRTPCR_876_Fw	gacggtgaaaaactgcttgg
q RT-PCR	Mouse mH2A1_qRTPCR_1035_Rv	ggaggaggacatcgtggag
q RT-PCR	Mouse mH2A2_qRTPCR_867_Fw	gctggaagagaccatcaaaaa
q RT-PCR	Mouse mH2A2_qRTPCR_1015_Rv	cgaagtgagccgagatgg
q RT-PCR	mm_H2AFY_qRTPCR_E5s	cctacagacggcttcactgtc
q RT-PCR	mm_H2AFY_qRTPCR_E6as	ggtcaatgtcagcattggtagg
q RT-PCR	mm_H2AFY_qRTPCR_E7as	gtgtagaagtcagtgtttgtcg
q RT-PCR	mmGAPDH_qRTPCR_540_fwd	tgcaccaccaactgcttag
q RT-PCR	mmGAPDH_qRTPCR_698_rev	gatgcagggatgatgttc
q RT-PCR	mhRpo-qPCR-F	ttcattgtgggagcagac
q RT-PCR	mhRpo-qPCR-R	cagcagtttctccagagc
q RT-PCR	Ckm_qRTPCR_375_F (mouse)	acccacagacaagcataagaccga
q RT-PCR	Ckm_qRTPCR_478_R (mouse)	aggcagagtgtaacccttgatgct
q RT-PCR	mRpl7_qPCR_262_f	gaagctcatctatgagaaggc
q RT-PCR	mRpl7_qPCR_443_r	aagacgaaggagctgcagaac
q RT-PCR	macroH2A1_ex2_qRTPCR_254_f	gggaagaagaaatccaccaag
q RT-PCR	macroH2A1_ex2_qRTPCR_323_r	gcctttcttgatgtaccgaag
q RT-PCR	mDdx17 F	agaagtagcaagactgactcc
q RT-PCR	mDdx17 R	ccccctctcactgtaatctc
q RT-PCR	mDdx5 F	gtagctcagactggatctgg
q RT-PCR	mDdx5 R	tctctaggaatggctggtgg
q RT-PCR	mFOX2 F	cagtagttggagctgtgtatg
q RT-PCR	mFOX2 R	ggatgtaagtgttgatgcctc
q RT-PCR	mFOX1 F	caggagggatcttccatgtac
q RT-PCR	mFOX1 R	ggtatgcagctgcagcagtg
q RT-PCR	mMBNL1 F	gactgcaccaatgttggtcac
q RT-PCR	mMBNL1 R	gtgctgtcagcaggatgagc
q RT-PCR	mQKI F	tggaagatgctcagaacagag
q RT-PCR	mQKI R	tcttcttcaggctgtcttcac
q RT-PCR	mCugbp1 F	ctctcactacatccagcagtc
q RT-PCR	mCugbp1 R	gaattactgctgctggagctc
q RT-PCR	mCugbp2 F	cagatgaaacctgcagatagtg
q RT-PCR	mCugbp2 R	cactctgatatcattctcgttac
q RT-PCR	mCdhr1_qPCR_2156_f	gctccccatctttcagtacaac
q RT-PCR	mCdhr1_qPCR_2248_r	atgggattgtccttggtctg
q RT-PCR	mItga11_qPCR_3426_f	gttccacagccccttcatc
q RT-PCR	mItga11_qPCR_3488_r	tgccagtcttcttgcttgg
q RT-PCR	mTmem171_qPCR_841_f	aaacccaccttcctattccag
q RT-PCR	mTmem171_qPCR_937_r	atgaaccctgcccagaaatg

q RT-PCR	mAtp9a_qPCR_2828_f	tttgggtgttaatcagcatctatc
q RT-PCR	mAtp9a_qPCR_2919_r	ggatgagggatgtgaaggag
q RT-PCR	mFabp3_qPCR_222_f	gacagcagatgaccggaag
q RT-PCR	mFabp3_qPCR_294_r	gttgtctcctgcccgttc
q RT-PCR	mFoxo1_qPCR_1052_f	ataagggcgacagcaacag
q RT-PCR	mFoxo1_qPCR_1110_r	cgaataaacttgctgtgaagg
q RT-PCR	mMyh1_qPCR_5518_f	ctgaagggcggcaagaag
q RT-PCR	mMyh1_qPCR_5581_r	cgcttctgttcattttccac
q RT-PCR	mMyh8_qPCR_5606_f	ctgaagggcggcaagaag
q RT-PCR	mMyh8_qPCR_5672_r	ttgcgtttctgttcattttc
q RT-PCR	mItga11_qPCR_3345_f	gggaaacctgtggctgac
q RT-PCR	mItga11_qPCR_3426_r	atgaaggggctgtggaac
q RT-PCR	mChdr1_qPCR_1901_f	tacagagcgtccaggaaaag
q RT-PCR	mChdr1_qPCR_1966_r	ttgttaggctcctctgcatc
q RT-PCR	mMyf6_qPCR_507_f	gcgtggacccctacagctac
q RT-PCR	mMyf6_qPCR_730_r	cgtggaggaggtggtggagaag
q RT-PCR	mMyh7b_qPCR_905_f	gcctctgcggacattgatag
q RT-PCR	mMyh7b_qPCR_946_r	gggcagctggaagatcact
q RT-PCR	mMyh7_qPCR_2005_f	gccaactatgctggagctgatgccc
q RT-PCR	mMyh7_qPCR_2140_r	ggtgcgtggagcgcaagtttgtcataag
q RT-PCR	mMyh4_qRTPCR_5235_F	gagctactggatgccagtgagcgc
q RT-PCR	mMyh4_qRTPCR_5337_R	ctggacgatgtcttccatctctcc
q RT-PCR	mMyh2_qRTPCR_2003_F	ggcacaaactgctgaagcagaggc
q RT-PCR	mMyh2_qRTPCR_2117_R	ggtgctcctgaggttggtcatcagc
q RT-PCR	mCoxVb_qRTPCR_259_f	agcagcacagaagggactg
q RT-PCR	mCoxVb_qRTPCR_328_r	tggacgggactagattaggg
q RT-PCR	mCycs_qRTPCR_159_f	caaatctccacggtctgttc
q RT-PCR	mCycs_qRTPCR_248_r	tccatcagggtatcctctcc
q RT-PCR	mCpt1b_qRTPCR_1362 _f	ttgctacaaccctgacgatg
q RT-PCR	mCpt1b_qRTPCR_1452_r	tgcaggagataagggtgaaag
q RT-PCR	mAcadm_qRTPCR_885_f	attgtggaagccgacacc
q RT-PCR	mAcadm_qRTPCR_980_r	tttccttaggcactctgacg
q RT-PCR	mPdgfb_qRTPCR_1209_f	ctgcaataaccgcaatgtg
q RT-PCR	mPdgfb_qRTPCR_1279_r	ggcttctttcgcacaatctc
q RT-PCR	mEsrra_qRTPCR_752_f	ggaggacccaggaagacag
q RT-PCR	mEsrra_qRTPCR_815_r	gcatggcgtacagcttctc
q RT-PCR	mVegfa_qRTPCR_1359_f	gccagcacataggagagatg
q RT-PCR	mVegfa_qRTPCR_1455_r	tttttgacccttttccctttc
q RT-PCR	mIfg1_qRTPCR_467_f	tggtggatgctcttcagttc
q RT-PCR	mIfg1_qRTPCR_551_r	cacaatgcctgtctgaggtg
q RT-PCR	mIfg1_qRTPCR_880_f	catcgaaacacctaccaaataac
q RT-PCR	mIfg1_qRTPCR_964_r	tcctaaagacgatgttggaatg
q RT-PCR	mIgf2_qRTPCR_564_f	cacgcttcagtttgtctgttc

q RT-PCR	mIgf2_qRTPCR_642_r	agcagcactcttccacgatg
q RT-PCR	mFst_qRTPCR_582_f	caaggccagatgcaaagag
q RT-PCR	mFst_qRTPCR_677_r	ggtctgatccaccacacaag
q RT-PCR	mFstl1_qRTPCR_492_f	attccagatggctggttctc
q RT-PCR	mFstl1_qRTPCR_569_r	ggagtccaggtgagagtcg
q RT-PCR	mMyf5_qRTPCR_616_f	tgagggaacaggtggagaac
q RT-PCR	mMyf5_qRTPCR_705_r	acagggctgttacattcagg
q RT-PCR	mFbxo32_qRTPCR_864_f	atgtgggtgtatcggatgg
q RT-PCR	mFbxo32_qRTPCR_960_r	tgtaagcacacaggcaggtc
q RT-PCR	mPdgfr_qRTPCR_1972_f	ggtggagattcgcaggag
q RT-PCR	mPdgfr_qRTPCR_2053_r	gagagatgacggtaaggaccac
q RT-PCR	mSlc2a4_qRTPCR_695_f	aatcgcccccactcatc
q RT-PCR	mSlc2a4_qRTPCR_774_r	tagactccaagcccagcac
q RT-PCR	mPdk4_qRTPCR_749_f	aaagatgctctgcgaccag
q RT-PCR	mPdk4_qRTPCR_824_r	cacaatgtggattggttgg
q RT-PCR	mMstn_qRTPCR_442_f	cgctaccacggaaacaatc
q RT-PCR	mMstn_qRTPCR_505_r	aaagcaacatttgggcttg
q RT-PCR	mTrim63_qRTPCR_878_f	acttgtggagaccgccatc
q RT-PCR	mTrim63_qRTPCR_949_r	ctcttgatgagctgcttgg
RFLP	hs_H2AFY_E6_715_fwd	gcttcacagtcctcctctccacc
RFLP	hs_H2AFY_E9_914_rev	gagttccaggacagcttccac
RFLP	mm_H2AFY_E8_928_rev	cgcccttcttctccagtgtg
RFLP	mm_H2AFY_E8_928_rev	cgcccttcttctccagtgtg
q RT-PCR	hH2AFYE6/7s	tccttggccagaagctgaac
q RT-PCR	hH2AFYE8s	ttcacccgacaaacactgac
q RT-PCR	hH2AFYE9as	gagttccaggacagcttccac
q RT-PCR	h mH2A1_qPCR_897_fw	cctggctgatgataagaagctg
q RT-PCR	h mH2A1_qPCR_1019_Rv	gacacgaagtaactggagatgg
q RT-PCR	H2AFY2_qRTPCR_603_F	catggcggcagtcattgag
q RT-PCR	H2AFY2_qRTPCR_638_R	attgccggccaattctagaa
q RT-PCR	MYOD1_qRTPCR_844_f	cggcatgatggactacagcg
q RT-PCR	MYOD1_qRTPCR_958_	caggcagtctaggctcgac
q RT-PCR	CKM_qRTPCR_483_f	ctgacaagcacaagactgacc
q RT-PCR	CKM_qRTPCR_541_r	ctgctgagcacgtagttaggg
q RT-PCR	MYOG_qRTPCR_485_F	cagctccctcaaccaggag
q RT-PCR	MYOG_qRTPCR_586_R	cactgccccactctggac
q RT-PCR	HPRT1_qRTPCR_295_F	tggacaggactgaacgtcttg
q RT-PCR	HPRT1_qRTPCR_405_R	ccagcaggtcagcaaagaatt

Table 18. List of primers used in ChIP.

Method	Primer name	Sequence

qChIP	m Ranbp6_qChIP_-3929_ Fw	tgtatgtggcatttttgttgg
qChIP	m Ranbp6_qChIP_-4025_Rv	ttagagccaaatgagagggatag
qChIP	m Wnt8a_qChIP_+1403_Fw	tgtgtgcatgtgcaatgtatg
qChIP	m Wnt8a_qChIP_+1503_Rv	caccactcatacccacagacc

Table 19. List of cloning and mutagenesis primers.

Method	Primer name	Sequence
cloning	pCMV_FLAG_Bgl2_fwd	ggagatctgccaccatggattacaagg
cloning	mm_mH2A1.1_aa1_EcoRI_F	gc gaattccatgtcgagccgcggcgggaagaag
cloning	mm_mH2A1.1_STOP_XhoI_R	gg ctcgag tcagcctagttggcgtccagcttgg
mutagenesis	m mH2A1.1 silent_mut_887/890_F	gtgatgctgtcgttcacccgaccaatactgacttctacac cggtgg
mutagenesis	m mH2A1.1 silent_mut_887/890_R	ccaccggtgtagaagtcagtattggtcgggtgaacgac agcatcac
mutagenesis	m mH2A1.1 silent_mut_893/896_F	ctgtcgttcacccgaccaatacggatttctacaccggtg gtgaagt
mutagenesis	m mH2A1.1 silent_mut_893/896_R	acttcaccaccggtgtagaaatccgtattggtcgggtga acgacag
mutagenesis	m mH2A1.1 silent_GGT667GAG_F	ccgaccaatacggatttctacaccggtgaggaagt aggaaacacactggagaag
mutagenesis	m mH2A1.1 silent_GGT667GAG_R	cttctccagtgtgtttcctacttcctcaccggtgtagaaat ccgtattggtcgg

BIBLIOGRAPHY

Agathocleous, M., Love, N.K., Randlett, O., Harris, J.J., Liu, J., Murray, A.J., and Harris, W.A. (2012). Metabolic differentiation in the embryonic retina. Nat Cell Biol *14*, 859-864.

Agelopoulos, M., and Thanos, D. (2006). Epigenetic determination of a cell-specific gene expression program by ATF-2 and the histone variant macroH2A. Embo J *25*, 4843-4853.

Aguilar, V., Alliouachene, S., Sotiropoulos, A., Sobering, A., Athea, Y., Djouadi, F., Miraux, S., Thiaudiere, E., Foretz, M., Viollet, B.*, et al.* (2007). S6 kinase deletion suppresses muscle growth adaptations to nutrient availability by activating AMP kinase. Cell Metab *5*, 476-487.

Ahel, I., Ahel, D., Matsusaka, T., Clark, A.J., Pines, J., Boulton, S.J., and West, S.C. (2008). Poly(ADP-ribose)-binding zinc finger motifs in DNA repair/checkpoint proteins. Nature *451*, 81-85.

Alderton, J.M., and Steinhardt, R.A. (2000). How calcium influx through calcium leak channels is responsible for the elevated levels of calcium-dependent proteolysis in dystrophic myotubes. Trends Cardiovasc Med *10*, 268-272.

Alexander, P.B., Wang, J., and McKnight, S.L. (2011). Targeted killing of a mammalian cell based upon its specialized metabolic state. Proc Natl Acad Sci U S A *108*, 15828-15833.

Allbrook, D.B., Han, M.F., and Hellmuth, A.E. (1971). Population of muscle satellite cells in relation to age and mitotic activity. Pathology *3*, 223-243.

Allen, D.L., Cleary, A.S., Speaker, K.J., Lindsay, S.F., Uyenishi, J., Reed, J.M., Madden, M.C., and Mehan, R.S. (2008). Myostatin, activin receptor IIb, and follistatin-like-3 gene expression are altered in adipose tissue and skeletal muscle of obese mice. Am J Physiol Endocrinol Metab *294*, E918-927.

Allen, D.L., Hittel, D.S., and McPherron, A.C. (2011). Expression and function of myostatin in obesity, diabetes, and exercise adaptation. Med Sci Sports Exerc *43*, 1828-1835.

Allen, M.D., Buckle, A.M., Cordell, S.C., Lowe, J., and Bycroft, M. (2003). The crystal structure of AF1521 a protein from Archaeoglobus fulgidus with homology to the non-histone domain of macroH2A. J Mol Biol *330*, 503-511.

Allfrey, V.G., Faulkner, R., and Mirsky, A.E. (1964). Acetylation and Methylation of Histones and Their Possible Role in the Regulation of Rna Synthesis. Proc Natl Acad Sci U S A *51*, 786-794.

Angelov, D., Bondarenko, V.A., Almagro, S., Menoni, H., Mongelard, F., Hans, F., Mietton, F., Studitsky, V.M., Hamiche, A., Dimitrov, S.*, et al.* (2006). Nucleolin is a histone chaperone with FACT-like activity and assists remodeling of nucleosomes. EMBO J *25*, 1669-1679.

Angelov, D., Molla, A., Perche, P.Y., Hans, F., Cote, J., Khochbin, S., Bouvet, P., and Dimitrov, S. (2003). The histone variant macroH2A interferes with transcription factor binding and SWI/SNF nucleosome remodeling. Mol Cell *11*, 1033-1041.

Armstrong, R.B. (1990). Initial events in exercise-induced muscular injury. Med Sci Sports Exerc *22*, 429-435.

Asp, P., Blum, R., Vethantham, V., Parisi, F., Micsinai, M., Cheng, J., Bowman, C., Kluger, Y., and Dynlacht, B.D. (2011). Genome-wide remodeling of the epigenetic landscape during myogenic differentiation. Proc Natl Acad Sci U S A *108*, E149-158.

Aul, R.B., and Oko, R.J. (2002). The major subacrosomal occupant of bull spermatozoa is a novel histone H2B variant associated with the forming acrosome during spermiogenesis. Dev Biol *242*, 376-387.

Aziz, A., Sebastian, S., and Dilworth, F.J. (2012). The origin and fate of muscle satellite cells. Stem Cell Rev *8*, 609-622.

Bannister, A.J., and Kouzarides, T. (2011). Regulation of chromatin by histone modifications. Cell Res *21*, 381-395.

Barnhart, M.C., Kuich, P.H., Stellfox, M.E., Ward, J.A., Bassett, E.A., Black, B.E., and Foltz, D.R. (2011). HJURP is a CENP-A chromatin assembly factor sufficient to form a functional de novo kinetochore. J Cell Biol *194*, 229-243.

Barrero, M.J., Sese, B., Kuebler, B., Bilic, J., Boue, S., Marti, M., and Izpisua Belmonte, J.C. (2013a). Macrohistone variants preserve cell identity by preventing the gain of H3K4me2 during reprogramming to pluripotency. Cell Rep *3*, 1005-1011.

Barrero, M.J., Sese, B., Marti, M., and Izpisua Belmonte, J.C. (2013b). Macro histone variants are critical for the differentiation of human pluripotent cells. J Biol Chem *288*, 16110-16116.

Belcastro, A.N., Shewchuk, L.D., and Raj, D.A. (1998). Exercise-induced muscle injury: a calpain hypothesis. Mol Cell Biochem *179*, 135-145.

Bentzinger, C.F., Romanino, K., Cloetta, D., Lin, S., Mascarenhas, J.B., Oliveri, F., Xia, J., Casanova, E., Costa, C.F., Brink, M.*, et al.* (2008). Skeletal muscle-specific ablation of raptor, but not of rictor, causes metabolic changes and results in muscle dystrophy. Cell Metab *8*, 411-424.

Berger, F., Lau, C., Dahlmann, M., and Ziegler, M. (2005). Subcellular compartmentation and differential catalytic properties of the three human nicotinamide mononucleotide adenylyltransferase isoforms. J Biol Chem *280*, 36334-36341.

Bergman, Y., and Cedar, H. (2013). DNA methylation dynamics in health and disease. Nat Struct Mol Biol *20*, 274-281.

Bernstein, E., Muratore-Schroeder, T.L., Diaz, R.L., Chow, J.C., Changolkar, L.N., Shabanowitz, J., Heard, E., Pehrson, J.R., Hunt, D.F., and Allis, C.D. (2008). A phosphorylated subpopulation of the histone variant macroH2A1 is excluded from the inactive X chromosome and enriched during mitosis. Proc Natl Acad Sci U S A *105*, 1533-1538.

Bird, A. (2007). Perceptions of epigenetics. Nature *447*, 396-398.

Bird, A.P. (1978). Use of restriction enzymes to study eukaryotic DNA methylation: II. The symmetry of methylated sites supports semi-conservative copying of the methylation pattern. J Mol Biol *118*, 49-60.

Bischoff, R. (1975). Regeneration of single skeletal muscle fibers in vitro. Anat Rec *182*, 215-235.

Black, B.E., and Cleveland, D.W. (2011). Epigenetic centromere propagation and the nature of CENP-a nucleosomes. Cell *144*, 471-479.

Bland, C.S., Wang, E.T., Vu, A., David, M.P., Castle, J.C., Johnson, J.M., Burge, C.B., and Cooper, T.A. (2010). Global regulation of alternative splicing during myogenic differentiation. Nucleic Acids Res *38*, 7651-7664.

Blau, H.M., Pavlath, G.K., Hardeman, E.C., Chiu, C.P., Silberstein, L., Webster, S.G., Miller, S.C., and Webster, C. (1985). Plasticity of the differentiated state. Science *230*, 758-766.

Blum, R., and Dynlacht, B.D. (2013). The role of MyoD1 and histone modifications in the activation of muscle enhancers. Epigenetics *8*, 778-784.

Blum, R., Vethantham, V., Bowman, C., Rudnicki, M., and Dynlacht, B.D. (2012). Genome-wide identification of enhancers in skeletal muscle: the role of MyoD1. Genes Dev *26*, 2763-2779.

Bodine, S.C., Stitt, T.N., Gonzalez, M., Kline, W.O., Stover, G.L., Bauerlein, R., Zlotchenko, E., Scrimgeour, A., Lawrence, J.C., Glass, D.J.*, et al.* (2001). Akt/mTOR pathway is a crucial regulator of skeletal muscle hypertrophy and can prevent muscle atrophy in vivo. Nat Cell Biol *3*, 1014-1019.

Bonisch, C., and Hake, S.B. (2012). Histone H2A variants in nucleosomes and chromatin: more or less stable? Nucleic Acids Res *40*, 10719-10741.

Borer, K.T. (2005). Physical activity in the prevention and amelioration of osteoporosis in women : interaction of mechanical, hormonal and dietary factors. Sports Med *35*, 779-830.

Borra, M.T., O'Neill, F.J., Jackson, M.D., Marshall, B., Verdin, E., Foltz, K.R., and Denu, J.M. (2002). Conserved enzymatic production and biological effect of O-acetyl-ADP-ribose by silent information regulator 2-like NAD+-dependent deacetylases. J Biol Chem *277*, 12632-12641.

Boulard, M., Storck, S., Cong, R., Pinto, R., Delage, H., and Bouvet, P. (2010). Histone variant macroH2A1 deletion in mice causes female-specific steatosis. Epigenetics Chromatin *3*, 8.

Braun, T., and Gautel, M. (2011). Transcriptional mechanisms regulating skeletal muscle differentiation, growth and homeostasis. Nat Rev Mol Cell Biol *12*, 349-361.

Buschbeck, M., and Di Croce, L. (2010). Approaching the molecular and physiological function of macroH2A variants. Epigenetics *5*.

Buschbeck, M., Uribesalgo, I., Wibowo, I., Rue, P., Martin, D., Gutierrez, A., Morey, L., Guigo, R., Lopez-Schier, H., and Di Croce, L. (2009). The histone variant macroH2A is an epigenetic regulator of key developmental genes. Nat Struct Mol Biol *16*, 1074-1079.

Cantarino, N., Douet, J., and Buschbeck, M. (2013). MacroH2A--an epigenetic regulator of cancer. Cancer Lett *336*, 247-252.

Canto, C., Gerhart-Hines, Z., Feige, J.N., Lagouge, M., Noriega, L., Milne, J.C., Elliott, P.J., Puigserver, P., and Auwerx, J. (2009). AMPK regulates energy expenditure by modulating NAD+ metabolism and SIRT1 activity. Nature *458*, 1056-1060.

Canto, C., Jiang, L.Q., Deshmukh, A.S., Mataki, C., Coste, A., Lagouge, M., Zierath, J.R., and Auwerx, J. (2010). Interdependence of AMPK and SIRT1 for metabolic adaptation to fasting and exercise in skeletal muscle. Cell Metab *11*, 213-219.

Cao, Y., Yao, Z., Sarkar, D., Lawrence, M., Sanchez, G.J., Parker, M.H., MacQuarrie, K.L., Davison, J., Morgan, M.T., Ruzzo, W.L.*, et al.* (2010). Genome-wide MyoD binding in skeletal muscle cells: a potential for broad cellular reprogramming. Dev Cell *18*, 662-674.

Caretti, G., Di Padova, M., Micales, B., Lyons, G.E., and Sartorelli, V. (2004). The Polycomb Ezh2 methyltransferase regulates muscle gene expression and skeletal muscle differentiation. Genes Dev *18*, 2627-2638.

Cavalli, G., and Misteli, T. (2013). Functional implications of genome topology. Nat Struct Mol Biol *20*, 290-299.

Cerletti, M., Jang, Y.C., Finley, L.W., Haigis, M.C., and Wagers, A.J. (2012). Short-term calorie restriction enhances skeletal muscle stem cell function. Cell Stem Cell *10*, 515-519.

Chakravarthy, S., Gundimella, S.K., Caron, C., Perche, P.Y., Pehrson, J.R., Khochbin, S., and Luger, K. (2005). Structural characterization of the histone variant macroH2A. Mol Cell Biol *25*, 7616-7624.

Chakravarthy, S., Patel, A., and Bowman, G.D. (2012). The basic linker of macroH2A stabilizes DNA at the entry/exit site of the nucleosome. Nucleic Acids Res *40*, 8285-8295.

Chang, C.C., Ma, Y., Jacobs, S., Tian, X.C., Yang, X., and Rasmussen, T.P. (2005). A maternal store of macroH2A is removed from pronuclei prior to onset of somatic macroH2A expression in preimplantation embryos. Dev Biol *278*, 367-380.

Chang, E.Y., Ferreira, H., Somers, J., Nusinow, D.A., Owen-Hughes, T., and Narlikar, G.J. (2008). MacroH2A allows ATP-dependent chromatin remodeling by SWI/SNF and ACF complexes but specifically reduces recruitment of SWI/SNF. Biochemistry *47*, 13726-13732.

Changolkar, L.N., Costanzi, C., Leu, N.A., Chen, D., McLaughlin, K.J., and Pehrson, J.R. (2007). Developmental changes in histone macroH2A1-mediated gene regulation. Mol Cell Biol *27*, 2758-2764.

Changolkar, L.N., Singh, G., Cui, K., Berletch, J.B., Zhao, K., Disteche, C.M., and Pehrson, J.R. (2010). Genome-wide distribution of macroH2A1 histone variants in mouse liver chromatin. Mol Cell Biol *30*, 5473-5483.

Chawla, G., Lin, C.H., Han, A., Shiue, L., Ares, M., Jr., and Black, D.L. (2009). Sam68 regulates a set of alternatively spliced exons during neurogenesis. Mol Cell Biol *29*, 201-213.

Chazaud, B., Brigitte, M., Yacoub-Youssef, H., Arnold, L., Gherardi, R., Sonnet, C., Lafuste, P., and Chretien, F. (2009). Dual and beneficial roles of macrophages during skeletal muscle regeneration. Exerc Sport Sci Rev *37*, 18-22.

Chen, D., Vollmar, M., Rossi, M.N., Phillips, C., Kraehenbuehl, R., Slade, D., Mehrotra, P.V., von Delft, F., Crosthwaite, S.K., Gileadi, O.*, et al.* (2011). Identification of macrodomain proteins as novel O-acetyl-ADP-ribose deacetylases. J Biol Chem *286*, 13261-13271.

Chen, M., and Manley, J.L. (2009). Mechanisms of alternative splicing regulation: insights from molecular and genomics approaches. Nat Rev Mol Cell Biol *10*, 741-754.

Chiarugi, A., Dolle, C., Felici, R., and Ziegler, M. (2012). The NAD metabolome--a key determinant of cancer cell biology. Nat Rev Cancer *12*, 741-752.

Christov, C., Chretien, F., Abou-Khalil, R., Bassez, G., Vallet, G., Authier, F.J., Bassaglia, Y., Shinin, V., Tajbakhsh, S., Chazaud, B*., et al.* (2007). Muscle satellite cells and endothelial cells: close neighbors and privileged partners. Mol Biol Cell *18*, 1397-1409.

Chu, F., Nusinow, D.A., Chalkley, R.J., Plath, K., Panning, B., and Burlingame, A.L. (2006). Mapping post-translational modifications of the histone variant MacroH2A1 using tandem mass spectrometry. Mol Cell Proteomics *5*, 194-203.

Clarke, B.A., Drujan, D., Willis, M.S., Murphy, L.O., Corpina, R.A., Burova, E., Rakhilin, S.V., Stitt, T.N., Patterson, C., Latres, E*., et al.* (2007). The E3 Ligase MuRF1 degrades myosin heavy chain protein in dexamethasone-treated skeletal muscle. Cell Metab *6*, 376-385.

Collins, C.A., Olsen, I., Zammit, P.S., Heslop, L., Petrie, A., Partridge, T.A., and Morgan, J.E. (2005). Stem cell function, self-renewal, and behavioral heterogeneity of cells from the adult muscle satellite cell niche. Cell *122*, 289-301.

Comalada, M., Bailon, E., de Haro, O., Lara-Villoslada, F., Xaus, J., Zarzuelo, A., and Galvez, J. (2006). The effects of short-chain fatty acids on colon epithelial proliferation and survival depend on the cellular phenotype. J Cancer Res Clin Oncol *132*, 487-497.

Condon, K., Silberstein, L., Blau, H.M., and Thompson, W.J. (1990a). Development of muscle fiber types in the prenatal rat hindlimb. Dev Biol *138*, 256-274.

Condon, K., Silberstein, L., Blau, H.M., and Thompson, W.J. (1990b). Differentiation of fiber types in aneural musculature of the prenatal rat hindlimb. Dev Biol *138*, 275-295.

Cooper, T.A., Wan, L., and Dreyfuss, G. (2009). RNA and disease. Cell *136*, 777-793.

Cornelison, D.D., Olwin, B.B., Rudnicki, M.A., and Wold, B.J. (2000). MyoD(-/-) satellite cells in single-fiber culture are differentiation defective and MRF4 deficient. Dev Biol *224*, 122-137.

Cornelison, D.D., and Wold, B.J. (1997). Single-cell analysis of regulatory gene expression in quiescent and activated mouse skeletal muscle satellite cells. Dev Biol *191*, 270-283.

Cosgrove, B.D., Sacco, A., Gilbert, P.M., and Blau, H.M. (2009). A home away from home: challenges and opportunities in engineering in vitro muscle satellite cell niches. Differentiation *78*, 185-194.

Costanzi, C., and Pehrson, J.R. (1998). Histone macroH2A1 is concentrated in the inactive X chromosome of female mammals. Nature *393*, 599-601.

Creppe, C., Janich, P., Cantarino, N., Noguera, M., Valero, V., Musulen, E., Douet, J., Posavec, M., Martin-Caballero, J., Sumoy, L*., et al.* (2012). MacroH2A1 regulates the balance between self-renewal and differentiation commitment in embryonic and adult stem cells. Mol Cell Biol *32*, 1442-1452.

Crescenzi, M., Fleming, T.P., Lassar, A.B., Weintraub, H., and Aaronson, S.A. (1990). MyoD induces growth arrest independent of differentiation in normal and transformed cells. Proc Natl Acad Sci U S A *87*, 8442-8446.

Crose, L.E., Etheridge, K.T., Chen, C., Belyea, B., Talbot, L.J., Bentley, R.C., and Linardic, C.M. (2012). FGFR4 blockade exerts distinct antitumorigenic effects in human embryonal versus alveolar rhabdomyosarcoma. Clin Cancer Res *18*, 3780-3790.

d'Albis, A., Chanoine, C., Janmot, C., Mira, J.C., and Couteaux, R. (1990). Muscle-specific response to thyroid hormone of myosin isoform transitions during rat postnatal development. Eur J Biochem *193*, 155-161.

Dai, B., and Rasmussen, T.P. (2007). Global epiproteomic signatures distinguish embryonic stem cells from differentiated cells. Stem Cells *25*, 2567-2574.

Dalla Libera, L., Sabbadini, R., Renken, C., Ravara, B., Sandri, M., Betto, R., Angelini, A., and Vescovo, G. (2001). Apoptosis in the skeletal muscle of rats with heart failure is associated with increased serum levels of TNF-alpha and sphingosine. J Mol Cell Cardiol *33*, 1871-1878.

Dang, L., Jin, S., and Su, S.M. (2010). IDH mutations in glioma and acute myeloid leukemia. Trends Mol Med *16*, 387-397.

Dardenne, E., Pierredon, S., Driouch, K., Gratadou, L., Lacroix-Triki, M., Espinoza, M.P., Zonta, E., Germann, S., Mortada, H., Villemin, J.P.*, et al.* (2012). Splicing switch of an epigenetic regulator by RNA helicases promotes tumor-cell invasiveness. Nat Struct Mol Biol.

Daugaard, J.R., Nielsen, J.N., Kristiansen, S., Andersen, J.L., Hargreaves, M., and Richter, E.A. (2000). Fiber type-specific expression of GLUT4 in human skeletal muscle: influence of exercise training. Diabetes *49*, 1092-1095.

DeFronzo, R.A., and Tripathy, D. (2009). Skeletal muscle insulin resistance is the primary defect in type 2 diabetes. Diabetes Care *32 Suppl 2*, S157-163.

DeNardi, C., Ausoni, S., Moretti, P., Gorza, L., Velleca, M., Buckingham, M., and Schiaffino, S. (1993). Type 2X-myosin heavy chain is coded by a muscle fiber type-specific and developmentally regulated gene. J Cell Biol *123*, 823-835.

Dias, P., Chen, B., Dilday, B., Palmer, H., Hosoi, H., Singh, S., Wu, C., Li, X., Thompson, J., Parham, D.*, et al.* (2000). Strong immunostaining for myogenin in rhabdomyosarcoma is significantly associated with tumors of the alveolar subclass. Am J Pathol *156*, 399-408.

Divakaruni, A.S., and Brand, M.D. (2011). The regulation and physiology of mitochondrial proton leak. Physiology (Bethesda) *26*, 192-205.

Dole, V.P. (1956). A relation between non-esterified fatty acids in plasma and the metabolism of glucose. J Clin Invest *35*, 150-154.

Dominguez-Salas, P., Cox, S.E., Prentice, A.M., Hennig, B.J., and Moore, S.E. (2012). Maternal nutritional status, C(1) metabolism and offspring DNA methylation: a review of current evidence in human subjects. Proc Nutr Soc *71*, 154-165.

Donohoe, D.R., Collins, L.B., Wali, A., Bigler, R., Sun, W., and Bultman, S.J. (2012). The Warburg effect dictates the mechanism of butyrate-mediated histone acetylation and cell proliferation. Mol Cell *48*, 612-626.

Doyen, C.M., An, W., Angelov, D., Bondarenko, V., Mietton, F., Studitsky, V.M., Hamiche, A., Roeder, R.G., Bouvet, P., and Dimitrov, S. (2006). Mechanism of

Polymerase II Transcription Repression by the Histone Variant macroH2A. Mol Cell Biol *26*, 1156-1164.

Durieux, A.C., Amirouche, A., Banzet, S., Koulmann, N., Bonnefoy, R., Pasdeloup, M., Mouret, C., Bigard, X., Peinnequin, A., and Freyssenet, D. (2007). Ectopic expression of myostatin induces atrophy of adult skeletal muscle by decreasing muscle gene expression. Endocrinology *148*, 3140-3147.

Eason, J.M., Schwartz, G.A., Pavlath, G.K., and English, A.W. (2000). Sexually dimorphic expression of myosin heavy chains in the adult mouse masseter. J Appl Physiol (1985) *89*, 251-258.

Epstein, J.A., Shapiro, D.N., Cheng, J., Lam, P.Y., and Maas, R.L. (1996). Pax3 modulates expression of the c-Met receptor during limb muscle development. Proc Natl Acad Sci U S A *93*, 4213-4218.

Fearon, K.C., Glass, D.J., and Guttridge, D.C. (2012). Cancer cachexia: mediators, signaling, and metabolic pathways. Cell Metab *16*, 153-166.

Feinberg, A.P. (2007). Phenotypic plasticity and the epigenetics of human disease. Nature *447*, 433-440.

Ferreira, R., Neuparth, M.J., Vitorino, R., Appell, H.J., Amado, F., and Duarte, J.A. (2008). Evidences of apoptosis during the early phases of soleus muscle atrophy in hindlimb suspended mice. Physiol Res *57*, 601-611.

Fielding, R.A., Manfredi, T.J., Ding, W., Fiatarone, M.A., Evans, W.J., and Cannon, J.G. (1993). Acute phase response in exercise. III. Neutrophil and IL-1 beta accumulation in skeletal muscle. Am J Physiol *265*, R166-172.

Foltz, D.R., Jansen, L.E., Black, B.E., Bailey, A.O., Yates, J.R., 3rd, and Cleveland, D.W. (2006). The human CENP-A centromeric nucleosome-associated complex. Nat Cell Biol *8*, 458-469.

Forcales, S.V., Albini, S., Giordani, L., Malecova, B., Cignolo, L., Chernov, A., Coutinho, P., Saccone, V., Consalvi, S., Williams, R.*, et al.* (2012). Signal-dependent incorporation of MyoD-BAF60c into Brg1-based SWI/SNF chromatin-remodelling complex. EMBO J *31*, 301-316.

Fredrickson, D.S., and Gordon, R.S., Jr. (1958). Transport of fatty acids. Physiol Rev *38*, 585-630.

Fukada, S., Uezumi, A., Ikemoto, M., Masuda, S., Segawa, M., Tanimura, N., Yamamoto, H., Miyagoe-Suzuki, Y., and Takeda, S. (2007). Molecular signature of quiescent satellite cells in adult skeletal muscle. Stem Cells *25*, 2448-2459.

Fulco, M., Cen, Y., Zhao, P., Hoffman, E.P., McBurney, M.W., Sauve, A.A., and Sartorelli, V. (2008). Glucose restriction inhibits skeletal myoblast differentiation by activating SIRT1 through AMPK-mediated regulation of Nampt. Dev Cell *14*, 661-673.

Fulco, M., Schiltz, R.L., Iezzi, S., King, M.T., Zhao, P., Kashiwaya, Y., Hoffman, E., Veech, R.L., and Sartorelli, V. (2003). Sir2 regulates skeletal muscle differentiation as a potential sensor of the redox state. Mol Cell *12*, 51-62.

Gambke, B., Lyons, G.E., Haselgrove, J., Kelly, A.M., and Rubinstein, N.A. (1983). Thyroidal and neural control of myosin transitions during development of rat fast and slow muscles. FEBS Lett *156*, 335-339.

Gamble, M.J., Frizzell, K.M., Yang, C., Krishnakumar, R., and Kraus, W.L. (2010). The histone variant macroH2A1 marks repressed autosomal chromatin, but protects a subset of its target genes from silencing. Genes Dev *24*, 21-32.

Gan, Z., Rumsey, J., Hazen, B.C., Lai, L., Leone, T.C., Vega, R.B., Xie, H., Conley, K.E., Auwerx, J., Smith, S.R.*, et al.* (2013). Nuclear receptor/microRNA circuitry links muscle fiber type to energy metabolism. J Clin Invest *123*, 2564-2575.

Gao, Z., and Cooper, T.A. (2013). Reexpression of pyruvate kinase M2 in type 1 myofibers correlates with altered glucose metabolism in myotonic dystrophy. Proc Natl Acad Sci U S A *110*, 13570-13575.

Gaspar-Maia, A., Qadeer, Z.A., Hasson, D., Ratnakumar, K., Leu, N.A., Leroy, G., Liu, S., Costanzi, C., Valle-Garcia, D., Schaniel, C.*, et al.* (2013). MacroH2A histone variants act as a barrier upon reprogramming towards pluripotency. Nat Commun *4*, 1565.

Gibson, B.A., and Kraus, W.L. (2012). New insights into the molecular and cellular functions of poly(ADP-ribose) and PARPs. Nat Rev Mol Cell Biol *13*, 411-424.

Gordon, R.S., Jr., and Cherkes, A. (1956). Unesterified fatty acid in human blood plasma. J Clin Invest *35*, 206-212.

Gros, J., Manceau, M., Thome, V., and Marcelle, C. (2005). A common somitic origin for embryonic muscle progenitors and satellite cells. Nature *435*, 954-958.

Grosso, A.R., Martins, S., and Carmo-Fonseca, M. (2008). The emerging role of splicing factors in cancer. EMBO Rep *9*, 1087-1093.

Grounds, M.D., Garrett, K.L., Lai, M.C., Wright, W.E., and Beilharz, M.W. (1992). Identification of skeletal muscle precursor cells in vivo by use of MyoD1 and myogenin probes. Cell Tissue Res *267*, 99-104.

Grubisha, O., Rafty, L.A., Takanishi, C.L., Xu, X., Tong, L., Perraud, A.L., Scharenberg, A.M., and Denu, J.M. (2006). Metabolite of SIR2 reaction modulates TRPM2 ion channel. J Biol Chem *281*, 14057-14065.

Guasconi, V., and Puri, P.L. (2009). Chromatin: the interface between extrinsic cues and the epigenetic regulation of muscle regeneration. Trends Cell Biol *19*, 286-294.

Guenther, M.G., Levine, S.S., Boyer, L.A., Jaenisch, R., and Young, R.A. (2007). A chromatin landmark and transcription initiation at most promoters in human cells. Cell *130*, 77-88.

Guo, K., Wang, J., Andres, V., Smith, R.C., and Walsh, K. (1995). MyoD-induced expression of p21 inhibits cyclin-dependent kinase activity upon myocyte terminal differentiation. Mol Cell Biol *15*, 3823-3829.

Gut, P., and Verdin, E. (2013). The nexus of chromatin regulation and intermediary metabolism. Nature *502*, 489-498.

Hackett, J.D., Scheetz, T.E., Yoon, H.S., Soares, M.B., Bonaldo, M.F., Casavant, T.L., and Bhattacharya, D. (2005). Insights into a dinoflagellate genome through expressed sequence tag analysis. BMC Genomics *6*, 80.

Halevy, O., Novitch, B.G., Spicer, D.B., Skapek, S.X., Rhee, J., Hannon, G.J., Beach, D., and Lassar, A.B. (1995). Correlation of terminal cell cycle arrest of skeletal muscle with induction of p21 by MyoD. Science *267*, 1018-1021.

Han, W., Li, X., and Fu, X. (2011). The macro domain protein family: structure, functions, and their potential therapeutic implications. Mutat Res *727*, 86-103.

Hansen, J., Brandt, C., Nielsen, A.R., Hojman, P., Whitham, M., Febbraio, M.A., Pedersen, B.K., and Plomgaard, P. (2011). Exercise induces a marked increase in plasma follistatin: evidence that follistatin is a contraction-induced hepatokine. Endocrinology *152*, 164-171.

Hansen, J.M., Klass, M., Harris, C., and Csete, M. (2007). A reducing redox environment promotes C2C12 myogenesis: implications for regeneration in aged muscle. Cell Biol Int *31*, 546-553.

Harper, P. (2001). Myotonic Dystrophy. (Saunders, London).

Hassa, P.O., Haenni, S.S., Elser, M., and Hottiger, M.O. (2006). Nuclear ADP-ribosylation reactions in mammalian cells: where are we today and where are we going? Microbiol Mol Biol Rev *70*, 789-829.

Hatley, M.E., Tang, W., Garcia, M.R., Finkelstein, D., Millay, D.P., Liu, N., Graff, J., Galindo, R.L., and Olson, E.N. (2012). A mouse model of rhabdomyosarcoma originating from the adipocyte lineage. Cancer Cell *22*, 536-546.

Hellmuth, A.E., and Allbrook, D.B. (1971). Muscle satellite cell numbers during the postnatal period. J Anat *110*, 503.

Henriksen, E.J., Bourey, R.E., Rodnick, K.J., Koranyi, L., Permutt, M.A., and Holloszy, J.O. (1990). Glucose transporter protein content and glucose transport capacity in rat skeletal muscles. Am J Physiol *259*, E593-598.

Hernandez-Munoz, I., Lund, A.H., van der Stoop, P., Boutsma, E., Muijrers, I., Verhoeven, E., Nusinow, D.A., Panning, B., Marahrens, Y., and van Lohuizen, M. (2005). Stable X chromosome inactivation involves the PRC1 Polycomb complex and requires histone MACROH2A1 and the CULLIN3/SPOP ubiquitin E3 ligase. Proc Natl Acad Sci U S A *102*, 7635-7640.

Hindi, S.M., Tajrishi, M.M., and Kumar, A. (2013). Signaling mechanisms in mammalian myoblast fusion. Sci Signal *6*, re2.

Hittel, D.S., Axelson, M., Sarna, N., Shearer, J., Huffman, K.M., and Kraus, W.E. (2010). Myostatin decreases with aerobic exercise and associates with insulin resistance. Med Sci Sports Exerc *42*, 2023-2029.

Holliday, R. (1987). The inheritance of epigenetic defects. Science *238*, 163-170.

Holliday, R. (1990). Mechanism for the control of gene activity during development. Biological Reviews.

Holliday, R. (2006). Epigenetics: a historical overview. Epigenetics *1*, 76-80.

Holliday, R., and Pugh, J.E. (1975). DNA modification mechanisms and gene activity during development. Science *187*, 226-232.

Horsley, V., Friday, B.B., Matteson, S., Kegley, K.M., Gephart, J., and Pavlath, G.K. (2001). Regulation of the growth of multinucleated muscle cells by an NFATC2-dependent pathway. J Cell Biol *153*, 329-338.

Horsley, V., Jansen, K.M., Mills, S.T., and Pavlath, G.K. (2003). IL-4 acts as a myoblast recruitment factor during mammalian muscle growth. Cell *113*, 483-494.

Hosoyama, T., Aslam, M.I., Abraham, J., Prajapati, S.I., Nishijo, K., Michalek, J.E., Zarzabal, L.A., Nelon, L.D., Guttridge, D.C., Rubin, B.P*., et al.* (2011). IL-4R drives dedifferentiation, mitogenesis, and metastasis in rhabdomyosarcoma. Clin Cancer Res *17*, 2757-2766.

Huang, T.T., Naeemuddin, M., Elchuri, S., Yamaguchi, M., Kozy, H.M., Carlson, E.J., and Epstein, C.J. (2006). Genetic modifiers of the phenotype of mice deficient in mitochondrial superoxide dismutase. Hum Mol Genet *15*, 1187-1194.

Ibebunjo, C., Chick, J.M., Kendall, T., Eash, J.K., Li, C., Zhang, Y., Vickers, C., Wu, Z., Clarke, B.A., Shi, J.*, et al.* (2013). Genomic and proteomic profiling reveals reduced mitochondrial function and disruption of the neuromuscular junction driving rat sarcopenia. Mol Cell Biol *33*, 194-212.

Ibebunjo, C., Eash, J.K., Li, C., Ma, Q., and Glass, D.J. (2011). Voluntary running, skeletal muscle gene expression, and signaling inversely regulated by orchidectomy and testosterone replacement. Am J Physiol Endocrinol Metab *300*, E327-340.

Ignatius, M.S., Chen, E., Elpek, N.M., Fuller, A.Z., Tenente, I.M., Clagg, R., Liu, S., Blackburn, J.S., Linardic, C.M., Rosenberg, A.E.*, et al.* (2012). In vivo imaging of tumor-propagating cells, regional tumor heterogeneity, and dynamic cell movements in embryonal rhabdomyosarcoma. Cancer Cell *21*, 680-693.

Ioudinkova, E.S., Barat, A., Pichugin, A., Markova, E., Sklyar, I., Pirozhkova, I., Robin, C., Lipinski, M., Ogryzko, V., Vassetzky, Y.S.*, et al.* (2012). Distinct distribution of ectopically expressed histone variants H2A.Bbd and MacroH2A in open and closed chromatin domains. PLoS One *7*, e47157.

Jaenisch, A.B.R. (2003). Epigenetic regulation of gene expression: how the genome integrates intrinsic and environmental signals. Nature Genetics.

Jansen, K.M., and Pavlath, G.K. (2006). Mannose receptor regulates myoblast motility and muscle growth. J Cell Biol *174*, 403-413.

Jenuwein, T., and Allis, C.D. (2001). Translating the histone code. Science *293*, 1074-1080.

Johnson, M.T., Mahmood, S., and Patel, M.S. (2003). Intermediary metabolism and energetics during murine early embryogenesis. J Biol Chem *278*, 31457-31460.

Joshi, N. (2011). Sickle: A sliding-window, adaptive, quality-based trimming tool for FastQ files. https://githubcom/najoshi/sickle.

Juan, A.H., Derfoul, A., Feng, X., Ryall, J.G., Dell'Orso, S., Pasut, A., Zare, H., Simone, J.M., Rudnicki, M.A., and Sartorelli, V. (2011). Polycomb EZH2 controls self-renewal and safeguards the transcriptional identity of skeletal muscle stem cells. Genes Dev *25*, 789-794.

Kaelin, W.G., Jr., and McKnight, S.L. (2013). Influence of metabolism on epigenetics and disease. Cell *153*, 56-69.

Kalsotra, A., Xiao, X., Ward, A.J., Castle, J.C., Johnson, J.M., Burge, C.B., and Cooper, T.A. (2008). A postnatal switch of CELF and MBNL proteins reprograms alternative splicing in the developing heart. Proc Natl Acad Sci U S A *105*, 20333-20338.

Kamei, Y., Miura, S., Suzuki, M., Kai, Y., Mizukami, J., Taniguchi, T., Mochida, K., Hata, T., Matsuda, J., Aburatani, H.*, et al.* (2004). Skeletal muscle FOXO1 (FKHR) transgenic mice have less skeletal muscle mass, down-regulated Type I (slow twitch/red muscle) fiber genes, and impaired glycemic control. J Biol Chem *279*, 41114-41123.

Kapoor, A., Goldberg, M.S., Cumberland, L.K., Ratnakumar, K., Segura, M.F., Emanuel, P.O., Menendez, S., Vardabasso, C., Leroy, G., Vidal, C.I., *et al.* (2010). The histone variant macroH2A suppresses melanoma progression through regulation of CDK8. Nature *468*, 1105-1109.

Karras, G.I., Kustatscher, G., Buhecha, H.R., Allen, M.D., Pugieux, C., Sait, F., Bycroft, M., and Ladurner, A.G. (2005). The macro domain is an ADP-ribose binding module. Embo J *24*, 1911-1920.

Kelley, D.E., and Mandarino, L.J. (2000). Fuel selection in human skeletal muscle in insulin resistance: a reexamination. Diabetes *49*, 677-683.

Kim, I.K., Kiefer, J.R., Ho, C.M., Stegeman, R.A., Classen, S., Tainer, J.A., and Ellenberger, T. (2012a). Structure of mammalian poly(ADP-ribose) glycohydrolase reveals a flexible tyrosine clasp as a substrate-binding element. Nat Struct Mol Biol *19*, 653-656.

Kim, J.K., Fillmore, J.J., Chen, Y., Yu, C., Moore, I.K., Pypaert, M., Lutz, E.P., Kako, Y., Velez-Carrasco, W., Goldberg, I.J., *et al.* (2001). Tissue-specific overexpression of lipoprotein lipase causes tissue-specific insulin resistance. Proc Natl Acad Sci U S A *98*, 7522-7527.

Kim, M.Y., Zhang, T., and Kraus, W.L. (2005). Poly(ADP-ribosyl)ation by PARP-1: 'PAR-laying' NAD+ into a nuclear signal. Genes Dev *19*, 1951-1967.

Kim, S.C., Sprung, R., Chen, Y., Xu, Y., Ball, H., Pei, J., Cheng, T., Kho, Y., Xiao, H., Xiao, L., *et al.* (2006a). Substrate and functional diversity of lysine acetylation revealed by a proteomics survey. Mol Cell *23*, 607-618.

Kim, W., Chakraborty, G., Kim, S., Shin, J., Park, C.H., Jeong, M.W., Bharatham, N., Yoon, H.S., and Kim, K.T. (2012b). Macro histone H2A1.2 (macroH2A1) protein suppresses mitotic kinase VRK1 during interphase. J Biol Chem *287*, 5278-5289.

Kim, Y.I., Lee, F.N., Choi, W.S., Lee, S., and Youn, J.H. (2006b). Insulin regulation of skeletal muscle PDK4 mRNA expression is impaired in acute insulin-resistant states. Diabetes *55*, 2311-2317.

Kim, Y.S., and Milner, J.A. (2007). Dietary modulation of colon cancer risk. J Nutr *137*, 2576S-2579S.

Kleiber, M. (1947). Body size and metabolic rate. Physiol Rev *27*, 511-541.

Kline, W.O., Panaro, F.J., Yang, H., and Bodine, S.C. (2007). Rapamycin inhibits the growth and muscle-sparing effects of clenbuterol. J Appl Physiol (1985) *102*, 740-747.

Knowler, W.C., Barrett-Connor, E., Fowler, S.E., Hamman, R.F., Lachin, J.M., Walker, E.A., and Nathan, D.M. (2002). Reduction in the incidence of type 2 diabetes with lifestyle intervention or metformin. N Engl J Med *346*, 393-403.

Konigsberg, U.R., Lipton, B.H., and Konigsberg, I.R. (1975). The regenerative response of single mature muscle fibers isolated in vitro. Dev Biol *45*, 260-275.

Kornberg, R.D. (1977). Structure of chromatin. Annu Rev Biochem *46*, 931-954.

Kouzarides, T. (2007). Chromatin modifications and their function. Cell *128*, 693-705.

Kraft, C.S., LeMoine, C.M., Lyons, C.N., Michaud, D., Mueller, C.R., and Moyes, C.D. (2006). Control of mitochondrial biogenesis during myogenesis. Am J Physiol Cell Physiol *290*, C1119-1127.

Krauss, R.S., Cole, F., Gaio, U., Takaesu, G., Zhang, W., and Kang, J.S. (2005). Close encounters: regulation of vertebrate skeletal myogenesis by cell-cell contact. J Cell Sci *118*, 2355-2362.

Krebs, H. (1969). Pyridine nucleotide interrelations The Energy Level and Metabolic Control in Mitochondria.

Krogh-Madsen, R., Thyfault, J.P., Broholm, C., Mortensen, O.H., Olsen, R.H., Mounier, R., Plomgaard, P., van Hall, G., Booth, F.W., and Pedersen, B.K. (2010). A 2-wk reduction of ambulatory activity attenuates peripheral insulin sensitivity. J Appl Physiol (1985) *108*, 1034-1040.

Kuang, S., Gillespie, M.A., and Rudnicki, M.A. (2008). Niche regulation of muscle satellite cell self-renewal and differentiation. Cell Stem Cell *2*, 22-31.

Kuang, S., Kuroda, K., Le Grand, F., and Rudnicki, M.A. (2007). Asymmetric self-renewal and commitment of satellite stem cells in muscle. Cell *129*, 999-1010.

Kucharski, R., Maleszka, J., Foret, S., and Maleszka, R. (2008). Nutritional control of reproductive status in honeybees via DNA methylation. Science *319*, 1827-1830.

Kurisu, S., and Takenawa, T. (2009). The WASP and WAVE family proteins. Genome Biol *10*, 226.

Kustatscher, G., Hothorn, M., Pugieux, C., Scheffzek, K., and Ladurner, A.G. (2005). Splicing regulates NAD metabolite binding to histone macroH2A. Nat Struct Mol Biol *12*, 624-625.

Kuyumcu-Martinez, N.M., and Cooper, T.A. (2006). Misregulation of alternative splicing causes pathogenesis in myotonic dystrophy. Prog Mol Subcell Biol *44*, 133-159.

Ladurner, A.G. (2006). Rheostat control of gene expression by metabolites. Mol Cell *24*, 1-11.

Langmead, B., Trapnell, C., Pop, M., and Salzberg, S.L. (2009). Ultrafast and memory-efficient alignment of short DNA sequences to the human genome. Genome Biol *10*, R25.

Laporte, D., Lebaudy, A., Sahin, A., Pinson, B., Ceschin, J., Daignan-Fornier, B., and Sagot, I. (2011). Metabolic status rather than cell cycle signals control quiescence entry and exit. J Cell Biol *192*, 949-957.

Latil, M., Rocheteau, P., Chatre, L., Sanulli, S., Memet, S., Ricchetti, M., Tajbakhsh, S., and Chretien, F. (2012). Skeletal muscle stem cells adopt a dormant cell state post mortem and retain regenerative capacity. Nat Commun *3*, 903.

Lau, C., Niere, M., and Ziegler, M. (2009). The NMN/NaMN adenylyltransferase (NMNAT) protein family. Front Biosci (Landmark Ed) *14*, 410-431.

Le Grand, F., Jones, A.E., Seale, V., Scime, A., and Rudnicki, M.A. (2009). Wnt7a activates the planar cell polarity pathway to drive the symmetric expansion of satellite stem cells. Cell Stem Cell *4*, 535-547.

Leary, S.C., Battersby, B.J., Hansford, R.G., and Moyes, C.D. (1998). Interactions between bioenergetics and mitochondrial biogenesis. Biochim Biophys Acta *1365*, 522-530.

Lee, S.J. (2004). Regulation of muscle mass by myostatin. Annu Rev Cell Dev Biol *20*, 61-86.

Lee, S.J., and McPherron, A.C. (1999). Myostatin and the control of skeletal muscle mass. Curr Opin Genet Dev *9*, 604-607.

Lee, S.J., and McPherron, A.C. (2001). Regulation of myostatin activity and muscle growth. Proc Natl Acad Sci U S A *98*, 9306-9311.

Lee, S.W., Dai, G., Hu, Z., Wang, X., Du, J., and Mitch, W.E. (2004). Regulation of muscle protein degradation: coordinated control of apoptotic and ubiquitin-proteasome systems by phosphatidylinositol 3 kinase. J Am Soc Nephrol *15*, 1537-1545.

Lepper, C., Partridge, T.A., and Fan, C.M. (2011). An absolute requirement for Pax7-positive satellite cells in acute injury-induced skeletal muscle regeneration. Development *138*, 3639-3646.

Lexell, J., Taylor, C.C., and Sjostrom, M. (1988). What is the cause of the ageing atrophy? Total number, size and proportion of different fiber types studied in whole vastus lateralis muscle from 15- to 83-year-old men. J Neurol Sci *84*, 275-294.

Li, P., Waters, R.E., Redfern, S.I., Zhang, M., Mao, L., Annex, B.H., and Yan, Z. (2007a). Oxidative phenotype protects myofibers from pathological insults induced by chronic heart failure in mice. Am J Pathol *170*, 599-608.

Li, Q., Lee, J.A., and Black, D.L. (2007b). Neuronal regulation of alternative pre-mRNA splicing. Nat Rev Neurosci *8*, 819-831.

Li, X., Kuang, J., Shen, Y., Majer, M.M., Nelson, C.C., Parsawar, K., Heichman, K.A., and Kuwada, S.K. (2012). The atypical histone macroH2A1.2 interacts with HER-2 protein in cancer cells. J Biol Chem *287*, 23171-23183.

Licatalosi, D.D., Mele, A., Fak, J.J., Ule, J., Kayikci, M., Chi, S.W., Clark, T.A., Schweitzer, A.C., Blume, J.E., Wang, X.*, et al.* (2008). HITS-CLIP yields genome-wide insights into brain alternative RNA processing. Nature *456*, 464-469.

Lillioja, S., Young, A.A., Culter, C.L., Ivy, J.L., Abbott, W.G., Zawadzki, J.K., Yki-Jarvinen, H., Christin, L., Secomb, T.W., and Bogardus, C. (1987). Skeletal muscle capillary density and fiber type are possible determinants of in vivo insulin resistance in man. J Clin Invest *80*, 415-424.

Liou, G.G., Tanny, J.C., Kruger, R.G., Walz, T., and Moazed, D. (2005). Assembly of the SIR complex and its regulation by O-acetyl-ADP-ribose, a product of NAD-dependent histone deacetylation. Cell *121*, 515-527.

Lipton, B.H., and Schultz, E. (1979). Developmental fate of skeletal muscle satellite cells. Science *205*, 1292-1294.

Liu, C.M., Yang, Z., Liu, C.W., Wang, R., Tien, P., Dale, R., and Sun, L.Q. (2007). Effect of RNA oligonucleotide targeting Foxo-1 on muscle growth in normal and cancer cachexia mice. Cancer Gene Ther *14*, 945-952.

Lu, C., and Thompson, C.B. (2012). Metabolic regulation of epigenetics. Cell Metab *16*, 9-17.

Luger, K., Mader, A.W., Richmond, R.K., Sargent, D.F., and Richmond, T.J. (1997). Crystal structure of the nucleosome core particle at 2.8 A resolution. Nature *389*, 251-260.

Lyons, C.N., Leary, S.C., and Moyes, C.D. (2004). Bioenergetic remodeling during cellular differentiation: changes in cytochrome c oxidase regulation do not affect the metabolic phenotype. Biochem Cell Biol *82*, 391-399.

Magni, G., Orsomando, G., Raffelli, N., and Ruggieri, S. (2008). Enzymology of mammalian NAD metabolism in health and disease. Front Biosci *13*, 6135-6154.

Maiolica, A., De Medina Redondo, M., Schoof, E.M., Chaikuad, A., Villa, F., Gatti, M., Jeganatgan, S., Lou, H.J., Novy, K., Hauri, S., *et al.* (2014). Modulation of the chromatin phosphoproteome by the Haspin protein kinase. Mol Cell Proteomics.

Mal, A.K. (2006). Histone methyltransferase Suv39h1 represses MyoD-stimulated myogenic differentiation. EMBO J *25*, 3323-3334.

Malik, H.S., and Henikoff, S. (2003). Phylogenomics of the nucleosome. Nat Struct Biol *10*, 882-891.

Manzano, R., Toivonen, J.M., Calvo, A.C., Miana-Mena, F.J., Zaragoza, P., Munoz, M.J., Montarras, D., and Osta, R. (2011). Sex, fiber-type, and age dependent in vitro proliferation of mouse muscle satellite cells. J Cell Biochem *112*, 2825-2836.

Margueron, R., and Reinberg, D. (2010). Chromatin structure and the inheritance of epigenetic information. Nat Rev Genet *11*, 285-296.

Martin, M. (2011). Cutadapt removes adapter sequences from high-throughput sequencing reads. . EMBnetjournal.

Martino, F., Kueng, S., Robinson, P., Tsai-Pflugfelder, M., van Leeuwen, F., Ziegler, M., Cubizolles, F., Cockell, M.M., Rhodes, D., and Gasser, S.M. (2009). Reconstitution of yeast silent chromatin: multiple contact sites and O-AADPR binding load SIR complexes onto nucleosomes in vitro. Mol Cell *33*, 323-334.

Marzluff, W.F., Gongidi, P., Woods, K.R., Jin, J., and Maltais, L.J. (2002). The human and mouse replication-dependent histone genes. Genomics *80*, 487-498.

Mauro, A. (1961). Satellite cell of skeletal muscle fibers. J Biophys Biochem Cytol *9*, 493-495.

McCarthy, J.J., Mula, J., Miyazaki, M., Erfani, R., Garrison, K., Farooqui, A.B., Srikuea, R., Lawson, B.A., Grimes, B., Keller, C., *et al.* (2011). Effective fiber hypertrophy in satellite cell-depleted skeletal muscle. Development *138*, 3657-3666.

McFarlane, C., Plummer, E., Thomas, M., Hennebry, A., Ashby, M., Ling, N., Smith, H., Sharma, M., and Kambadur, R. (2006). Myostatin induces cachexia by activating the ubiquitin proteolytic system through an NF-kappaB-independent, FoxO1-dependent mechanism. J Cell Physiol *209*, 501-514.

McKnight, S.L. (2010). On getting there from here. Science *330*, 1338-1339.

McPherron, A.C., Lawler, A.M., and Lee, S.J. (1997). Regulation of skeletal muscle mass in mice by a new TGF-beta superfamily member. Nature *387*, 83-90.

Mehrotra, P.V. (2012). DNA Repair Factor APLF Is a Histone Chaperone. Molecular Cell, 46–55.

Messner, S., and Hottiger, M.O. (2011). Histone ADP-ribosylation in DNA repair, replication and transcription. Trends Cell Biol *21*, 534-542.

Miekus, K., Lukasiewicz, E., Jarocha, D., Sekula, M., Drabik, G., and Majka, M. (2013). The decreased metastatic potential of rhabdomyosarcoma cells obtained through MET receptor downregulation and the induction of differentiation. Cell Death Dis *4*, e459.

Mietton, F., Sengupta, A.K., Molla, A., Picchi, G., Barral, S., Heliot, L., Grange, T., Wutz, A., and Dimitrov, S. (2009). Weak but uniform enrichment of the histone variant macroH2A1 along the inactive X chromosome. Mol Cell Biol *29*, 150-156.

Minetti, G.C., Feige, J.N., Rosenstiel, A., Bombard, F., Meier, V., Werner, A., Bassilana, F., Sailer, A.W., Kahle, P., Lambert, C.*, et al.* (2011). Galphai2 signaling promotes skeletal muscle hypertrophy, myoblast differentiation, and muscle regeneration. Sci Signal *4*, ra80.

Minsky, A., Ghirlando, R., and Reich, Z. (1997). Nucleosomes: a solution to a crowded intracellular environment? J Theor Biol *188*, 379-385.

Monninkhof, E.M., Elias, S.G., Vlems, F.A., van der Tweel, I., Schuit, A.J., Voskuil, D.W., and van Leeuwen, F.E. (2007). Physical activity and breast cancer: a systematic review. Epidemiology *18*, 137-157.

Montarras, D., Morgan, J., Collins, C., Relaix, F., Zaffran, S., Cumano, A., Partridge, T., and Buckingham, M. (2005). Direct isolation of satellite cells for skeletal muscle regeneration. Science *309*, 2064-2067.

Montellier, E., Boussouar, F., Rousseaux, S., Zhang, K., Buchou, T., Fenaille, F., Shiota, H., Debernardi, A., Hery, P., Curtet, S.*, et al.* (2013). Chromatin-to-nucleoprotamine transition is controlled by the histone H2B variant TH2B. Genes Dev *27*, 1680-1692.

Moosmann, A., Campsteijn, C., Jansen, P.W., Nasrallah, C., Raasholm, M., Stunnenberg, H.G., and Thompson, E.M. (2011). Histone variant innovation in a rapidly evolving chordate lineage. BMC Evol Biol *11*, 208.

Moss, F.P., and Leblond, C.P. (1971). Satellite cells as the source of nuclei in muscles of growing rats. Anat Rec *170*, 421-435.

Mukai, A., Kurisaki, T., Sato, S.B., Kobayashi, T., Kondoh, G., and Hashimoto, N. (2009). Dynamic clustering and dispersion of lipid rafts contribute to fusion competence of myogenic cells. Exp Cell Res *315*, 3052-3063.

Murayama, A., Ohmori, K., Fujimura, A., Minami, H., Yasuzawa-Tanaka, K., Kuroda, T., Oie, S., Daitoku, H., Okuwaki, M., Nagata, K.*, et al.* (2008). Epigenetic control of rDNA loci in response to intracellular energy status. Cell *133*, 627-639.

Muroya, S., Takagi, H., Tajima, S., and Asano, A. (1994). Selective inhibition of a step of myotube formation with wheat germ agglutinin in a murine myoblast cell line, C2C12. Cell Struct Funct *19*, 241-252.

Murphy, M.M., Lawson, J.A., Mathew, S.J., Hutcheson, D.A., and Kardon, G. (2011). Satellite cells, connective tissue fibroblasts and their interactions are crucial for muscle regeneration. Development *138*, 3625-3637.

Musaro, A., McCullagh, K., Paul, A., Houghton, L., Dobrowolny, G., Molinaro, M., Barton, E.R., Sweeney, H.L., and Rosenthal, N. (2001). Localized Igf-1 transgene

expression sustains hypertrophy and regeneration in senescent skeletal muscle. Nat Genet *27*, 195-200.

Muthurajan, U.M., McBryant, S.J., Lu, X., Hansen, J.C., and Luger, K. (2011). The linker region of macroH2A promotes self-association of nucleosomal arrays. J Biol Chem *286*, 23852-23864.

Nahle, Z., Hsieh, M., Pietka, T., Coburn, C.T., Grimaldi, P.A., Zhang, M.Q., Das, D., and Abumrad, N.A. (2008). CD36-dependent regulation of muscle FoxO1 and PDK4 in the PPAR delta/beta-mediated adaptation to metabolic stress. J Biol Chem *283*, 14317-14326.

Nanni, P., Nicoletti, G., Palladini, A., Astolfi, A., Rinella, P., Croci, S., Landuzzi, L., Monduzzi, G., Stivani, V., Antognoli, A., *et al.* (2009). Opposing control of rhabdomyosarcoma growth and differentiation by myogenin and interleukin 4. Mol Cancer Ther *8*, 754-761.

Nashun, B., Yukawa, M., Liu, H., Akiyama, T., and Aoki, F. (2010). Changes in the nuclear deposition of histone H2A variants during pre-implantation development in mice. Development *137*, 3785-3794.

Nesterova, T.B., Mermoud, J.E., Hilton, K., Pehrson, J., Surani, M.A., McLaren, A., and Brockdorff, N. (2002). Xist expression and macroH2A1.2 localisation in mouse primordial and pluripotent embryonic germ cells. Differentiation *69*, 216-225.

Neuvonen, M., and Ahola, T. (2009). Differential activities of cellular and viral macro domain proteins in binding of ADP-ribose metabolites. J Mol Biol *385*, 212-225.

Nocon, M., Hiemann, T., Muller-Riemenschneider, F., Thalau, F., Roll, S., and Willich, S.N. (2008). Association of physical activity with all-cause and cardiovascular mortality: a systematic review and meta-analysis. Eur J Cardiovasc Prev Rehabil *15*, 239-246.

Novikov, L., Park, J.W., Chen, H., Klerman, H., Jalloh, A.S., and Gamble, M.J. (2011). QKI-Mediated Alternative Splicing of the Histone Variant MacroH2A1 Regulates Cancer Cell Proliferation. Mol Cell Biol *31*, 4244-4255.

Nowak, S.J., Nahirney, P.C., Hadjantonakis, A.K., and Baylies, M.K. (2009). Nap1-mediated actin remodeling is essential for mammalian myoblast fusion. J Cell Sci *122*, 3282-3293.

O'Gorman, D.J., Karlsson, H.K., McQuaid, S., Yousif, O., Rahman, Y., Gasparro, D., Glund, S., Chibalin, A.V., Zierath, J.R., and Nolan, J.J. (2006). Exercise training increases insulin-stimulated glucose disposal and GLUT4 (SLC2A4) protein content in patients with type 2 diabetes. Diabetologia *49*, 2983-2992.

O'Neill, H.M. (2013). AMPK and Exercise: Glucose Uptake and Insulin Sensitivity. Diabetes Metab J *37*, 1-21.

Ogawa, Y., Ono, T., Wakata, Y., Okawa, K., Tagami, H., and Shibahara, K.I. (2005). Histone variant macroH2A1.2 is mono-ubiquitinated at its histone domain. Biochem Biophys Res Commun *336*, 204-209.

Ohno, S. (1967). Chromosomes and Sex-linked Genes. Springer-Verlag, Heidelberg.

Olsen, R.H., Krogh-Madsen, R., Thomsen, C., Booth, F.W., and Pedersen, B.K. (2008). Metabolic responses to reduced daily steps in healthy nonexercising men. JAMA *299*, 1261-1263.

Orimo, S., Hiyamuta, E., Arahata, K., and Sugita, H. (1991). Analysis of inflammatory cells and complement C3 in bupivacaine-induced myonecrosis. Muscle Nerve *14*, 515-520.

Ouararhni, K., Hadj-Slimane, R., Ait-Si-Ali, S., Robin, P., Mietton, F., Harel-Bellan, A., Dimitrov, S., and Hamiche, A. (2006). The histone variant mH2A1.1 interferes with transcription by down-regulating PARP-1 enzymatic activity. Genes Dev *20*, 3324-3336.

Ozbudak, E.M., Tassy, O., and Pourquie, O. (2010). Spatiotemporal compartmentalization of key physiological processes during muscle precursor differentiation. Proc Natl Acad Sci U S A *107*, 4224-4229.

Palsgaard, J., Brons, C., Friedrichsen, M., Dominguez, H., Jensen, M., Storgaard, H., Spohr, C., Torp-Pedersen, C., Borup, R., De Meyts, P.*, et al.* (2009). Gene expression in skeletal muscle biopsies from people with type 2 diabetes and relatives: differential regulation of insulin signaling pathways. PLoS One *4*, e6575.

Pan, Q., Shai, O., Lee, L.J., Frey, B.J., and Blencowe, B.J. (2008). Deep surveying of alternative splicing complexity in the human transcriptome by high-throughput sequencing. Nat Genet *40*, 1413-1415.

Panopoulos, A.D., Yanes, O., Ruiz, S., Kida, Y.S., Diep, D., Tautenhahn, R., Herrerias, A., Batchelder, E.M., Plongthongkum, N., Lutz, M.*, et al.* (2012). The metabolome of induced pluripotent stem cells reveals metabolic changes occurring in somatic cell reprogramming. Cell Res *22*, 168-177.

Pasque, V., Gillich, A., Garrett, N., and Gurdon, J.B. (2011). Histone variant macroH2A confers resistance to nuclear reprogramming. EMBO J *30*, 2373-2387.

Pasque, V., Radzisheuskaya, A., Gillich, A., Halley-Stott, R.P., Panamarova, M., Zernicka-Goetz, M., Surani, M.A., and Silva, J.C. (2012). Histone variant macroH2A marks embryonic differentiation in vivo and acts as an epigenetic barrier to induced pluripotency. J Cell Sci.

Pavlath, G.K. (2010). Spatial and functional restriction of regulatory molecules during mammalian myoblast fusion. Exp Cell Res *316*, 3067-3072.

Pavlath, G.K., and Horsley, V. (2003). Cell fusion in skeletal muscle--central role of NFATC2 in regulating muscle cell size. Cell Cycle *2*, 420-423.

Pazienza, V., Borghesan, M., Mazza, T., Sheedfar, F., Panebianco, C., Williams, R., Mazzoccoli, G., Andriulli, A., Nakanishi, T., and Vinciguerra, M. (2014). SIRT1-metabolite binding histone macroH2A1.1 protects hepatocytes against lipid accumulation. Aging (Albany NY) *6*, 35-47.

Pedersen, B.K., and Febbraio, M.A. (2012). Muscles, exercise and obesity: skeletal muscle as a secretory organ. Nat Rev Endocrinol *8*, 457-465.

Pehrson, J.R., Costanzi, C., and Dharia, C. (1997). Developmental and tissue expression patterns of histone macroH2A1 subtypes. J Cell Biochem *65*, 107-113.

Pehrson, J.R., and Fried, V.A. (1992). MacroH2A, a core histone containing a large nonhistone region. Science *257*, 1398-1400.

Pehrson, J.R., and Fuji, R.N. (1998). Evolutionary conservation of histone macroH2A subtypes and domains. Nucleic Acids Res *26*, 2837-2842.

Penn, B.H., Bergstrom, D.A., Dilworth, F.J., Bengal, E., and Tapscott, S.J. (2004). A MyoD-generated feed-forward circuit temporally patterns gene expression during skeletal muscle differentiation. Genes Dev *18*, 2348-2353.

Perdiguero, E., Sousa-Victor, P., Ballestar, E., and Munoz-Canoves, P. (2009). Epigenetic regulation of myogenesis. Epigenetics *4*, 541-550.

Perez, E.A., Kassira, N., Cheung, M.C., Koniaris, L.G., Neville, H.L., and Sola, J.E. (2011). Rhabdomyosarcoma in children: a SEER population based study. J Surg Res *170*, e243-251.

Perraud, A.L., Takanishi, C.L., Shen, B., Kang, S., Smith, M.K., Schmitz, C., Knowles, H.M., Ferraris, D., Li, W., Zhang, J.*, et al.* (2005). Accumulation of free ADP-ribose from mitochondria mediates oxidative stress-induced gating of TRPM2 cation channels. J Biol Chem *280*, 6138-6148.

Peterson, F.C., Chen, D., Lytle, B.L., Rossi, M.N., Ahel, I., Denu, J.M., and Volkman, B.F. (2011). Orphan macrodomain protein (human C6orf130) is an O-acyl-ADP-ribose deacylase: solution structure and catalytic properties. J Biol Chem *286*, 35955-35965.

Philippou, A., Halapas, A., Maridaki, M., and Koutsilieris, M. (2007). Type I insulin-like growth factor receptor signaling in skeletal muscle regeneration and hypertrophy. J Musculoskelet Neuronal Interact *7*, 208-218.

Phillips, D.M. (1963). The presence of acetyl groups of histones. Biochem J *87*, 258-263.

Phillips, S.M., Green, H.J., Tarnopolsky, M.A., Heigenhauser, G.J., and Grant, S.M. (1996). Progressive effect of endurance training on metabolic adaptations in working skeletal muscle. Am J Physiol *270*, E265-272.

Pinto, R., Ivaldi, C., Reyes, M., Doyen, C., Mietton, F., Mongelard, F., Alvarez, M., Molina, A., Dimitrov, S., Krauskopf, M.*, et al.* (2005). Seasonal environmental changes regulate the expression of the histone variant macroH2A in an eurythermal fish. FEBS Lett *579*, 5553-5558.

Pleschke, J.M., Kleczkowska, H.E., Strohm, M., and Althaus, F.R. (2000). Poly(ADP-ribose) binds to specific domains in DNA damage checkpoint proteins. J Biol Chem *275*, 40974-40980.

Pogribny, I.P., Tryndyak, V.P., Bagnyukova, T.V., Melnyk, S., Montgomery, B., Ross, S.A., Latendresse, J.R., Rusyn, I., and Beland, F.A. (2009). Hepatic epigenetic phenotype predetermines individual susceptibility to hepatic steatosis in mice fed a lipogenic methyl-deficient diet. J Hepatol *51*, 176-186.

Poirier, G.G., de Murcia, G., Jongstra-Bilen, J., Niedergang, C., and Mandel, P. (1982). Poly(ADP-ribosyl)ation of polynucleosomes causes relaxation of chromatin structure. Proc Natl Acad Sci U S A *79*, 3423-3427.

Posavec, M., Timinszky, G., and Buschbeck, M. (2013). Macro domains as metabolite sensors on chromatin. Cell Mol Life Sci *70*, 1509-1524.

Potthoff, M.J., Wu, H., Arnold, M.A., Shelton, J.M., Backs, J., McAnally, J., Richardson, J.A., Bassel-Duby, R., and Olson, E.N. (2007). Histone deacetylase degradation and

MEF2 activation promote the formation of slow-twitch myofibers. J Clin Invest *117*, 2459-2467.

Pugh, T.D., Conklin, M.W., Evans, T.D., Polewski, M.A., Barbian, H.J., Pass, R., Anderson, B.D., Colman, R.J., Eliceiri, K.W., Keely, P.J.*, et al.* (2013). A shift in energy metabolism anticipates the onset of sarcopenia in rhesus monkeys. Aging Cell *12*, 672-681.

Pujadas, E., and Feinberg, A.P. (2012). Regulated noise in the epigenetic landscape of development and disease. Cell *148*, 1123-1131.

Raben, N., Hill, V., Shea, L., Takikita, S., Baum, R., Mizushima, N., Ralston, E., and Plotz, P. (2008). Suppression of autophagy in skeletal muscle uncovers the accumulation of ubiquitinated proteins and their potential role in muscle damage in Pompe disease. Hum Mol Genet *17*, 3897-3908.

Rafty, L.A., Schmidt, M.T., Perraud, A.L., Scharenberg, A.M., and Denu, J.M. (2002). Analysis of O-acetyl-ADP-ribose as a target for Nudix ADP-ribose hydrolases. J Biol Chem *277*, 47114-47122.

Rampalli, S., Li, L., Mak, E., Ge, K., Brand, M., Tapscott, S.J., and Dilworth, F.J. (2007). p38 MAPK signaling regulates recruitment of Ash2L-containing methyltransferase complexes to specific genes during differentiation. Nat Struct Mol Biol *14*, 1150-1156.

Rappa, F., Greco, A., Podrini, C., Cappello, F., Foti, M., Bourgoin, L., Peyrou, M., Marino, A., Scibetta, N., Williams, R.*, et al.* (2013). Immunopositivity for histone macroH2A1 isoforms marks steatosis-associated hepatocellular carcinoma. PLoS One *8*, e54458.

Ratnakumar, K., Duarte, L.F., LeRoy, G., Hasson, D., Smeets, D., Vardabasso, C., Bonisch, C., Zeng, T., Xiang, B., Zhang, D.Y.*, et al.* (2012). ATRX-mediated chromatin association of histone variant macroH2A1 regulates alpha-globin expression. Genes Dev *26*, 433-438.

Reisz-Porszasz, S., Bhasin, S., Artaza, J.N., Shen, R., Sinha-Hikim, I., Hogue, A., Fielder, T.J., and Gonzalez-Cadavid, N.F. (2003). Lower skeletal muscle mass in male transgenic mice with muscle-specific overexpression of myostatin. Am J Physiol Endocrinol Metab *285*, E876-888.

Relaix, F., Rocancourt, D., Mansouri, A., and Buckingham, M. (2005). A Pax3/Pax7-dependent population of skeletal muscle progenitor cells. Nature *435*, 948-953.

Relaix, F., and Zammit, P.S. (2012). Satellite cells are essential for skeletal muscle regeneration: the cell on the edge returns centre stage. Development *139*, 2845-2856.

Revollo, J.R., Grimm, A.A., and Imai, S. (2004). The NAD biosynthesis pathway mediated by nicotinamide phosphoribosyltransferase regulates Sir2 activity in mammalian cells. J Biol Chem *279*, 50754-50763.

Riggs, A.D. (2002). X chromosome inactivation, differentiation, and DNA methylation revisited, with a tribute to Susumu Ohno. Cytogenet Genome Res *99*, 17-24.

Rios, R., Fernandez-Nocelos, S., Carneiro, I., Arce, V.M., and Devesa, J. (2004). Differential response to exogenous and endogenous myostatin in myoblasts

suggests that myostatin acts as an autocrine factor in vivo. Endocrinology *145*, 2795-2803.

Risson, V., Mazelin, L., Roceri, M., Sanchez, H., Moncollin, V., Corneloup, C., Richard-Bulteau, H., Vignaud, A., Baas, D., Defour, A.*, et al.* (2009). Muscle inactivation of mTOR causes metabolic and dystrophin defects leading to severe myopathy. J Cell Biol *187*, 859-874.

Rongvaux, A., Shea, R.J., Mulks, M.H., Gigot, D., Urbain, J., Leo, O., and Andris, F. (2002). Pre-B-cell colony-enhancing factor, whose expression is up-regulated in activated lymphocytes, is a nicotinamide phosphoribosyltransferase, a cytosolic enzyme involved in NAD biosynthesis. Eur J Immunol *32*, 3225-3234.

Rossi, S., Stoppani, E., Puri, P.L., and Fanzani, A. (2011). Differentiation of human rhabdomyosarcoma RD cells is regulated by reciprocal, functional interactions between myostatin, p38 and extracellular regulated kinase signalling pathways. Eur J Cancer *47*, 1095-1105.

Russell, S.D., Cambon, N., Nadal-Ginard, B., and Whalen, R.G. (1988). Thyroid hormone induces a nerve-independent precocious expression of fast myosin heavy chain mRNA in rat hindlimb skeletal muscle. J Biol Chem *263*, 6370-6374.

Ryall, J.G. (2013). Metabolic reprogramming as a novel regulator of skeletal muscle development and regeneration. FEBS J *280*, 4004-4013.

Sacheck, J.M., Hyatt, J.P., Raffaello, A., Jagoe, R.T., Roy, R.R., Edgerton, V.R., Lecker, S.H., and Goldberg, A.L. (2007). Rapid disuse and denervation atrophy involve transcriptional changes similar to those of muscle wasting during systemic diseases. FASEB J *21*, 140-155.

Sacheck, J.M., Ohtsuka, A., McLary, S.C., and Goldberg, A.L. (2004). IGF-I stimulates muscle growth by suppressing protein breakdown and expression of atrophy-related ubiquitin ligases, atrogin-1 and MuRF1. Am J Physiol Endocrinol Metab *287*, E591-601.

Sakabe, K., Wang, Z., and Hart, G.W. (2010). Beta-N-acetylglucosamine (O-GlcNAc) is part of the histone code. Proc Natl Acad Sci U S A *107*, 19915-19920.

Samal, B., Sun, Y., Stearns, G., Xie, C., Suggs, S., and McNiece, I. (1994). Cloning and characterization of the cDNA encoding a novel human pre-B-cell colony-enhancing factor. Mol Cell Biol *14*, 1431-1437.

Sambasivan, R., Yao, R., Kissenpfennig, A., Van Wittenberghe, L., Paldi, A., Gayraud-Morel, B., Guenou, H., Malissen, B., Tajbakhsh, S., and Galy, A. (2011). Pax7-expressing satellite cells are indispensable for adult skeletal muscle regeneration. Development *138*, 3647-3656.

Sandman, K., Pereira, S.L., and Reeve, J.N. (1998). Diversity of prokaryotic chromosomal proteins and the origin of the nucleosome. Cell Mol Life Sci *54*, 1350-1364.

Sandri, M. (2008). Signaling in muscle atrophy and hypertrophy. Physiology (Bethesda) *23*, 160-170.

Sandri, M., Lin, J., Handschin, C., Yang, W., Arany, Z.P., Lecker, S.H., Goldberg, A.L., and Spiegelman, B.M. (2006). PGC-1alpha protects skeletal muscle from atrophy by

suppressing FoxO3 action and atrophy-specific gene transcription. Proc Natl Acad Sci U S A *103*, 16260-16265.

Sandri, M., Sandri, C., Gilbert, A., Skurk, C., Calabria, E., Picard, A., Walsh, K., Schiaffino, S., Lecker, S.H., and Goldberg, A.L. (2004). Foxo transcription factors induce the atrophy-related ubiquitin ligase atrogin-1 and cause skeletal muscle atrophy. Cell *117*, 399-412.

Schakman, O., Gilson, H., and Thissen, J.P. (2008). Mechanisms of glucocorticoid-induced myopathy. J Endocrinol *197*, 1-10.

Schiaffino, S. (2010). Fibre types in skeletal muscle: a personal account. Acta Physiol (Oxf) *199*, 451-463.

Schiaffino, S., Dyar, K.A., Ciciliot, S., Blaauw, B., and Sandri, M. (2013). Mechanisms regulating skeletal muscle growth and atrophy. FEBS J *280*, 4294-4314.

Schiaffino, S., Gorza, L., Pitton, G., Saggin, L., Ausoni, S., Sartore, S., and Lomo, T. (1988). Embryonic and neonatal myosin heavy chain in denervated and paralyzed rat skeletal muscle. Dev Biol *127*, 1-11.

Schiaffino, S., and Reggiani, C. (2011). Fiber types in mammalian skeletal muscles. Physiol Rev *91*, 1447-1531.

Schuelke, M., Wagner, K.R., Stolz, L.E., Hubner, C., Riebel, T., Komen, W., Braun, T., Tobin, J.F., and Lee, S.J. (2004). Myostatin mutation associated with gross muscle hypertrophy in a child. N Engl J Med *350*, 2682-2688.

Schultz, E. (1996). Satellite cell proliferative compartments in growing skeletal muscles. Dev Biol *175*, 84-94.

Schultz, E., Jaryszak, D.L., and Valliere, C.R. (1985). Response of satellite cells to focal skeletal muscle injury. Muscle Nerve *8*, 217-222.

Scott, W., Stevens, J., and Binder-Macleod, S.A. (2001). Human skeletal muscle fiber type classifications. Phys Ther *81*, 1810-1816.

Sebastian, S., Faralli, H., Yao, Z., Rakopoulos, P., Palii, C., Cao, Y., Singh, K., Liu, Q.C., Chu, A., Aziz, A*., et al.* (2013). Tissue-specific splicing of a ubiquitously expressed transcription factor is essential for muscle differentiation. Genes Dev *27*, 1247-1259.

Sebire, N.J., and Malone, M. (2003). Myogenin and MyoD1 expression in paediatric rhabdomyosarcomas. J Clin Pathol *56*, 412-416.

Seenundun, S., Rampalli, S., Liu, Q.C., Aziz, A., Palii, C., Hong, S., Blais, A., Brand, M., Ge, K., and Dilworth, F.J. (2010). UTX mediates demethylation of H3K27me3 at muscle-specific genes during myogenesis. EMBO J *29*, 1401-1411.

Serra, C., Palacios, D., Mozzetta, C., Forcales, S.V., Morantte, I., Ripani, M., Jones, D.R., Du, K., Jhala, U.S., Simone, C*., et al.* (2007). Functional interdependence at the chromatin level between the MKK6/p38 and IGF1/PI3K/AKT pathways during muscle differentiation. Mol Cell *28*, 200-213.

Serrano, M., Lin, A.W., McCurrach, M.E., Beach, D., and Lowe, S.W. (1997). Oncogenic ras provokes premature cell senescence associated with accumulation of p53 and p16INK4a. Cell *88*, 593-602.

Shefer, G., Van de Mark, D.P., Richardson, J.B., and Yablonka-Reuveni, Z. (2006). Satellite-cell pool size does matter: defining the myogenic potency of aging skeletal muscle. Dev Biol *294*, 50-66.

Shen, L., Shao, N., Liu, X., and Nestler, E. (2014). ngs.plot: Quick mining and visualization of next-generation sequencing data by integrating genomic databases. BMC Genomics *15*, 284.

Sherwood, R.I., Christensen, J.L., Conboy, I.M., Conboy, M.J., Rando, T.A., Weissman, I.L., and Wagers, A.J. (2004). Isolation of adult mouse myogenic progenitors: functional heterogeneity of cells within and engrafting skeletal muscle. Cell *119*, 543-554.

Shi, Y. (2004). Metabolic enzymes and coenzymes in transcription--a direct link between metabolism and transcription? Trends Genet *20*, 445-452.

Shi, Y., Lan, F., Matson, C., Mulligan, P., Whetstine, J.R., Cole, P.A., and Casero, R.A. (2004). Histone demethylation mediated by the nuclear amine oxidase homolog LSD1. Cell *119*, 941-953.

Shyh-Chang, N., Locasale, J.W., Lyssiotis, C.A., Zheng, Y., Teo, R.Y., Ratanasirintrawoot, S., Zhang, J., Onder, T., Unternaehrer, J.J., Zhu, H.*, et al.* (2013). Influence of threonine metabolism on S-adenosylmethionine and histone methylation. Science *339*, 222-226.

Simionescu, A., and Pavlath, G.K. (2011). Molecular mechanisms of myoblast fusion across species. Adv Exp Med Biol *713*, 113-135.

Skene, P.J., and Henikoff, S. (2013). Histone variants in pluripotency and disease. Development *140*, 2513-2524.

Slack, J.M. (2002). Conrad Hal Waddington: the last Renaissance biologist? Nat Rev Genet *3*, 889-895.

Slade, D., Dunstan, M.S., Barkauskaite, E., Weston, R., Lafite, P., Dixon, N., Ahel, M., Leys, D., and Ahel, I. (2011). The structure and catalytic mechanism of a poly(ADP-ribose) glycohydrolase. Nature *477*, 616-620.

Slater, C.R. (1982). Postnatal maturation of nerve-muscle junctions in hindlimb muscles of the mouse. Dev Biol *94*, 11-22.

Smith, C.K., 2nd, Janney, M.J., and Allen, R.E. (1994). Temporal expression of myogenic regulatory genes during activation, proliferation, and differentiation of rat skeletal muscle satellite cells. J Cell Physiol *159*, 379-385.

Smith, Z.D., Chan, M.M., Mikkelsen, T.S., Gu, H., Gnirke, A., Regev, A., and Meissner, A. (2012). A unique regulatory phase of DNA methylation in the early mammalian embryo. Nature *484*, 339-344.

Smyth, G.K. (2004). Linear models and empirical bayes methods for assessing differential expression in microarray experiments. Stat Appl Genet Mol Biol *3*, Article3.

Snow, M.H. (1978). An autoradiographic study of satellite cell differentiation into regenerating myotubes following transplantation of muscles in young rats. Cell Tissue Res *186*, 535-540.

Song, R., Peng, W., Zhang, Y., Lv, F., Wu, H.K., Guo, J., Cao, Y., Pi, Y., Zhang, X., Jin, L.*, et al.* (2013). Central role of E3 ubiquitin ligase MG53 in insulin resistance and metabolic disorders. Nature *494*, 375-379.

Song, X.M., Kawano, Y., Krook, A., Ryder, J.W., Efendic, S., Roth, R.A., Wallberg-Henriksson, H., and Zierath, J.R. (1999). Muscle fiber type-specific defects in insulin signal transduction to glucose transport in diabetic GK rats. Diabetes *48*, 664-670.

Sousa-Victor, P., Gutarra, S., Garcia-Prat, L., Rodriguez-Ubreva, J., Ortet, L., Ruiz-Bonilla, V., Jardi, M., Ballestar, E., Gonzalez, S., Serrano, A.L.*, et al.* (2014). Geriatric muscle stem cells switch reversible quiescence into senescence. Nature *506*, 316-321.

Southgate, R.J., Neill, B., Prelovsek, O., El-Osta, A., Kamei, Y., Miura, S., Ezaki, O., McLoughlin, T.J., Zhang, W., Unterman, T.G.*, et al.* (2007). FOXO1 regulates the expression of 4E-BP1 and inhibits mTOR signaling in mammalian skeletal muscle. J Biol Chem *282*, 21176-21186.

Spalding, K.L., Bhardwaj, R.D., Buchholz, B.A., Druid, H., and Frisen, J. (2005). Retrospective birth dating of cells in humans. Cell *122*, 133-143.

Sporn, J.C., and Jung, B. (2012). Differential regulation and predictive potential of MacroH2A1 isoforms in colon cancer. Am J Pathol *180*, 2516-2526.

Sporn, J.C., Kustatscher, G., Hothorn, T., Collado, M., Serrano, M., Muley, T., Schnabel, P., and Ladurner, A.G. (2009). Histone macroH2A isoforms predict the risk of lung cancer recurrence. Oncogene.

Steffen, J.D., and Pascal, J.M. (2013). New players to the field of ADP-ribosylation make the final cut. EMBO J *32*, 1205-1207.

Stitt, T.N., Drujan, D., Clarke, B.A., Panaro, F., Timofeyva, Y., Kline, W.O., Gonzalez, M., Yancopoulos, G.D., and Glass, D.J. (2004). The IGF-1/PI3K/Akt pathway prevents expression of muscle atrophy-induced ubiquitin ligases by inhibiting FOXO transcription factors. Mol Cell *14*, 395-403.

Stuart, C.A., South, M.A., Lee, M.L., McCurry, M.P., Howell, M.E., Ramsey, M.W., and Stone, M.H. (2013). Insulin responsiveness in metabolic syndrome after eight weeks of cycle training. Med Sci Sports Exerc *45*, 2021-2029.

Supek, F., Bosnjak, M., Skunca, N., and Smuc, T. (2011). REVIGO summarizes and visualizes long lists of gene ontology terms. PLoS One *6*, e21800.

Suzuki, T., Maruyama, A., Sugiura, T., Machida, S., and Miyata, H. (2009). Age-related changes in two- and three-dimensional morphology of type-identified endplates in the rat diaphragm. J Physiol Sci *59*, 57-62.

Tachiwana, H., Osakabe, A., Shiga, T., Miya, Y., Kimura, H., Kagawa, W., and Kurumizaka, H. (2011). Structures of human nucleosomes containing major histone H3 variants. Acta Crystallogr D Biol Crystallogr *67*, 578-583.

Takahashi, I., Kameoka, Y., and Hashimoto, K. (2002). MacroH2A1.2 binds the nuclear protein Spop. Biochim Biophys Acta *1591*, 63-68.

Talbert, P.B., and Henikoff, S. (2010). Histone variants--ancient wrap artists of the epigenome. Nat Rev Mol Cell Biol *11*, 264-275.

Tan, M., Luo, H., Lee, S., Jin, F., Yang, J.S., Montellier, E., Buchou, T., Cheng, Z., Rousseaux, S., Rajagopal, N.*, et al.* (2011). Identification of 67 histone marks and

histone lysine crotonylation as a new type of histone modification. Cell *146*, 1016-1028.

Tanasijevic, B., and Rasmussen, T.P. (2011). X chromosome inactivation and differentiation occur readily in ES cells doubly-deficient for macroH2A1 and macroH2A2. PLoS One *6*, e21512.

Tanner, K.G., Landry, J., Sternglanz, R., and Denu, J.M. (2000). Silent information regulator 2 family of NAD- dependent histone/protein deacetylases generates a unique product, 1-O-acetyl-ADP-ribose. Proc Natl Acad Sci U S A *97*, 14178-14182.

Tanny, J.C., and Moazed, D. (2001). Coupling of histone deacetylation to NAD breakdown by the yeast silencing protein Sir2: Evidence for acetyl transfer from substrate to an NAD breakdown product. Proc Natl Acad Sci U S A *98*, 415-420.

Tapscott, S.J. (2005). The circuitry of a master switch: Myod and the regulation of skeletal muscle gene transcription. Development *132*, 2685-2695.

Teperino, R., Schoonjans, K., and Auwerx, J. (2010). Histone methyl transferases and demethylases; can they link metabolism and transcription? Cell Metab *12*, 321-327.

Tiku, P.E., Gracey, A.Y., Macartney, A.I., Beynon, R.J., and Cossins, A.R. (1996). Cold-induced expression of delta 9-desaturase in carp by transcriptional and posttranslational mechanisms. Science *271*, 815-818.

Till, S., and Ladurner, A.G. (2009). Sensing NAD metabolites through macro domains. Front Biosci *14*, 3246-3258.

Timinszky, G., Till, S., Hassa, P.O., Hothorn, M., Kustatscher, G., Nijmeijer, B., Colombelli, J., Altmeyer, M., Stelzer, E.H., Scheffzek, K.*, et al.* (2009). A macrodomain-containing histone rearranges chromatin upon sensing PARP1 activation. Nat Struct Mol Biol *16*, 923-929.

Tong, L., and Denu, J.M. (2010). Function and metabolism of sirtuin metabolite O-acetyl-ADP-ribose. Biochim Biophys Acta *1804*, 1617-1625.

Tong, L., Lee, S., and Denu, J.M. (2009). Hydrolase regulates NAD+ metabolites and modulates cellular redox. J Biol Chem *284*, 11256-11266.

Tonin, P.N., Scrable, H., Shimada, H., and Cavenee, W.K. (1991). Muscle-specific gene expression in rhabdomyosarcomas and stages of human fetal skeletal muscle development. Cancer Res *51*, 5100-5106.

Tropberger, P., and Schneider, R. (2013). Scratching the (lateral) surface of chromatin regulation by histone modifications. Nat Struct Mol Biol *20*, 657-661.

Tuomilehto, J., Lindstrom, J., Eriksson, J.G., Valle, T.T., Hamalainen, H., Ilanne-Parikka, P., Keinanen-Kiukaanniemi, S., Laakso, M., Louheranta, A., Rastas, M.*, et al.* (2001). Prevention of type 2 diabetes mellitus by changes in lifestyle among subjects with impaired glucose tolerance. N Engl J Med *344*, 1343-1350.

Turcan, S., Rohle, D., Goenka, A., Walsh, L.A., Fang, F., Yilmaz, E., Campos, C., Fabius, A.W., Lu, C., Ward, P.S.*, et al.* (2012). IDH1 mutation is sufficient to establish the glioma hypermethylator phenotype. Nature *483*, 479-483.

Ueda, K., Kinoshita, Y., Xu, Z.J., Ide, N., Ono, M., Akahori, Y., Tanaka, I., and Inoue, M. (2000). Unusual core histones specifically expressed in male gametic cells of Lilium longiflorum. Chromosoma *108*, 491-500.

Van Doninck, K., Mandigo, M.L., Hur, J.H., Wang, P., Guglielmini, J., Milinkovitch, M.C., Lane, W.S., and Meselson, M. (2009). Phylogenomics of unusual histone H2A Variants in Bdelloid rotifers. PLoS Genet *5*, e1000401.

Vander Heiden, M.G., Cantley, L.C., and Thompson, C.B. (2009). Understanding the Warburg effect: the metabolic requirements of cell proliferation. Science *324*, 1029-1033.

Vaquero, A., and Reinberg, D. (2009). Calorie restriction and the exercise of chromatin. Genes Dev *23*, 1849-1869.

Vardabasso, C., Hasson, D., Ratnakumar, K., Chung, C.Y., Duarte, L.F., and Bernstein, E. (2014). Histone variants: emerging players in cancer biology. Cell Mol Life Sci *71*, 379-404.

Veech, R.L., Eggleston, L.V., and Krebs, H.A. (1969). The redox state of free nicotinamide-adenine dinucleotide phosphate in the cytoplasm of rat liver. Biochem J *115*, 609-619.

Vera, M.I., Norambuena, L., Alvarez, M., Figueroa, J., Molina, A., Leon, G., and Krauskopf, M. (1993). Reprogramming of nucleolar gene expression during the acclimatization of the carp. Cell Mol Biol Res *39*, 665-674.

Vethantham, V., Yang, Y., Bowman, C., Asp, P., Lee, J.H., Skalnik, D.G., and Dynlacht, B.D. (2012). Dynamic loss of H2B ubiquitylation without corresponding changes in H3K4 trimethylation during myogenic differentiation. Mol Cell Biol *32*, 1044-1055.

Waddington, C.H. (1953). The Epigenetics of birds. Cambridge University Press.

Waddington, C.H. (1957). The Strategy of the Genes. Allen&Unwin.

Wang, E.T., Sandberg, R., Luo, S., Khrebtukova, I., Zhang, L., Mayr, C., Kingsmore, S.F., Schroth, G.P., and Burge, C.B. (2008). Alternative isoform regulation in human tissue transcriptomes. Nature *456*, 470-476.

Wang, J., Alexander, P., and McKnight, S.L. (2011). Metabolic specialization of mouse embryonic stem cells. Cold Spring Harb Symp Quant Biol *76*, 183-193.

Wang, J., Alexander, P., Wu, L., Hammer, R., Cleaver, O., and McKnight, S.L. (2009). Dependence of mouse embryonic stem cells on threonine catabolism. Science *325*, 435-439.

Wang, X. (2012). Satellite cells, the engines of muscle repair. Molecular Cell Biology *13*, 127.

Warburton, P.E. (2001). Epigenetic analysis of kinetochore assembly on variant human centromeres. Trends Genet *17*, 243-247.

Warburton, P.E. (2004). Chromosomal dynamics of human neocentromere formation. Chromosome Res *12*, 617-626.

Welle, S., Tawil, R., and Thornton, C.A. (2008). Sex-related differences in gene expression in human skeletal muscle. PLoS One *3*, e1385.

Wellen, K.E., Hatzivassiliou, G., Sachdeva, U.M., Bui, T.V., Cross, J.R., and Thompson, C.B. (2009). ATP-citrate lyase links cellular metabolism to histone acetylation. Science *324*, 1076-1080.

Wellen, K.E., and Thompson, C.B. (2012). A two-way street: reciprocal regulation of metabolism and signalling. Nat Rev Mol Cell Biol *13*, 270-276.

Wenz, T., Rossi, S.G., Rotundo, R.L., Spiegelman, B.M., and Moraes, C.T. (2009). Increased muscle PGC-1alpha expression protects from sarcopenia and metabolic disease during aging. Proc Natl Acad Sci U S A *106*, 20405-20410.

Whetstine, J.R., Nottke, A., Lan, F., Huarte, M., Smolikov, S., Chen, Z., Spooner, E., Li, E., Zhang, G., Colaiacovo, M.*, et al.* (2006). Reversal of histone lysine trimethylation by the JMJD2 family of histone demethylases. Cell *125*, 467-481.

White, R.B., Bierinx, A.S., Gnocchi, V.F., and Zammit, P.S. (2010). Dynamics of muscle fibre growth during postnatal mouse development. BMC Dev Biol *10*, 21.

Wolin, K.Y., Yan, Y., Colditz, G.A., and Lee, I.M. (2009). Physical activity and colon cancer prevention: a meta-analysis. Br J Cancer *100*, 611-616.

Wu, H., and Zhang, Y. (2014). Reversing DNA methylation: mechanisms, genomics, and biological functions. Cell *156*, 45-68.

Wu, S.C., and Zhang, Y. (2010). Active DNA demethylation: many roads lead to Rome. Nat Rev Mol Cell Biol *11*, 607-620.

Xiao, M., Yang, H., Xu, W., Ma, S., Lin, H., Zhu, H., Liu, L., Liu, Y., Yang, C., Xu, Y.*, et al.* (2012). Inhibition of alpha-KG-dependent histone and DNA demethylases by fumarate and succinate that are accumulated in mutations of FH and SDH tumor suppressors. Genes Dev *26*, 1326-1338.

Xu, C., Xu, Y., Gursoy-Yuzugullu, O., and Price, B.D. (2012). The histone variant macroH2A1.1 is recruited to DSBs through a mechanism involving PARP1. FEBS Lett *586*, 3920-3925.

Yablonka-Reuveni, Z., and Rivera, A.J. (1994). Temporal expression of regulatory and structural muscle proteins during myogenesis of satellite cells on isolated adult rat fibers. Dev Biol *164*, 588-603.

Yaffe, D., and Saxel, O. (1977). Serial passaging and differentiation of myogenic cells isolated from dystrophic mouse muscle. Nature *270*, 725-727.

Yanes, O., Clark, J., Wong, D.M., Patti, G.J., Sanchez-Ruiz, A., Benton, H.P., Trauger, S.A., Desponts, C., Ding, S., and Siuzdak, G. (2010). Metabolic oxidation regulates embryonic stem cell differentiation. Nat Chem Biol *6*, 411-417.

Yin, H., Price, F., and Rudnicki, M.A. (2013). Satellite cells and the muscle stem cell niche. Physiol Rev *93*, 23-67.

Young, J.M., and Weser, E. (1971). The metabolism of circulating maltose in man. J Clin Invest *50*, 986-991.

Zang, C., Schones, D.E., Zeng, C., Cui, K., Zhao, K., and Peng, W. (2009). A clustering approach for identification of enriched domains from histone modification ChIP-Seq data. Bioinformatics *25*, 1952-1958.

Zhang, R., Poustovoitov, M.V., Ye, X., Santos, H.A., Chen, W., Daganzo, S.M., Erzberger, J.P., Serebriiskii, I.G., Canutescu, A.A., Dunbrack, R.L.*, et al.* (2005). Formation of MacroH2A-containing senescence-associated heterochromatin foci and senescence driven by ASF1a and HIRA. Dev Cell *8*, 19-30.

Zhang, S., Hulver, M.W., McMillan, R.P., Cline, M.A., and Gilbert, E.R. (2014). The pivotal role of pyruvate dehydrogenase kinases in metabolic flexibility. Nutr Metab (Lond) *11*, 10.

Zhou, X., Wang, J.L., Lu, J., Song, Y., Kwak, K.S., Jiao, Q., Rosenfeld, R., Chen, Q., Boone, T., Simonet, W.S*., et al.* (2010). Reversal of cancer cachexia and muscle wasting by ActRIIB antagonism leads to prolonged survival. Cell *142*, 531-543.

Zhu, L.J., Gazin, C., Lawson, N.D., Pages, H., Lin, S.M., Lapointe, D.S., and Green, M.R. (2010). ChIPpeakAnno: a Bioconductor package to annotate ChIP-seq and ChIP-chip data. BMC Bioinformatics *11*, 237.

Zimmers, T.A., Davies, M.V., Koniaris, L.G., Haynes, P., Esquela, A.F., Tomkinson, K.N., McPherron, A.C., Wolfman, N.M., and Lee, S.J. (2002). Induction of cachexia in mice by systemically administered myostatin. Science *296*, 1486-1488.